ROLE OF ERAP1 IN ANTIGEN-PRESENTATION AND ANKYLOSING SPONDYLITIS

By

David Patric Werner Rastall

A DISSERTATION

Submitted to
Michigan State University
in partial fulfillment of the requirements
for the degree of

Cell and Molecular Biology – Doctor of Philosophy

2017

ABSTRACT

ROLE OF ERAP1 IN ANTIGEN-PRESENTATION AND ANKYLOSING SPONDYLITIS

By

David Patric Werner Rastall

Ankylosing spondylitis (AS) is a crippling autoimmune disorder that causes inflammation, fusion of the spinal vertebrae and osteoporosis. Over 40 years ago the strong association of AS to the *HLA-B* gene was discovered, but the pathogenesis of the disease is still completely unknown. More recent genetic studies have identified the association of another antigen presentation gene, endoplasmic reticulum aminopeptidase 1 (*ERAP1*) to AS. After *HLA-B*, *ERAP1* has the strongest association, and highest odds ratio of any gene in AS and epistatic (non-additive) interactions between *ERAP1* and *HLA-B* further increase risk for developing AS. Because both genes were known to contribute to antigen presentation, their epistatic interaction led to the hypothesis that antigen presentation may be responsible for the pathogenesis of the disease. However, the extent to which ERAP1 contributes to antigen presentation and how antigen presentation may be affecting bone homeostasis are not known.

For that reason we investigated the role that ERAP1 plays in antigen presentation. Using ERAP1$^{-/-}$ mice, we demonstrated that ERAP1 is required to create and destroy immunogenic epitopes and could result in a complete inversion of the immunodominant T-cell response. We then demonstrated that similar changes could be mediated by polymorphic disease-associated human ERAP1 variants in cells and in transgenic mice. These studies furthered our understanding of how *ERAP1* and AS-associated *ERAP1* polymorphisms impacted antigen presentation, and supported the antigen-presentation hypothesis of AS. However, the central question in the field remained: can antigen presentation impact bone homeostasis? To investigate

if ERAP1 and/or antigen presentation played a role in bone homeostasis, we performed a detailed skeletal analysis of mice deficient in ERAP1. Surprisingly, loss of ERAP1 was sufficient to cause spontaneous vertebral fusion, osteoporosis, and cellular infiltrate in the spine. This result demonstrated that ERAP1 was directly linked to bone homeostasis within the axial skeleton, but did not address if ERAP1 was mediating this effect via its role in antigen presentation or via a non-canonical function. To help discern the molecular mechanisms underlying this phenotype, we repeated the analysis in β-2-microglobulin knockout ($\beta2m^{-/-}$) mice, that lack all cell-surface presentation of MHC-I. $\beta2m^{-/-}$ mice developed similar patterns of vertebral fusion and osteoporosis and appeared to have a later-onset of disease. Additionally, in the ERAP1 transgenic mice we uncovered multiple effects of ERAP1 outside of antigen presentation, such as modulation of NK-mediated cytotoxicity, modulation of NKG2D signaling on NK cells, and we determined that a variant of ERAP1 associated with a high risk for AS is a dominant lethal allele in male mice, independent of it's function in antigen presentation.

These important findings define the role of ERAP1 in antigen presentation, directly connect ERAP1 to bone homeostasis and pathology in the axial skeleton, and suggest that antigen presentation plays a role in bone homeostasis. This work also provides the first simple genetic animal model of AS that spontaneously develops all of the key symptoms of AS and therefore will be valuable for the development and testing of therapeutics for the disease.

This work is dedicated to patients with ankylosing spondylitis and related disorders. While it is easy as scientists to become consumed by the progress of human knowledge, our end goal should always be the ending of human suffering and bettering of the human condition in the universe.

ACKNOWLEDGMENTS

I would sincerely like to thank the large number of scientists, colleges, collaborators and funding sources that have allowed me to participate in the discoveries outlined in this thesis. I would like to thank Dr. McCormick for trusting in me despite my background in professional fine art and supporting my application into the physician scientist training program. He saw potential in me that many others may have overlooked and I greatly appreciate his wisdom and support. I would also like to thank Dr. Amalfitano, who took a similar chance on me, letting me prove myself in his lab, and always reminding me to see the "big-picture" in science, stressing the economic and social ramifications of translational science and encouraging a pragmatic and practical approach.

I received mentoring from many colleagues in the laboratory and chief among them is Dr. Yasser Aldhamen, who has supported my scientific efforts throughout my stay at MSU. He took responsibility in helping me develop in the laboratory, teaching me how to develop scientific thoughts, design experiments, write papers, and construct grants. I would also like to thank Dr. Sergey Seregin who trained me in basic scientific techniques and instructed me in my first experiments in the lab.

I have also revived phenomenal support from other graduate students including Yuliya Pepelyayeva and Patrick O'Connell who have spent countless hours assisting with experiments from the early morning to late at night and who contributed greatly to this thesis. Additionally, I would not have been able to complete this work without the constant assistance of our laboratory manager Sarah Roosa, and laboratory technician Cristiane Pereira-Hicks who maintain a laboratory environment in which we can efficiently conduct research and who helped directly on a

many experiments. I would also like to thank all past and current members of the Amalfitano laboratory who have all directly or indirectly supported this work.

I greatly appreciate the help provided by my guidance committee: Dr. Andrea Amalfitano, Dr. Katheryn Meek, Dr. Brian Schutte, Dr. Nara Parameswaran, and Dr. Kefei Yu. Their insightful comments and criticisms helped improve this research and helped me develop as a scientist.

Without funding from the NIH, the MSU Foundation, the MSU graduate school, the College of Osteopathic Medicine, as well the Osteopathic Heritage Foundation this thesis could not have been completed. I greatly appreciate the support that we received as a lab, and the individual awards and fellowships granted to me by the MSU graduate school and the College of Osteopathic Medicine.

I also owe a tremendous thanks to Bethany Heinlein who served to organize the dual degree program, organized my schedules, and maintained the dual degree program.

I would also like to thank my family, my step father Dr. Micheal Henderson who supported my transition from an artist to a scientist, and my mother and father who also provided support.

Finally, I would like to thank all the members of the institutional departments that supported this thesis including MMG, COM, ULAR, the histopathology core, the flow cytometry core, and the graduate school. Special thanks to Amy Porter and Kathy Joseph of the Investigative Histopathology Lab, who provided endless help and advice and went above and beyond on multiple occasions to facilitate scientific discovery. Special thanks to Dr. Louis King of the Flow Cytometry Core, who provided help, advice, and similarly went above and beyond to support this work.

TABLE OF CONTENTS

LIST OF TABLES

LIST OF FIGURES

KEY TO ABBREVIATIONS

Ad5	adenovirus serotype 5
Ad5-TA	adenovirus serotype 5 expressing Clostridium difficile Toxin A
AIRE	autoimmune regulator
ALL	anterior longitudinal ligament
APS1	autoimmune polyendocrinopathy syndrome type 1
AS	ankylosing spondylitis
ASAS20	Assessment of SpondyloArthritis international Society 20 improvement criteria
ASspiMRI-a	AS spinal MRI activity
BMC	bone mineral content
BMD	bone mineral density
BV/TV%	bone mineral volume percent
CD 107a	cluster of differentiation 107a, lysosomal-associated membrane protein 1
CD 127	cluster of differentiation 127
CD 62	cluster of differentiation 62
CD 69	cluster of differentiation 69
CD 8	cluster of differentiation 8
CD 97	cluster of differentiation 97
CD3	cluster of differentiation 3
CFSE	carboxyfluorescein succinimidyl ester
CFSEhigh	cells stained with 10 μM carboxyfluorescein succinimidyl ester
CFSElow	cells stained with 1 μM carboxyfluorescein succinimidyl ester

CIA	collagen induced arthritis
CMV	cytomegalovirus (promoter)
CRP	C-reactive protein
dpi	days post-injection
E:T	effector to target
ER	endoplasmic reticulum
ERAP1	endoplasmic reticulum aminopeptidase 1
ERAP1−/− IDTAP	ERAP1-independent TA-derived immunodominant peptides only responsive in Ad-TA-vaccinated ERAP1−/− mice
ESR	erythrocyte sedimentation rate
FBS	fetal bovine serum
FHC	free heavy chain
GFP	green fluorescent protein
GWAS	genome-wide association studies
HLA	human leukocyte antigen
HPLC	high performance liquid chromatography
hβ2m	human β2 microglobulin
I.M.	intramuscularly
IBD	inflammatory bowel disease
ICP47	infected cell protein
IFN-γ	interferon gamma
IgG	immunoglobulin g
IL	interleukin

IL-1	interleukin 1
IL-12B	interleukin-12 subunit p40
IL-23	interleukin 23
IL-23A	interleukin-23 subunit alpha
IL-23R	interleukin-23 receptor
IL-6Rα	interleukin-6 receptor alpha
KIR	killer-cell immunoglobulin-like receptor
L6	6th lumbar vertebrea
mERAP1	murine endoplasmic reticulum aminopeptidase 1
MFI	mean fluorescent intensity
MHC-I	major histocompatibility complex I
MRI	magnetic resonance imaging
NK	natural killer
NSAID	non-steroidal anti-inflammatories
PIA	proteoglycan-induced arthritis
RA	rheumatoid arthritis
RFP	red fluorescent protein
SEM	standard error measurement
SI	sacroiliac
SNPs	single nucleotide polymorphisms
SPF	specific pathogen free
TA	toxin A

TAP1	transporter associated with antigen presentation 1
Tb. N.	trabecular number
Tb. Sp.	trabecular spacing
Tb. Th.	trabecular thickness
TCM	T central memory
TCR	T-cell receptor
TEM	T effector memory
TNF-α	tumor necrosis factor alpha
TNFR1	type I tumor necrosis factor receptor
UPR	unfolded protein response
WT	wildtype
WT IDTAP	ERAP1-dependent TA-derived immunodominant peptides only responsive in Ad-TA-vaccinated WT mice
β2m	β2 microglobulin
μCT	micro computed tomography

Chapter 1

Introduction

Seronegative Spondyloarthropathies

Ankylosing spondylitis (AS) is the prototypical disease of the seronegative spondyloarthropathies, a group of autoimmune diseases that share common clinical features and genetic predispositions. AS is the most common of these disorders with a prevalence of 0.15-1.8%; the overall prevalence of the seronegative spondyloarthropathies is 0.2-9.4% depending on the population studied.[1] The initial description of these disease was made over 50 years ago by the International League against Rheumatism who believed these diseases to be atypical presentations of rheumatoid arthritis.[2] In 1974 Moll et al. recognized these diseases as a distinct entity and named them the seronegative spondyloarthropathies.[3] This grouping was based on the observation that these diseases had similar clinical presentation, including the absence of rheumatoid factor in the serum, the absence of joint nodules, and the tendency to develop sacroiliitis.[3] Subsequent genome-wide association studies (GWAS) identified many overlapping risk loci, suggesting that these diseases not only shared clinical features, but genetic risk factors as well. Today the seronegative spondyloarthropathies are generally understood to include ankylosing spondylitis (AS), psoriasis, psoriatic arthritis, reactive arthritis, Behçet's syndrome, and arthritis associated with inflammatory bowel disease (IBD).

These disorders share overlapping clinical symptoms including inflammatory back pain, sacroiliitis, asymmetric peripheral arthritis, enthesitis and dactylitis, skin involvement, nail bed changes, inflammation in the eye, and inflammatory bowel disease.[2,4–12] Shared genetic risk loci include many antigen-presentation genes (*HLA-B, HLA-C, ERAP1*)[13–16] and genes in the IL-23 pathway (*IL23-R, IL12B, IL23A*).[17–20] The shared clinical features and genetic risk loci are summarized in chapter 1 table 1 below. It is important to note with many of these diseases that

definitions and classification criteria have changed over time, potentially blurring the boundaries of these disorders further.

Table 1 – Seronegative Spondyloarthropathies Symptoms and Genetic Risks

Disease	Associated Signs and Symptoms	Primary Associated Genes
Ankylosing spondylitis	Sacroiliitis,[4] Spinal Ankylosis,[4] Inflammatory Back Pain,[4,7] Uveitis,[8,9] Osteoporosis,[10,21] Asymmetric Peripheral Arthritis,[7] Enthesitis and Dactylitis,[7]	HLA-B,[13,14,22–24] ERAP1,[13,14,25] IL-23R,[17] CARD8,[26] IL6R,[27] HLA-A,[28] HLA-DR,[14,29–31] TNFRSF1A[13]
Psoriatic arthritis	Skin Lesions (Psoriatic Plaques), Uveitis,[9,11] Asymmetric Peripheral Arthritis,[5] Sacroiliitis,[6] Spinal Ankylosis (syndesmophyte formation, paravertebral ossification),[6] Enthesitis[32]	HLA-C,[33,34] HLA-B,[33] IL-12B,[18] IL-23R,[18,35] KIR,[36]
Reactive arthritis	Asymmetric Peripheral Arthritis[37]	HLA-B,[37] *Note: limited genetic studies have been conducted on RA
Psoriasis	Skin Lesions (Psoriatic Plaques),[18] Asymmetric Peripheral Arthritis[38]	HLA-C,[33,34,39] HLA-B,[33] ERAP1,[38] IL-12B,[18,39] IL-23R,[18,38] IL-23A,[40] TNIP1,[40] TNFAIP3,[40] IL4,[40] IL13,[40]
Behçet's syndrome	Oral Ulcers,[41] Genital Ulcers,[41] Skin Lesions,[41] Uveitis,[41] Peripheral Arthritis,[42] Sacroiliitis,[42] Osteoporosis,[42] Vascular Pathology,[41]	HLA-B,[15,43] ERAP1,[15,43] IL-23R,[43] IL-10,[43]
IBD/ IBD-associated arthritis	Colitis,[44] Asymmetric Peripheral Arthritis,[12,44] Uveitis[45]	HLA-B,[44] NOD2,[46] IL-23R,[19]

Clinical Presentation of AS

Ankylosing spondylitis (AS) is the prototypical seronegative spondyloarthropathy. It affects around 0.55% of people with European ancestry, 0.35% of people with Chinese ancestry, and is uncommon in people with Japanese or African ancestry. This pattern correlates with the frequency of specific HLA-B27 and ERAP1 alleles in those populations. It is one of few autoimmune diseases that affects men more frequently than women, and compared to other forms of arthritis has a relatively early onset, with a mean age of 20-26 at diagnosis.[47] AS patients develop gradual fusion of the bones of the axial skeleton (the spine and pelvis) alongside systemic inflammation and osteoporosis.[4,48] Together with these key features, AS is associated with many lower-frequency comorbidities including uveitis,[8] subclinical colitis,[49,50] and peripheral arthritis.[51,52]

Primary Skeletal Features of AS

Ankylosis is the hallmark feature of AS and can affect any joint within the axial skeleton, but is frequently first observed and diagnosed within the sacroiliac (SI) joint.[53] Ankylosis of the SI joint progresses through three stages and typically is bilateral and symmetrical. First, the SI joint loses bone, causing a focal widening of the joint on radiography. Prominent erosions are observed along the iliac side of the joint, where subchondral bone loss leads to a loss of definition and osteoporosis.[54] Second, the joint shows signs of reactive sclerosis, which blur the joint margins on radiography and the ligaments between the joints begin to calcify. Finally, new bone forms along the joint, obliterating the joint margins on radiography, and the bones eventually fuse. A similar three-stage progression is observed sporadically between vertebrae in

the spine. Within an intervertebral joint, the first change observed is the "shiny corner sign," erosions and bone loss along the superior and inferior endplates of the intervertebral joints that look like shiny corners on a lateral radiograph.[55] These erosions are followed by the formation of syndesmophytes, calcifications that form within intervertebral ligaments and grow from one or both sides of the joint, until they form a bridge.[55] As bridging syndesmophytes progress and widen, eventually all ligaments of the joint calcify and the two vertebrae fuse. Without treatment, all of the bones of the spine and pelvis may eventually fuse into a single bone.[54] This unique pathology was recognized in cadavers as early as the 1800's and led to the initial identification of the disease.[48]

Inflammation in AS

Although 70-80% of AS patients develop inflammation and inflammatory back pain,[56] the exact nature of this inflammation is not understood, and there is conflicting evidence on which cytokines and inflammatory biomarkers are increased in AS. Erythrocyte sedimentation rate (ESR) and C-reactive protein (CRP) are traditional clinical measures of inflammation, but neither has proven sensitive or specific for AS.[57] IL-6 has been studied extensively and is frequently,[58–61] but not always[62] found to be elevated in the serum of AS patients. The same is true for TNF-α,[58–60,63] IL-23,[60,64] and IL-17.[60,64] IL-1β[58,59] and IFN-γ[58] have also been studied, but do not appear to be elevated in the serum of AS patients. The variance in these results may arise from confounding factors such as differing medications and comorbidities between subjects, or may be a genuine variance within differing manifestations of the disease. Furthermore, while evaluating serum cytokines is convenient, they may not be the best measure of inflammation in

AS. MRI imaging of spines shows that inflammation is highly localized and is not constant,[65] but occurs in sporadic patterns of exacerbation and remission. Therefore the key cytokines responsible for ankylosis may only be present focally during flare-ups and not necessarily chronically elevated. To address this limitation, biopsies have been performed on disco-vertebral lesions from AS patients. These biopsies identified plasma cells, macrophages, and T-cells within spinal lesions in AS, suggesting that these cells may be involved in the pathogenesis of the disease.[66,67]

The relationship between inflammation and ankylosis is also not clear. In the clinic, AS patients typically complain of inflammatory back pain for years before there is radiologic evidence of spinal ankylosis. Because clinical evidence of back pain precedes evidence of spinal ankylosis, many physicians and scientists have theorized that inflammation causes spinal ankylosis in AS,[4] however there is now evidence suggesting that inflammation is not essential for the development of spinal ankylosis.[65,68] TNF-α inhibitors effectively treat inflammation and back pain in AS patients,[69] but fail to halt progression of spinal ankylosis.[70,71] Additional evidence comes from studies that directly tracked inflammation and the development of spinal ankylosis by MRI.[68,72,73] Multiple studies found that syndesmophytes could form at sites with or without local inflammation, and that they were more likely to form at sites where inflammation had receded, than at sites of active inflammation.[68,72] Based on these results it appears inflammation may affect the development of spinal ankylosis, but that neither local nor systemic inflammation is essential for it.

Osteoporosis in AS

Paradoxically, while excessive bone develops within the axial skeleton, osteoporosis develops within all the bones of the body, including the spine, of As patients.[10] This critical feature of AS was missed for years because on x-ray the excess bone formed by ankylosis masks the underlying osteoporosis of spinal vertebrae and was only recognized when more advanced imaging became broadly accessible.[10] AS patients have decreased bone mineral density (BMD), and bone mineral content (BMC) in the trabecular space of their spines, femurs, and radii,[10,74,75] as well as overall decreases in the trabecular thickness of the spine.[76] Osteoporosis is a critical symptom in AS, as the combination of osteoporosis and ankylosis leads to a high (10%) incidence of spinal fractures.[77,78] Because of the unique structure of their spines, these fractures are frequently severe leading to permanent damage and neurological sequelae.[21,79]

Comorbidities in AS

AS is frequently accompanied by several comorbidities including uveitis, peripheral arthritis, and colitis. Acute anterior uveitis will spontaneously develop in 25-40% of AS patients.[80] A single patient will usually have multiple episodes of unilateral uveitis throughout their life and subsequent episodes may affect the same eye or the contralateral eye with equal likelihood. These attacks may be accompanied by hypopyon, immune cells in the anterior chamber of the eye and typically respond well to antiinflammatories (prednisolone acetate) and cycloplegic therapy.[11] AS-associated uveitis is thought to be mediated by inflammation or immune cells, as AS patients being treated with TNF-α inhibitors have a reduced risk for

developing uveitis.[81,82]

Peripheral arthritis will also develop in ~35% of AS patients.[51,52] Peripheral arthritis in AS is usually asymmetrical, monoarticular or oligoarticular, and effects joints of the lower extremities significantly more frequently than upper extremities.[83] Importantly, while pathology in the axial skeleton begins at a relatively young age (mean of 26) peripheral arthritis appears to affect AS patients at much later ages.[84]

It has also been reported that AS patients have an increased risk for colitis;[85] however, the prevalence of inflammatory bowel disease (Chron's disease or ulcerative colitis) in AS is 5-10%[85] and the prevalence in the general population is 4-5%,[86] so without a more detailed study this claim is difficult to verify. Moreover, primary/idiopathic AS and AS associated with inflammatory bowel disease have distinct genetic backgrounds[4,85] leading to the hypotheses that they are separate populations with genetic overlap.[4] While only 5-10% of AS patients develop clinical colitis,[85] up to 70% develop subclinical inflammation within the gut, as histology revealed evidence of chronic inflammatory damage to the colonic epithelium in 50-70% of AS patients.[50,87]

Current Treatment for AS

Back pain is the most common reason that patients seek medical attention for AS and the majority of therapeutics are targeted towards this symptom, using the Assessment of SpondyloArthritis international Society 20 improvement criteria (ASAS20) to assess overall severity of disease. The ASAS 20 is an index invented specifically for clinical trials in AS and is composed of responses to a series of questions broken into four domains that assess: (1) the patient's global impression of their health, (2) their pain, (3) their ability to daily tasks and function, and (4) their flexibility.[88,89] A successful drug must typically achieve at least a 20% improvement in at least 3 of these domains.[90] Importantly, the ASAS20 is a subjective measure of quality of life and does not include any direct assessment of spinal ankylosis nor other skeletal changes.[90] As a result, the drugs that have been approved for AS show significant efficacy at improving quality of life, lessening pain, and reducing inflammation, but show mixed results at halting progressive ankylosis in the spine.[70,71,91–93] Currently, at least three classes of therapeutics are approved for AS: non-steroidal anti-inflammatories (NSAIDs), TNF-α inhibitors, and IL-17 inhibitors.

Non-steroidal anti-inflammatories

Non-steroidal anti-inflammatories (NSAIDs) were the first approved medication for AS and remain the first-line therapy.[7] NSAIDs are very effective at reducing pain in most AS patients[94] and have been shown to slow, but not prevent, skeletal progression of the disease if taken daily based on the modified Stokes Ankylosing Spondylitis Spinal Score (mSASSS).[91,95] However, for unknown reasons, 40% of AS patients don't respond to NSAIDs and are placed on

other therapeutics.[94]

TNF-α inhibitors

For the 40% of AS patients that don't respond to NSAIDs, treatment with TNF-α inhibitors are recommended as a second line therapy.[7] Thirteen independent clinical trials have demonstrated that TNF-α inhibitors are effective at treating the pain associated with AS, with only 20-50% of AS patients failing to respond.[69,96–98] However, multiple studies have confirmed that TNF-α inhibitors do not stop or reduce the disease progression within the spine.[70,71,99,100] Additionally some patients develop diminishing responses to TNF-α inhibitors over time, and these drugs are contraindicated in patients with latent infections such as *Mycobacterium tuberculosis*, *Histoplasma capsulatum* and *Coccidioides immitis*.[101]

IL-17 inhibitors

Most recently, IL-17 inhibitors have been approved for AS.[92] Similar to TNF-α inhibitors, initial studies suggest that IL-17 inhibitors are effective at treating inflammation and back pain, but may fail to prevent spinal ankylosis and other structural changes.[93] Thus, while there are several drugs that improve pain and quality of life in many AS patients, it appears that there are no therapeutics that directly target the cause of spinal ankylosis and bony pathology.

Failed Therapeutics

In addition to the previously mentioned therapeutics, several drugs failed in clinical trials, including apremilast, tocilizumab, and anakinra.[102–105] These trials provide valuable insight into the pathogenesis of AS because each of these agents targets a specific immune pathway.

Anakinra (Kineret) is a recombinant soluble form of the interleukin 1 (IL-1) receptor that blocks IL-1 signaling. The clinical trial that used anakinra to treat AS patients justified the study based on results from experimental arthritis in mice and the observation that IL-1 is increased in AS.[105] The initial trial showed improvement in several functional indexes,[104] but a subsequent trial found no significant improvement in the Assessment of SpondyloArthritis international Society 20 (ASAS20), ASAS40, or ASAS70, despite being an open label trial.[105] This resulted in some debate about the efficacy of anakinra in AS, and accordingly the FDA found insufficient evidence to approve it for use in AS patients.

Apremilast (Otezla) is a small molecule inhibitor of phosphodiesterase type 4 (PDE4). PDE4 is essential for cyclic adenosine monophosphate (cAMP) signaling in immune cells and neurons and inhibition of the pathway has anti-inflammatory effects, although the exact molecular mechanisms are not fully understood.[106] Apremilast was tested on AS after successful trials in psoriasis and psoriac arthritis.[107] The treatment arm failed to reach significance over placebo for the primary endpoint, ASAS20.[108]

Tocilizumab (Sarilumab) is a blocking antibody of interleukin-6 receptor-α, and was justified for use in a clinical trial based on its success in rheumatoid arthritis and the observation that IL-6 is increased in the serum and joints of AS patients.[109] Tocilizumab also failed to reach its primary endpoint, an improved ASAS20.[109]

While these trials failed to demonstrate therapeutic efficacy in AS patients, they still provide important insight into the mechanism of AS, as they were large-scale human trials. The results of these trials suggests that IL-1, IL-6 and PDE4 are not essential to inflammation or back pain in AS. The results from the trials antagonizing IL-17 and TNF-α suggest that IL-17 and TNF-α are critical mediators of pain or inflammation in AS, but that neither is essential for progressive ankylosis. In fact, no drug to date has halted spinal ankylosis in all of the AS patients given the drug. There remains the possibility that there are multiple sub-populations within these AS cohorts, and that better stratification may increase the success of these therapies. However, these findings suggest that AS has multiple redundant mechanisms of causation, and/or that no currently tested drug directly targets the pathway responsible for ankylosis.

Genetics of AS

Further insight into the pathogenesis of AS comes from genetic studies. Over 50 years ago it was noticed that AS frequently occurred in families,[110] and the heritability of AS is formally estimated to be >90%.[111,112] The monozygotic twin of an AS patient has a 60% chance of developing AS,[113] first-degree relatives of AS patients have a 6-8% risk of developing AS,[113–115] and the recurrence risk of AS drops off rapidly in second and third degree relatives.[113] This pattern suggests that a small number of genes are responsible for the disorder,[113] and the identity of these genes has been determined by increasingly sophisticated genetic studies as outlined below.

MHC Genes

Over 40 years ago *HLA-B* became the first gene associated with AS.[22–24] It is frequently said that AS is associated with *HLA-B*27*, but this is not entirely true. While initial studies identified the association between AS and *HLA-B*27*, they were reliant on methods that could not distinguish between *HLA-B*27* subtypes and were conducted in populations in which the *HLA-B*27:05* subtype was overrepresented.[22–24] More recent studies have identified many HLA-B alleles associated with AS including *HLA-B*27:05*, *B*27:04, B*27:02, B*07:02, B*13:02, B*40:01, B*40:02, B*47:01, B*51:01 and B*57:01*.[14,116] Of the *HLA-B*27* subtypes, *HLA-B*27:05* and *HLA-B*27:02* have the strongest association with AS, with odds ratios of 62 and 43 respectively.[14] Importantly, not all *HLA-B*27* subtypes increase risk for developing AS, and *HLA-B*27:06* and *B*27:09* appear to be protective, with odds ratios of 0.128 and 0.53

respectively.[117–120] The global distribution of AS closely follows the distribution of these alleles. *HLA-B*27:05* and *HLA-B*27:02* are common in caucasian and Chinese populations where the prevalence of AS is high, and *HLA-B*27:06* and *B*27:09* are common in Sardinian and Southeast Asia, where prevalence of AS is low. This distinction is critical since whatever causes AS must be shared by all of the AS-associated *HLA-B* genes, but not by *HLA-B*27:06* and *HLA-B*27:09*.

Despite the strong association of *HLA-B*, it only accounts for 20-40% of the total heritability of AS in AS-susceptible populations, suggesting the involvement of other genes.[4,121] A very small portion (<1%) of the heritability not explained by *HLA-B* is explained by other MHC genes including *HLA-A*0201,*[28] *HLA-DR*,[14,29–31] and *HLA-DP*.[14,122]

ERAP1

After *HLA-B*, *ERAP1* (also known as *ARTS1*) has the strongest association of any gene with AS,[123] and accounts for 20-30% of the population attributable risk fraction.[17,25] Moreover epistatic gene-gene interactions exist between *ERAP1* and *HLA-B* further increasing the risk for developing AS,[13,14] suggesting that these two genes are interacting in the pathogenesis of the disease.[13,14] The 5 ERAP1 SNPs specifically associated with AS are rs27044, rs17482078, rs10050860, rs30187, rs2287987.[25] Each of these SNPs is located in the coding region of the *ERAP1* gene and is non-synonymous.[124] The rs27044 (Q730E), rs17482078 (R725Q), and rs30187 (K528R), are located in ERAP1's active site while rs10050860 (D575N) and rs2287987 (M349V) are located in structural regions of the protein.[125] These SNPs are in strong linkage

disequilibrium, suggesting that they may be interacting to cause disease. Interestingly, the same pattern of epistasis between *ERAP1* and *HLA* is observed in psoriasis[16] and Behçet's disease,[15,43] and suggests that ERAP1-HLA interactions may underlie these diseases as well. In addition to these diseases, *ERAP1* has been associated with multiple sclerosis[126] and preeclampsia.[127]

IL-23R

After *HLA-B* and *ERAP1*, the interleukin-23 receptor gene (*IL-23R*) has the strongest association with AS, and accounts for ~10% of the population attributable risk fraction.[25] *IL-23R* polymorphisms do not show epistasis with other AS genes, and *IL-23R* polymorphisms are not specific for AS, but shared by other inflammatory disorders including psoriasis,[18] psoriatic arthritis,[20,128] Crohn's disease,[129] and ulcerative colitis.[130] In addition to associations with *IL23R*, polymorphisms in the two genes that form the heterodimeric IL-23 cytokine (*IL-12B* and *IL-23A*) have been associated with other seronegative spondyloarthropathies.[18,40]

Other Genes

HLA, ERAP1, and IL23 are the only genes to reach genome wide significance in all large studies in populations prone to AS. Beyond *HLA*, *ERAP1*, and *IL-23R*, 32 other genes have been weakly associated with AS in multiple studies. Of these 32 genes, 22 have known functions in the immune system.[123] *HLA-B, ERAP1*, *ERAP2*,[131] *HLA-A*0201*,[28] and *NPEPPS*[28] are associated with AS and all play important roles in antigen presentation. Other AS-associated immune genes are important in the IL-17/Il-23 axis including *IL23R*,[25,27] *IL12B,*[132] and *PTGER4.*[13] In addition to

antigen presentation and the IL-23 pathway, several pro-inflammatory genes are also associated including *IL6R*,[27] *CARD8*,[26] and *TNFRSF1A/LTBR*.[13] Despite these published associations, only *HLA-B* and *ERAP1* have been reproduced across all populations studied.

Function of AS-associated Genes – Antigen Presentation

HLA-B,[13,14,22–24] ERAP1,[13,14] ERAP2,[131] HLA-A,[28] and NPEPPS[28] function in the antigen-presentation pathway, suggesting that antigen presentation may be critical to AS. Antigen presentation occurs in all nucleated cells and serves to communicate the identity and current status of these cells to the immune system. The majority of peptides presented on MHC are derived from endogenous proteins, and induce tolerance by identifying a cell as 'self' to CD8+ T-cells and NK cells. However, when a cell is infected by intracellular pathogens (viruses, parasites, or bacteria) peptides derived from the foreign proteins are presented and mark the cell as 'non-self' to CD8+ T-cells. The same process occurs in cancer cells, when fusion proteins, or other abnormal proteins generated by cancer cells are broken down and presented to CD8+ T-cells. When these 'non-self' peptides are presented on MHC-I any CD8+ T-cells harboring T cell receptors capable of recognizing them will eliminate the cells presenting them, then divide and provide lasting immunity. In this way antigen-presentation allows the immune system to monitor which proteins are present within a cell, and destroy cells that have become infected or malignant.

Antigen Presentation – Mechanism

Antigen presentation begins within the cytosol, where proteins are degraded by the proteasome. Most peptides generated by proteasomal degradation are too small for antigen presentation, both biochemically, as they would not fit in the peptide-binding groove of MHC-I,[133,134] and informatically, as they contain too little information to uniquely identify the protein of origin.[135] For this reason under certain circumstances, an alternative proteasome, the

immunoproteasome is assembled. The immunoproteasome generates longer peptides that are more suitable for antigen-presentation.[136] A small fraction of all peptides generated by either proteasome is selected by the transporter associated with antigen presentation 1 (TAP1) and transported into the endoplasmic reticulum (ER). TAP1 selects peptides in a length- and sequence- dependent manner and favors peptides 9-16 residues long.[137] In the ER, ERAP1 selects peptides 9-16 residues long, and rapidly trims them to 8-13 residues, then stops.[138] These peptides then bind to the peptide-binding groove in an HLA molecule and HLA associates with β2 microglobulin (β2m). The completed MHC-I molecule, consisting of HLA, peptide, and β2m is then transported to the cell surface, where it interacts with CD8+ T-cells and NK cells.

Antigen Presentation – Peptide Selection

The peptides that are presented on MHC-I are determined primarily by three factors, the HLA variant, the ERAP1 variants present within the ER, and the antigens available. *HLA* genes are among the the most polymorphic genes of the genome,[139,140] and they maintain diversity even in small, isolated populations.[140,141] These polymorphisms are primarily located in regions of the gene that correspond to the two α-helices that form the peptide-binding groove in HLA.[142] As a result, each HLA variant presents unique peptides from a given antigen. It has been hypothesized that this diversity at the molecular level provides herd-protection from pathogens, pushing divergent selection at the MHC-I locus, although it may also be due to a more complex evolutionary selection.[143,144] Whatever the evolutionary cause, each HLA allele presents unique peptides based on the sequence of amino acids within the α-helices that form its peptide-binding groove.

ERAP1 also has a large affect on which peptides are presented, although prior to our work the extent to which ERAP1 altered peptide selection was not fully appreciated. ERAP1 is a interferon-γ inducible, metalloprotease that takes peptide substrates of 9-16 aa in length and trims them to 8-13 aa products.[138,145] Early reports of ERAP1 assumed that it existed primarily to create immunogenic epitopes by trimming peptides for MHC-I and demonstrated that it facilitated the loading of a few specific peptides (such as SIINFEKL, CMV NP396 and CMV GP34) onto MHC-I.[146,147] However in subsequent reports we demonstrated that ERAP1 is capable of both creating and destroying immunogenic epitopes by trimming peptides to the appropriate length for MHC-I, or over-trimming peptides beyond the appropriate length for MHC-I (detailed in Chapter 2).[148] We demonstrated that by creating and destroying peptide epitopes for MCH-I, ERAP1 was capable of completely shifting the immunodominant T-cell response to a given antigen, and capable of having as much impact on antigen presentation as MHC-I.[148] We then demonstrated that polymorphisms in the *ERAP1* gene could have similar effects. Specifically the 5 AS-associated SNPs (s27044, rs17482078, rs10050860, rs30187, rs2287987)[25] appeared to have an additive effect, as the ERAP1-variant with all 5 high-risk AS-associated SNPs (ERAP1-High) was able to trim peptides at a faster rate and reduce the amount of MHC-I on the surface of cells.[149] The combined effect of these SNPs *in vivo* was similarly able to reduce the steady state level of MHC-I on the surface of cells, and also able to generate and remove immunodominant T-cell epitopes, demonstrating a functional consequence of these ERAP1 SNPs on antigen presentation and T-cell immunodominance (detailed in Chapter 3). While many other proteins are critical for antigen presentation, these genes are not polymorphic, and so do not contribute to differences in antigen presentation in the manner that *HLA* and *ERAP1* do.

Antigen Presentation – Immunologic Consequences

On the surface of the cell, MHC-I is recognized by both CD8+ T-cells and NK cells and these interactions serve complementary functions. CD8+ T-cells recognize abnormal 'non-self' peptides and kill cells presenting them, thereby eliminating infected cells and neoplasms.[150] To evade CD8+ T-cell killing, many pathogens and neoplasms disrupt the antigen-presentation pathway and eliminate MHC-I from the surface of cells. To compensate for this MHC-I evasion, NK cells recognize any cell with insufficient surface MHC-I and kill them.[151] In this way, CD8+T-cells and NK cells work together to eliminate cells with abnormal MHC-I.

CD8+ T-cells recognize the individual peptide-loaded on the MHC-I molecule using the T-cell receptor (TCR). Because there is no way for the immune system to predict which peptides will be relevant to fight infections over the life of the organism, TCRs are randomly-generated via recombination of somatic DNA. The random generation of TCRs accounts for the robustness of the immune response. Because randomly generated TCRs can potentially react to any peptide that could exist, they allow a rapid, focused immune response to novel pathogens.[150] When a T-cell recognizes a peptide with its TCR in an immunogenic environment, it begins rapidly dividing, producing multiple clonal populations of T-cells capable of circulating throughout the body and eliminating the infection or neoplasm.[152] Because the TCR was rearranged in somatic DNA, all of its daughter cells will share the same TCR and be able to recognize the same MHC-I-bound peptide.

This random recombination accounts for the robustness of the adaptive immune system, however it introduces two potential problems: (1) many of the randomly rearranged TCRs may be non-functional,[153,154] and (2) some of the randomly rearranged TCRs may target self-derived

peptides, and therefore induce auto-immunity.[155,156] To address these limitations, immature T-cells migrate from the bone marrow to the thymus, where they undergo both positive selection and negative selection. During positive selection, T-cells that made non-functional TCRs, incapable of recognizing MHC-I are eliminated.[153,154] During negative selection auto-reactive T-cells that recognize self-peptides are eliminated, leaving only T-cells with functional TCRs that don't recognize self-derived peptides.[155,156] This process is called central tolerance, and antigen-presentation plays a vital role. For instance, when certain peptides are not presented at sufficient levels during negative selection, auto-reactive T-cells escape negative selection and cause an auto-immune disease in the periphery. This exact process causes autoimmune polyendocrinopathy syndrome type 1 (APS1),[157] where dysfunction of autoimmune regulator (AIRE) results in tissue-specific peptides not being presented on MHC-I and thereby allows a subset of auto-reactive T-cells to escape negative selection and cause autoimmune disease.[158] APS1 provides an example of how changes in antigen presentation can cause autoimmunity via a failure of thymic selection.

Unlike T-cells, NK cells do not undergo recombination and instead recognize MHC-I via killer-cell immunoglobulin-like receptors (KIRs) in humans and Ly49 receptors in mice. Although these receptors are different in mice and humans they serve a homologous function. In both cases the engagement of the NK receptor (KIR or Ly49) results in inhibition of the NK cell, preventing NK cells from killing healthy, MHC-I expressing cells. Each NK receptor recognizes only a subset of HLA subtypes. For instance, KIR3DL2 binds HLA-A*03 and HLA-A*11, while KIR2DL1 binds all HLA-C variants that have a lysine at position 80.[159] KIRs and Ly49 molecules differ in how they recognize MHC-I. KIRs make direct contact with the MHC-I-

bound peptide and show peptide-specific activation, while Ly49 molecules do not directly bind the peptide.[160–162] For instance, KIR2DL2 makes direct contact with the GAVDPLLAL peptide at the 7th and 8th residues within HLA-Cw*03 and becomes activated in a peptide-specific manner.[163,164] In contrast, Ly49 receptors recognize MHC-I with an interaction between their carboxy-terminal lectin domains and the α1, α2, and α3 domains of MHC-I located under the peptide-binding platform. For this reason it was believed that Ly49 receptors did not recognize peptides, however recent studies have demonstrated that at least some Ly49 molecules respond differently when a peptide is loaded on MHC-I. For instance, Ly49A does not recognize the bound peptide directly, but a portion of MHC-I that changes conformation when peptide is bound.[165] Activation of the Ly49C receptor is also dependent on which peptides are bound to MHC-I with aliphatic residues as P2 and P3 facilitating activation.[166,167] The effect of ERAP1 on these interactions has not been studied, although the data presented in this thesis shows that ERAP1 can effect both the identity and overall quantity of peptides displayed on MHC-I, and therefore suggests that ERAP1 may alter NK activation via KIR and Ly49 receptors. In Chapter 4 we identify specific effects of ERAP1 and disease-associated ERAP1 variants on NK cell phenotype and function.

Function of AS-associated Genes – Non-canonical Functions of ERAP1

ERAP1 may have functions beyond its canonical role in antigen-presentation, although the mechanism behind these functions remains unknown. Early reports demonstrated that ERAP1 could mediate shedding of several immune receptors including interleukin-6 receptor alpha (IL-6Rα),[168] type I tumor necrosis factor receptor (TNFR1),[169] and IL-1 decoy receptor,[170] although the immunological consequences of these effects remain unknown.

We have also reported that ERAP1 alters early interactions in host-pathogen recognition. Specifically, without ERAP1, mice developed an exaggerated immune response to adenovirus, characterized by increased activation of NK and NKT cells and increased production of pro-inflammatory cytokines and chemokines including IL-6, IL-12, TNFα, and MCP-1.[171] It was not apparent if the increased NK cell activity was due to changes in cytokine levels, as ERAP1-deficient mice had more terminally differentiated and licensed NK cells, suggesting that ERAP1 may impact the development and maintenance of NK cell populations.[171] Again, the mechanism behind these functions of ERAP1 remains unknown.

Another non-canonical function of ERAP1, is its ability to act outside the cell. ERAP1 is secreted in response to IFNγ,[172,173] and once secreted ERAP1 can generate nitric oxide,[174] enhance macrophage phagocytosis,[173] and stimulate the production of IL-18 and IL-1β.[175] Furthermore, it appears that at least some of these effects are influenced by the presence of AS-associated SNPs in ERAP1, as we demonstrated that the addition of extracellular ERAP1 variants with the rs30187 (K528R) or rs27044 (Q730E) SNP increased the production of IL-1β by human peripheral blood mononuclear cells (hPBMCs) more than the addition of ERAP1 variants lacking those SNPs.[175]

Each of these functions appear to require the aminopeptidase activity of ERAP1, but may be independent of antigen presentation. For instance, the production of nitric oxide by ERAP1 was tied to its ability to produce free arginine (a substrate in nitric oxide synthesis) by removing amino-terminal arginine residues from extracellular peptides.[174] Future experiments to define the specific mechanisms and outcomes of these non-canonical roles of ERAP1 will contribute to our understanding of how ERAP1 is promoting disease.

Function of AS-associated Genes – IL-23R and IL-17/23 Axis

The association of AS with *IL-23R* suggest that the IL-23 pathway may contribute to the pathogenesis of AS. IL-23 is a heterodimeric cytokine composed of IL-12p40 and IL-23p19 and is recognized by a heterodimeric cytokine receptor composed of IL-12R1β and IL23R.[176] Because the IL-23 shares the IL-12p40 subunit with IL-12, early studies falsely attributed effects of IL-23 to IL-12.[177] This has since been corrected, and the function of IL-23 as a key pro-inflammatory cytokine has been recognized.[178] In addition to its pro-inflammatory role, IL-23 induces Th17 cells to secrete IL-17 and promotes epithelial immune defense.[179] There are 6 subtypes of IL-17 (IL-17A-IL-17F) and each appears to play a specialized role in epithelial immune defense. For instance different subsets of Th17 cells were induced by *Staphylococcus aureus* and *Candida albicans* and each orchestrated specific epithelial immune responses to protect against these pathogens.[180] In general all IL-17 subsets promotes epithelial defense by: (1) increasing secretion of cytokines such as IL-6 and TNF-α, (2) increasing production of anti-microbial peptides such as β-defensins, and (3) strengthening tight junctions by increasing claudin expression.[181,182]

Beyond its role in epithelial defense, IL-17 and IL-23 have been implicated in the pathogenesis of several of the seronegative spondyloarthropathies. In psoriasis; dendritic cells,[183,184] keratinocytes,[185] mast cells,[186] and neutrophils[186] produce IL-23 that stimulates the pathogenic production of IL17 within psoriatic plaques.[187] Increased levels of IL-17 are also observed in the serum of patients with Behçet's disease[188,189] and AS.[190] How IL-17 and IL-23 are contributing to AS in humans remains unclear, however, mice injected with large doses of IL-23

developed enthesitis, an inflammation at the attachment of soft tissue to bone.[191] Enthesitis is a symptom shared by several of the seronegative spondyloarthropathies and the observation that it can be induced by IL-23 may explain the role of IL-23 in these diseases. The role of HLA-B and ERAP1 in this pathway remain to be elucidated. Furthermore, the IL-23 induction model of AS fails to explain why there is an increased production of IL-23 in AS, or why only the axial skeleton is effected, as the mice that received IL-23 had systemic enthesitis that was most prominent in their paws.[191]

Animal Models of Ankylosing Spondylitis

The etiology of AS is unknown, so putative animal models of AS must be analyzed with emphasis placed on the differences between the models and AS, rather than on their similarities. This is crucial, as there are potentially a very large number of animal models that mimic some phenotypic aspects of AS, but only a few of these will be truly homologous, and share a mechanism with the disease. With this caveat in mind, we examine and critique the various animal models that have been used to study AS.

HLA-B*27 Rat Model of Ankylosing Spondylitis

One of the first animal models of AS was the HLA-B27 rat model, produced by inserting 150 copies of the *HLA-B*27:05* gene and 90 copies of the human *β2m* gene into the Lewis rat.[192] These animals developed a phenotype that was described as similar to AS and have subsequently been used in a number of high-impact studies that are widely used to describe the pathology of AS. An example of this is the frequent assertion that CD8 T-cells are not required in the pathogenesis of AS[193,194] because they are dispensable for the phenotype in the HLA-B*27 rats.[195,196]

As a result, this model has been critical to the development of the field, however there are many troubling aspects of this model. Firstly, the model does not consist of one copy of *HLA-B*2705* and one copy of human *β2m* (*hβ2m*). That rat was constructed and reported in the same manuscript to have no phenotype.[192] The authors then inserted various copy numbers of the *HLA-B*2705* gene and the human β2m gene into the rats, and assayed for a phenotype. The following combinations of *HLA-B*27* and *hβ2m* failed to produce a phenotype: 1+0, 1+1, 6+6, 7+7, 20+15,

and 55+66. Only the combination of 150 copies of *HLA-B*27* and 90 copies of *hβ2m* reproducibility developed a phenotype. The proposed reason for increasing the copy number was to increase surface expression to a level that would be sufficient to trigger the disease, however the rat with 55 copies of HLA-B*27 and 66 copies of hβ2m actually had higher expression of both HLA-B*27 and hβ2m on the surface of cells, but did not develop the phenotype.[192] In the strain with 150 copies of HLA-B*27 and 90 copies of hβ2m the phenotype consisted of diarrhea in 100% of animals, peripheral arthritis in 41% of animals, and a neurologic syndrome in the majority of the animals (% not specified).[192] Subsequent studies have determined that in addition to those symptoms, ~30-50% of the HLA-B*27 rats develop a destructive spondylitis, with inflammatory destruction of ligaments and discs.[197]

Upon critical review, this phenotype more closely resembles β2m amyloidosis, a human disease caused by excessive β2m. β2m amyloidosis appears in patients undergoing long-term hemodialysis or continuous ambulatory peritoneal dialysis where a diminished capacity of renal catabolism increases production of β2m, and kidney failure decreases the elimination of β2m.[198] When the serum concentration of β2m is ~10-fold above normal, it begins to precipitate out of the blood and polymerize in the joints, activating focal inflammation and inflammatory bone damage.[199,200] This is highly relevant as the HLA-B*27 rats that developed the arthritic phenotype had 90 copies of *hβ2m*. Both the HLA-B*27 rats and humans with β2m amyloidosis develop gastrointestinal pathology,[201] peripheral arthritis dominated by erosions, and destructive spondyloarthropathy characterized by destruction of the paravertebral ligaments and intervertebral discs.[197,202,203] The destructive pattern observed in the spine of HLA-B*27 rats and β2m amyloidosis patients is not the same as observed in AS, where in the latter the ligaments

calcify, rather than get destroyed. Beyond phenotypic similarities there is further evidence suggesting that the disease developed by HLA-B*27 rats may be mediated by excessive β2m. Some of this evidence comes from a study that increased the copy number of *hβ2m* further by crossing the HLA-B*27 rats with another strain of rats that had a higher copy number of *hβ2m* within their genome. This study demonstrated that increasing the copy number of hβ2m in the rats increased the frequency of arthritis observed in the rats, suggesting that the excessive hβ2m may be causing the phenotype, rather than *HLA-B*27*.[204] Further evidence suggesting this possibility comes from the initial report describing the animals. Rats with 55 copies of HLA-B*27 and 60 copies of hβ2m expressed a higher amount of HLA-B*27 on their cell surface compared to (150:90) rats, but did not develop a phenotype.[192] Therefore, the phenotype in this model correlates with β2m copy number, but not with HLA-B*27 surface expression. Finally, in patients with β2m amyloidosis, β2m amyloid may deposit in affected joints and if found confirms the diagnosis.[198] These same amyloid deposits have been observed in the joints of HLA-B*27 rats.[205] These limitations do not rule out the HLA-B*27 rat model of AS or rule out observations made in the model from also contributing to the pathogenesis of AS, however they do suggest that results obtained in the HLA-B*27 rat must be interpreted very carefully.

HLA-B*27 Mouse Model of Ankylosing Spondylitis

HLA-B*27 mice have also been used to model AS.[206,207] These mice were constructed by inserting one copy of *HLA-B*27* and *hβ2m* in a single cassette and then knocking-out the endogenous murine *β2m*. Removal of β2m, removed all murine MHC-I from the surface of cells in these mice and allowed only HLA-B*27 to be presented.[207] This model was reported to

develop spontaneous arthritis in their hind feet that was only triggered when they were transferred into a non-specific pathogen free (non-SPF) environment. Similar to the HLA-B*27 rats, they primarily develop a peripheral arthritis, with limited or secondary spinal involvement.

It was subsequently observed that any disruption of the MHC-I pathway was enough to mimic this phenotype.[208] Loss of either *β2m* or *TAP1* prevents almost all MHC-I expression on the surface of cells and merely knocking out one of these genes was enough to cause spontaneous arthritis in mice transferred to non-SPF environments.[208] These results suggest that the phenotype in the HLA-B*27 mice was due to loss of *β2m*, rather than the addition of *HLA-B*27:05.* Because it was assumed that HLA-B*27:05 must have gained a pathogenic function, the observation that *HLA-B*27:05* was not essential in this model led to the conclusion that the disease in HLA-B*27 mice was not relevant to AS.[208] However, an alternative explanation would be that loss of normal MHC-I function causes an arthropathy and addition of *HLA-B*27:05* fails to rescue it. If AS-associated *HLA-B* genes like *HLA-B*27:05* have lost a critical function, rather than gaining one, this model may mimic components of the disease. This may be the case, as it appears that $\beta 2m^{-/-}$ mice transgenically expressing other human HLA molecules do not develop arthritis, however it may have been overlooked, as there is no evidence that an advanced skeletal screening of these animals has been performed.[209,210]

Induced Arthritis

When BALB/c mice are immunized with an emulsion of Freund's complete adjuvant and type II collagen they develop prominent arthritis in their feet. While this collagen induced arthritis (CIA) model has been used to study AS,[191] it is primarily used to study rheumatoid

arthritis (RA) because the phenotype closely resembles RA and not AS.[211] Similar to RA, affected joints in the feet develop mononuclear cell infiltration, synovial hyperplasia, and cartilage degradation.[211] Genetically this model also resembles RA and not AS, as predisposition to develop arthritis corresponds to MHC-II genes and not MHC-I genes.[212,213]

A similar model exists where female BALB/c mice are immunized with fetal human cartilage proteoglycan, rather than type II collagen. Similar to the CIA model, the proteoglycan-induced arthritis (PIA) model predominantly affects the feet, and affected joints demonstrated mononuclear cell infiltration, degradation of cartilage and bone, and synovial hyperplasia.[214] If repeatedly immunized, up to 60% of mice will develop inflammation in their tail vertebrae as well, which has ledmultiple groups to use PIA as a model for AS.[215–217] Unlike AS, PIA mice develop destructive changes within intervertebral joints and excess bone is rarely observed.[217] Furthermore involvement of vertebrae only was observed in 60% of mice and only after repeated immunization, while peripheral arthritis develops in 100% of mice after a single immunization. The opposite pattern is observed in AS, where peripheral arthritis is only present in 35% of cases and occurs years after spinal ankylosis.[51] While the possibility exists that these changes are due to differences between the murine and human physiology or anatomy, the possibility also exists that models inducing autoimmunity with Freund's complete adjuvant are more analogous to the autoimmunity triggered in humans by Freund's complete adjuvant.[218]

Hypotheses of the Pathogenesis of AS

Many hypotheses have been proposed to explain the unique pathogenesis of AS. The majority of them assume that HLA-B*27 has gained some novel pathological function that causes the disease.[219–221] However, these theories must be able to explain why only 1-5% of people with HLA-B*27 develop AS,[114] and why other HLA alleles are associated with developing AS.[14] The alternative hypothesis, that HLA-B*27 has lost a critical function that leaves AS patients vulnerable to develop the condition, has been explored substantially less.

Antigen Presentation Hypothesis

More than 40 years ago, the strong association of *HLA-B* with AS led to the hypothesis that antigen presentation may be involved in the pathogenesis of AS.[22–24] This theory has been supported by the subsequent observation of epistasis between *ERAP1* and *MHC-I* genes[13,14] as well as the identification of other antigen-presentation genes (*ERAP2*, *HLA-A*, and *NPEPPS*) that are associated with the disease.[28,131] Furthermore the only known functional difference between all HLA-B variants associated with AS and all HLA-B variants that are not associated with AS, is antigen presentation. This is illustrated best by *HLA-B*27:06* and *HLA-B*27:09*. Neither of these MHC-I molecules is associated with developing AS, but they differ from AS-associated HLA-B*27 variants only at 1-2 amino acids located at the peptide-binding groove.[117,118] These non-synonymous animo acid substitutions impact which peptides are loaded, suggesting that they may impact AS via antigen presentation, however it remains possible that these substitutions impact another unknown function of HLA.

Our work has further supported the antigen presentation hypothesis by demonstrating the

effect of ERAP1 on antigen presentation. Before our work, the impact of ERAP1 and AS-associated ERAP1 SNPs on antigen presentation were not fully understood. We demonstrated that ERAP1 completely reshapes the hierarchy of antigens presented and the subsequent T cell response (Chapter 2).[148] We then demonstrated that disease-associated ERAP1 variants had different enzymatic activities,[149] and that those activities had major impacts on antigen presentation in cells[149] and mice (Chapter 3&4). These findings build upon the genetic studies that showed interaction between *HLA* and *ERAP1* genes by providing biological evidence demonstrating interaction between HLA and ERAP1 proteins.

For all of these reasons, the theory that antigen presentation causes AS has been the predominant hypothesis in the field, although there are multiple ways that antigen presentation may cause the disease. There are only five basic mechanisms that are possible if antigen presentation is responsible for AS. 1) AS-associated combinations of MHC-I and ERAP1 facilitate the presentation of certain pathogenic peptides. 2) AS-associated combinations of MHC-I and ERAP1 prevent the presentation of certain protective, tolerance-inducing peptides. 3) AS-associated combinations of MHC-I and ERAP1 decrease the overall level of MHC-I presented within certain cells. 4) AS-associated combinations of MHC-I and ERAP1 increase the overall level of MHC-I presented within certain cells. 5) A combination of the above.

Mechanism 1 has been previously referred to as the arthritogenic peptide hypothesis,[222] and is the most widely accepted hypothesis in the medical community.[223] This hypothesis is supported by the observation that many HLA-B*27-positive reactive arthritis patients share the same T-cell receptors, suggesting that they may be reacting to the same HLA-B*27-restricted epitopes.[224] Because of the belief in this hypothesis, a great deal of effort has gone into

discovering the arthritogenic peptides by identifying proteins that are unique to the axial skeleton and determining if they are immunogenic.[225] However, even if the arthritogenic peptide hypothesis is correct, there is not necessarily a single peptide (or a small group of peptides) that causes the disease, because the disease could be triggered by different peptides in different patients. For instance, in autoimmune polyendocrinopathy syndrome type 1 (APS1) autoimmune disease is caused when tissue-specific peptides are presented in peripheral tissues, but not the thymus. This allows auto-reactive CD8 T-cells to escape negative selection and cause autoimmune disease.[157] This disease demonstrates that it may not be specific peptides, but a miss-matching of peptides presented between tolerance-inducing tissues (such as the thymus or peripheral tolerance-inducing cells) and the tissues targeted by autoimmune attack. Therefore, the search for a single arthritogenic peptide may be impossible and a more sophisticated approach that considers patterns of peptide presentation across multiple tissues may be required.

Mechanisms 3 and 4 have been explored less, however there is increasing evidence that mechanism 3—a failure of normal antigen presentation—may play a role in the pathogenesis of disease. A recent study searching for an arthritogenic peptides failed to identify specific peptides shared by AS patients, but did identity a global decrease in overall antigen presentation mediated by AS-associated HLA-B*27 variants.[222] It is also known that many of the forms of HLA-B associated with AS are deficient in antigen presentation. For instance multiple disease-associated HLA-B*27 molecules form homodimers that are deficient in antigen presentation,[226] and others fold very slowly in the ER and present peptide on the cell surface at a globally reduced rate.[220] Our work builds upon this hypothesis by demonstrating that the ERAP1 variant with all 5 AS-associated high-risk SNPs over-trims peptides due to increased enzymatic activity (Chapter 3),

and decreases the amount of MHC-I presentation in vitro (Chapter 4) and in vivo (Chapter 5). These data suggest that AS-associated ERAP1 variants may be over-trimming peptides leading to a reduction of MHC-I antigen presentation in AS patients, globally or in specific tissues.

In summary, there is convincing evidence from genetic studies that implicates antigen presentation in the pathogenesis of AS and there is now biological evidence to support the interaction of HLA and ERAP1 in antigen presentation. However, prior to the findings presented in Chapter 6, no connection between antigen presentation and bone homeostasis had been shown, and even with this important discovery the exact mechanism by which antigen presentation impacts the skeletal system remains elusive.

Homodimer Hypothesis

An alternative hypothesis stems from the observation that certain forms of HLA-B*27 are capable of forming β2m-free homodimers.[226] When MHC-I folds properly, it associates with a peptide and β2m, then is transported to the surface of the cell, however certain forms of HLA-B*27 are able to escape to the cell surface without β2m by forming a homodimers. These B*27 homodimers can then activate certain immune receptors such as KIR3DL2[227] and potentially trigger a variety of downstream effects on the immune system.[228]

While this theory is innovative and HLA-B*27 homodimers may contribute in some way to AS, there is mounting evidence that they are not a necessary component of the disease. First, not all forms of *HLA* associated with AS form homodimers (including *B*07:02*, *B*13:02*, *B*40:01*, *B*40:02*, *B*47:01*, *B*51:01* and *B*57:01*). Second, at least one MHC-I allele that is protective for AS (*HLA-B*27:06*) also forms homodimers but decreases the odds of developing

the disease.[228] Conversely, *HLA-B*15*, *HLA-B*38*, *HLA-B*39* and *HLA-B*75* also have the cysteine residue at position 67 that allows HLA-B*27 to form homodimers, but they are not associated with AS. Furthermore, multiple studies have compared HLA-B*27+ AS patients to HLA-B*27+ healthy controls and found no significant difference in the amount of HLA-B*27 homodimers.[229,230] For these reasons it appears that homodimers are not essential for the development of AS, however they may still play a role in promoting or worsening the disease.

Unfolded Protein Response Hypothesis

Another unique property of certain HLA-B*27 molecules is that they take an abnormally long amount of time to properly fold within the ER.[231] This observation led to the hypothesis that they may be triggering the unfolded protein response (UPR), and subsequently causing the secretion of cytokines that lead to pathology.[232]

Similar to the homodimer theory of AS, this theory does not match the known genetic risks for AS. There is no evidence that many of the AS-associated HLA molecules (including *B*07:02*, *B*13:02*, *B*40:01*, *B*40:02*, *B*47:01*, *B*51:01* and *B*57:01*) activate the UPR, as they have ordinary folding kinetics, while *HLA-B*27:06* and *HLA-B*27:09* have abnormal folding kinetics, but do not increase risk for AS.[117,118] Furthermore, no significant difference in activation of the UPR was observed between HLA-B*27+ AS patients or healthy HLA-B*27+ controls in multiple studies.[229,233,234]

IL23/IL17 Axis Hypothesis

The *IL-23R* gene has the third strongest association of any gene with AS[27], and an increased level of IL-17 and IL-23 has been observed in the serum of AS patients compared to healthy controls.[190]These findings implicate the IL-23/IL-17 axis as a contributing factor in AS, but the strongest evidence for the role of the IL-23/IL-17 axis in AS comes from the success of secukimab in a clinical trial.[92,93] In this trial, secukimab had a similar effect as TNF-α inhibitors, managing the pain and inflammation of AS without halting the spinal ankylosis.[92,93,100] It therefore appears that similar to TNF-α, IL-17 is not essential for developing spinal ankylosis, and plays a supporting role in bony pathology.

The nature of this supporting role may have been explained by recent experiments that demonstrate injecting a high amount of IL-23 into mice triggers enthesitis, inflammation at the attachments of soft tissues to bones.[191] IL-23 activated these enthesis-resident T-cells and triggered localized inflammation at the entheses throughout the organism, most prominently in the feet. This remarkable finding may explain the enthesitis shared by AS and the other seronegative spondyloarthropathies, and may explain the association of IL-23R with these diseases (summarized in Chapter 1 Table 1). However, it can not explain why the inflammation in AS is predominantly localized within the axial skeleton because the enthesitis in IL-23-exposed mice developed throughout the body and was most prominent in the feet.[191] This theory also fails to explain the role of AS-associated HLA molecules (such as B*27) and ERAP1. Therefore, while this research explains how IL-23 and IL-17 contribute to AS and the other seronegative spondyloarthropathies, it does not explain why bones of the axial skeleton fuse in AS or how HLA-B and ERAP1 contribute to the disease.

Microbiota Hypothesis

Despite the advances in understanding the genetics of AS, it is still unknown why more than 90% of cases are positive *HLA-B*27*, but only a 1-5% of *HLA-B*27* carriers develop AS.[4] Furthermore, while AS has been estimated to be 90% heritable,[111,123] all known AS-associated genes can only explain 24.4% of the risk.[28] This suggests that a shared environmental exposure may be playing a role.[123] Whatever this exposure is, it must be ubiquitous, as there are no reported outbreaks of AS, and the distribution of AS globally follows patterns of genetic susceptibility, rather than cultural or ecological boarders. This has led to a 50 year search for a ubiquitous environmental agent that may trigger AS in genetically prone individuals. While multiple infectious pathogens including *Klebsiella pneumoniae*[235] and *Chlamydia trachomatis*[236] have been investigated, a definitive environmental trigger has not been identified.

Recent findings have converged on the theory that this environmental trigger may be changes in the intestinal microbiome. After *HLA-B* and *ERAP1*, *IL-23R* is the gene with the strongest association with AS,[17,27] and plays an important role in the gut mucosa.[237,238] Patients who have a breakdown of this barrier, such as IBD patients, are 3 times more likely to develop AS[239] and up to 70% of AS patients develop subclinical inflammation in their gut which damages the epithelium.[232,240,241] Furthermore it has recently been shown that the addition of HLA-B*27:05 modifies the microbial communities in the gut of rats[242] and that AS

patients suffer from intestinal dysbiosis with a unique signature in the gut microbiome.[243] Still, it remains unclear if the inflammation in AS causes the dysbiosis, or if the dysbiosis causes the skeletal inflammation and damage.

While all of this evidence hints at the possibility that dysbiosis is a feature of AS, none of it demonstrates that dysbiosis causes AS. In fact, it may be more reasonable to assume that AS causes dysbiosis rather than to assume that dysbiosis causes AS. The systemic increase in pro-inflammatory cytokines triggered by AS could cause dysbiosis by altering the immune responses and endothelial permeability in the gut. The only evidence that the microbiome may impact arthritis came from the murine HLA-B*27 model of AS. In that model HLA-B*27/$\beta 2m^{-/-}$ mice only developed arthritis when transferred to a non-SPF facility.[207] The same spontaneous arthritis was subsequently observed in other mice deficient in MHC-I presentation ($\beta 2m^{-/-}$ mice and $TAP1^{-/-}$ mice) when they were transferred to a non-SPF facility.[208] While these findings may have occurred for a large number of reasons, one reason is that disruption of the antigen presentation pathway made the animals susceptible to pathogenic dysbiosis. This theory is supported by the recent observation that gut bacteria effect spinal inflammation and the association of expansion of specific genera of gut bacteria such as *Prevotella* with arthritis.[244,245] Still, there is no direct evidence for a causative role of microbiota in AS.

Conclusion

With a heritability of ~90%,[111] AS was one of the complex genetic disorders that was proposed to be solved by the revolution of genome-wide association studies.[246] However after many GWAS in AS patients,[13,14,27,247] all known genes only account for 24.4% of the heritable

risk.[28] While some of this missing heritability may be explained by the epistatic interaction of HLA-B and ERAP1,[248] the rest of this missing heritability may never be discovered by associative genetic studies. For this reason it is critical to investigate the functional interactions of GWAS-identified genes in biological systems. With that goal, we begin with the known association of antigen presentation genes *ERAP1* and *HLA* in AS, and investigate the biological function of ERAP1 in antigen-presentation and bone homeostasis. In Chapter 1 we define the role of ERAP1 in antigen presentation by demonstrating that it is required to create and destroy epitopes, thereby completely altering the immunodominant T-cell response. In Chapter 2 we determined that polymorphisms in human ERAP1 could mediate similar changes in a cell-based transfection system. In Chapter 3 we carried these discoveries into a murine model and demonstrated that mice transgenic for human ERAP1 variants presented unique sets of peptides and had global changes in MHC-I expression that impacted immune function, as well as other phenotypic changes. Finally in chapter 4 we defined a role for ERAP1 and antigen presentation in bone homeostasis. Together this work builds upon the current understanding of antigen presentation, osteoimmunology, and the pathogenesis of AS and provides new avenues of investigation into the pathogenesis of AS.

Chapter 2

ERAP1 functions override the intrinsic selection of specific antigens as immunodominant peptides, thereby altering the potency of antigen-specific cytolytic and effector memory T-cell responses

This chapter is adapted from an article published in International Immunology, Volume 26, Issue 12, Pp. 685-695 August 2, 2014.

Authors: David P. W. Rastall, Yasser A. Aldhamen, Sergey S. Seregin, Sarah Godbehere and Andrea Amalfitano

Introduction

After *HLA-B27*, DNA variations in the *ERAP1* gene have the strongest association with AS.[14] Because both genes are critical to antigen presentation, we investigated the impact that ERAP1 has on antigen presentation and adaptive immunity using ERAP1 deficient mice. ERAP1 has been identified as a central player in the process of antigen trimming and loading onto MHC class I molecules (MHC-I), and therefore adaptive immunity.[146,249,250] ERAP1 is an IFN-γ-inducible, M1 zinc-binding, metalloaminopeptidase of the oxytocinase subfamily.[251] ERAP1 is the only peptidase found in the ER of mice, and one of two highly homologous aminopeptidases (ERAP1 and ERAP2) found in the ER of humans.[252] The N-terminal moiety of ERAP1 binds and trims the N-terminal residues from peptides present within the ER in a length- and sequence-dependent manner that results in the generation of epitopes that are 8–10 amino acids long for loading onto MHC-I.[138,145,251,253–255] Because of this function, loss of ERAP1 activity can result in an increase in the average length of all peptides found on MHC-I molecules.[256] In addition to changing the length of peptides being presented to T cells by MHC-I molecules, ERAP1 functions are known to facilitate the loading of a few specific peptides (such as SIINFEKL, CMV NP396 and CMV GP34) onto MHC-I.[146,147] Additionally, and possibly as a result, peptide-MHC-I complexes generated in the absence of ERAP1 on average have a shorter half-life on the cell surface, resulting in a decreased number of peptide-MHC-I complexes on ERAP1-deficient cells.[257,258] Furthermore, these changes in MHC-I-loaded peptides can impact a cell's immunologic identity, since induced absence of ERAP1 can cause a cell to become immunologically recognized as non-self by otherwise syngenic T cells.[257]

Out of the thousands of potential epitopes present in a respective protein, only a few are maximally recognized by the cells of the adaptive immune system. This phenomenon is referred to as immunodominance and is critical for understanding and manipulating T-cell-mediated immunity.[259] In previous studies of ERAP1, known immunodominant peptides were tested and found to generate reduced CD8+ T-cell responses in the absence of ERAP1 functions, indirectly suggesting that ERAP1 may play a role in immunodominance.[147] However, ERAP1 functions also modulate the secretion of certain cytokines during innate immune responses, independent of its canonical role as an antigen-processing molecule.[171] These latter observations complicate the interpretation of prior results that relied on cytokine secretion profiles, or reporter cell lines to measure the potency of T-cell epitopes in the presence or absence of ERAP1 functionality.[146,250,257,260] In light of these issues, we wished to determine if immunodominance occurred in the absence of ERAP1 and to examine the extent to which immunodominance might be altered by loss of ERAP1 functions. To test these hypotheses, we queried the role that ERAP1 might have in a mouse model. Specifically, after vaccination of wild-type (WT) or ERAP1-deficient animals with a model antigen, the immunodominance profile of the antigen was assessed. We measured antigen-specific adaptive immune responses after vaccination with an adenovirus serotype 5 (Ad5) vector expressing the non-enzymatic portion of the toxin A (TA) protein from *Clostridium difficile* (Ad5-TA).[261] Surprisingly, vaccination of ERAP1$^{-/-}$ mice did not merely change the amount that certain peptides contributed to immunodominance, but resulted in an entirely new and distinct set of TA-derived epitopes becoming immunodominant. These changes in immunodominance selection were profound, as none of the immunodominant

TA-derived epitopes, respectively, identified in Ad5-TA-vaccinated WT or ERAP$^{-/-}$ mice were shared between the two strains of mice. As a result, these ERAP1-mediated changes on immunodominance also had profound effects on T-cell biology, including the generation of functionally distinct CTL populations and modulating the quantity of T-cell effector memory populations present in the vaccinated animals.

Results

ERAP1 overrides inherent immunodominant peptide selection to completely shift which antigen-derived peptides are identified as immunodominant by the adaptive immune system

ERAP1 facilitates efficient MHC-I presentation of certain epitopes, such as SIINFEKL[146,147] and the HF10 peptide from *Toxoplasma gondii*, the latter being required for T-cell-mediated immune clearance of the organism.[262] However, those studies could not determine if loss of ERAP1 eradicates the ability of the adaptive immune system to generate an alternative hierarchy of immunodominant epitopes to a specific antigen. To specifically determine if and how ERAP1 affects the breadth of T-cell clonal responses to a specific antigen, we immunized mice with an adenovirus-based vaccine expressing the *C. difficile*-derived antigen, TA (Ad-TA) and studied the breadth of the T-cell responses to this model antigen. Specifically, WT or ERAP1$^{-/-}$ mice were vaccinated with Ad-TA, and TA-specific T-cell responses were evaluated at 14 days post-injection (dpi). Splenocytes from the vaccinated mice were exposed to a 15-mer overlapping peptide library (peptides overlapping by five amino acids) that spanned the entire TA protein expressed by Ad-TA. T-cell responses to these peptides were quantified by IFN-γ ELISpot assay; 15-mer peptides were selected because peptides of this length are suitable substrates for both TAP and ERAP1, yet are longer than any classic MHC-I substrates, and therefore require processing prior to MHC-I loading. Among the 84 15-mer peptides that we interrogated, not a single peptide responded as immunodominant in both WT and ERAP1$^{-/-}$ mice (Figure 1). Rather, we identified a set of ERAP1-dependent TA-derived immunodominant peptides only responsive in Ad-TA-vaccinated WT mice (the WT IDTAPs) and a set of ERAP1-independent TA-derived immunodominant peptides only responsive in Ad-TA-vaccinated

ERAP1$^{-/-}$ mice (the ERAP1$^{-/-}$ IDTAPs) (Figure 1). Together, these results demonstrate that the presence of ERAP1 completely shifts the repertoire of antigen-derived peptides ultimately identified as immunodominant by the adaptive immune system.

It is also worth noting that of the ERAP1$^{-/-}$ IDTAPs, FAPANTDANNIEGQA and ANNIEGQAIRYQNRF were effectively immunologically silent in Ad5-TA-immunized WT mice, generating only 2.4 and 4 spot-forming cells per 10^6 splenocytes when the splenocytes used in these assays were derived from Ad5-TA-immunized WT mice. As previous studies relied on using peptides that were identified as potent or immunodominant peptides only in WT animals prior to their study in ERAP1$^{-/-}$ mice, to our knowledge the ERAP1$^{-/-}$ IDTAPs identified in this study are the first immunodominant antigen-derived sequences to be specifically identified as becoming immunodominant in the absence of ERAP1 activity.

Figure 1: ERAP1 reshapes the immunodominant focus by the creation and destruction of epitopes.

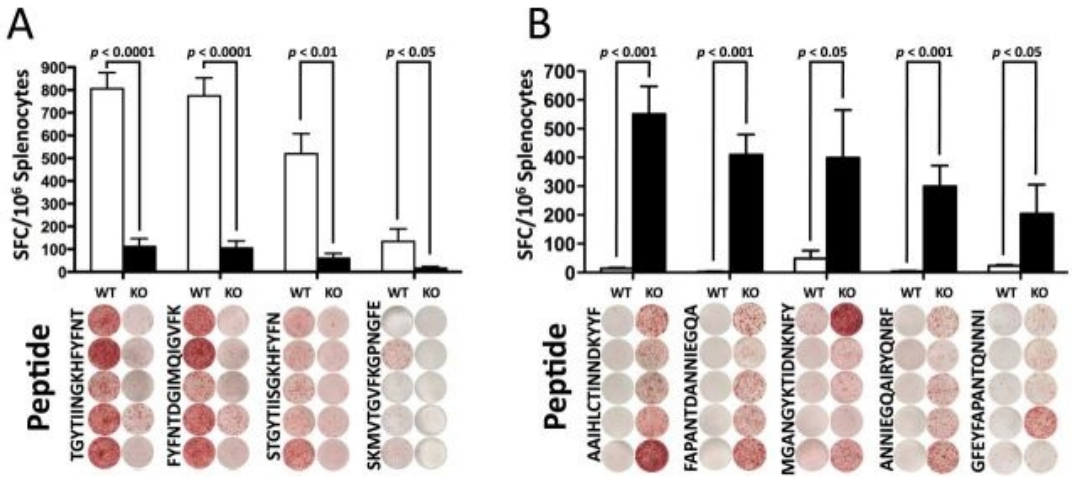

C56BL/6 mice (n = 5) or ERAP1$^{-/-}$ mice (n = 5) were immunized I.M. in the tibialis anterior with Ad5-*Clostridium difficile*-TA as described in Methods. At day 14, mice were sacrificed and splenocytes were harvested and stimulated with 2 μg per well of the listed 15-mer peptides. Splenocytes were then analyzed for IFN-γ production using IFN-γ ELISpot. From the 84 peptide library, the peptides that generated a strong response (100 or more spots) and showed an average of at least 100 less spots in the other strain of mouse were selected and repeated. (A) Peptides that had a very high response in WT mice compared with ERAP1$^{-/-}$ mice. (B) Peptides that had a very high response in ERAP1$^{-/-}$ mice compared with WT mice. Bars represent the mean number of spot-forming cells per 10^6 splenocytes ± SEM. Below are representative wells. All wells are shown in the order they appeared on the plate and all paired sets of wells are from the same plate. A P value < 0.05 was statistically significant. The figure is representative of two separate experiments.

ERAP1 destroys otherwise immunodominant epitopes via linear N-terminal trimming

It has been observed that certain epitopes are presented at a higher frequency in cells without ERAP1.[249] As it is also known that immunodominant epitopes are capable of suppressing the selection of sub-dominant epitopes,[259,263,264] one hypothesis suggests that peptides generated by ERAP1 (WT IDTAPs) are outcompeting and suppressing immunodominant peptides generated in the absence of ERAP1 (ERAP1$^{-/-}$ IDTAPs), resulting in the loss of recognition of these sub-dominant epitopes by T cells in the WT animal. An alternative hypothesis is that ERAP1 is actively degrading epitopes that would otherwise be presented on the cell surface and become immunodominant.[126,265,266] To investigate the latter hypothesis, we chose to study the peptide with the least response in WT mice, FAPANTDANNIEGQA. We constructed four 15-mer peptides with 1, 2, 3 or 4 additional N-terminal amino acids in front of the FAPANTDANNIEGQA sequence. If ERAP1 is degrading this epitope via N-terminal trimming, each N-terminal amino acid should provide incremental protection and result in increased response in WT mice. To further control for ERAP1's strong, length-dependent substrate specificity, each peptide produced in this manner was made the same overall length by removing a C-terminal amino acid for each N-terminal amino acid added. The resulting sequences were used to stimulate splenocytes harvested from Ad-TA-immunized WT or ERAP1−/− animals. We confirmed that with each additional N-terminus extension of the FAPANTDANNIEGQA peptide, a significantly higher number of splenocytes derived from Ad-TA-vaccinated WT mice responded to the extended peptide (Figure 1A). Furthermore, the N-terminal amino acids increased the Ad-TA-vaccinated splenocyte ELISpot responses in a linear manner, with each N-

terminal amino acid resulting in an additional 13.67 (± 1.302) IFN-γ-secreting WT cells per 106 splenocytes (Figure 2B). To further demonstrate this, a linear regression of the mean values was performed, yielding an R 2 of 0.9948 (Figure 2B). To demonstrate that this effect was specific to ERAP1, we included ERAP1−/− cells. ERAP1−/− cells had a uniformly high response to each peptide, independent of N-terminal amino acid additions, with an R 2 of 0.19 (Figure 2B). To our knowledge these are the first data suggesting that ERAP1 destroys potential alternative immunodominant peptide epitopes by virtue of its N-terminal trimming activity and that this destruction has functional significance on T-cell responses.

Figure 2: ERAP1 ablates response to ERAP1$^{-/-}$ IDTAP linearly with the number of N-terminal residues prior to a consensus sequence.

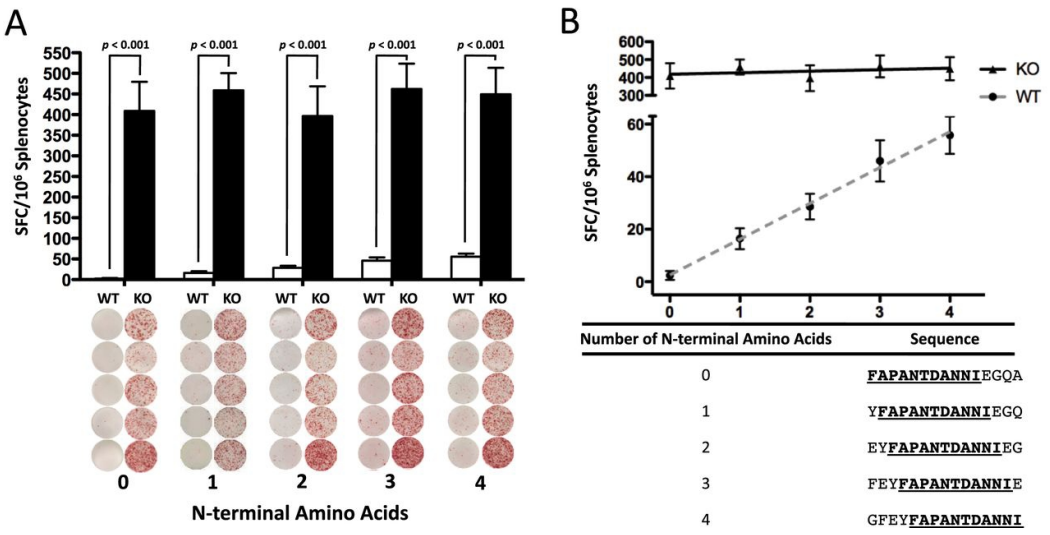

C56BL/6 mice (n = 5) or ERAP1$^{-/-}$ mice (n = 5) were immunized I.M. in the tibialis anterior with Ad5-*C. difficile*-TA as described in Methods. At day 14, mice were sacrificed and splenocytes were harvested and stimulated with 2 μg per well of the listed 15-mer peptides. Five peptides were generated that contained the consensus sequence FAPANTDANNI and 0, 1, 2, 3 or 4 additional N-terminal residues. These peptides were used to stimulate splenocytes using an ELISpot technique. As expected each peptide generated a strong response in ERAP1$^{-/-}$ mice, and very low responses in corresponding WT animals (A). A linear regression was performed (dotted gray line) to examine if N-terminal extension of the consensus sequence would provide incremental protection from ERAP1-mediated destruction (B). The number of specific spots per 10^6 splenocytes stimulated were graphed on the y-axis and the number of N-terminal amino acids before the consensus sequence were plotted on the x-axis. In WT cells, for each additional N-terminal amino acid in front of the consensus sequence, 13.67 (± 1.892) additional spots per

10^6 were observed to respond. There was no strong relationship observed in ERAP1$^{-/-}$ cells. R^2 of 0.9948 for WT and 0.1903 for ERAP1$^{-/-}$. Error is shown above and below each point. The figure is representative of two separate experiments.

Different cytokine secretion profiles of CD8+ T lymphocytes derived from Ad5-TA-vaccinated WT or ERAP1-deficient mice

To further characterize the ERAP1-dependent aspects of induction of peptide-specific T-cell responses to TA-derived epitopes, WT or ERAP1−/− mice were vaccinated with Ad5-TA, and at 14 dpi the splenocytes derived from these animals were stimulated with either a pool of the WT IDTAPs or a pool of the ERAP1−/− IDTAPs and then subjected to FACS analysis. We observed a significantly ($P < 0.001$) increased frequency of IFN-γ- and TNF-α-secreting CD3+ CD8+ T cells in splenocytes derived from WT mice vaccinated with Ad5-TA and exposed to the WT IDTAPs (Figure 3A), as compared with similar exposures of T cells derived from ERAP1−/− animals vaccinated with Ad5-TA (Figure 3B). In contrast, ERAP1−/− IDTAPs induced a significant ($P < 0.01$) increase in the frequency of IFN-γ- and TNF-α-expressing CD8+ T cells in splenocytes derived from Ad5-TA-vaccinated ERAP1−/− mice, as compared with splenocytes from Ad5-TA-vaccinated WT mice similarly exposed to the ERAP1−/− IDTAPs (Figure 3C and D).

Figure 3: Cytokine secretion profile of CD8+ T cells derived from WT C57BL/6 or ERAP1-deficient mice.

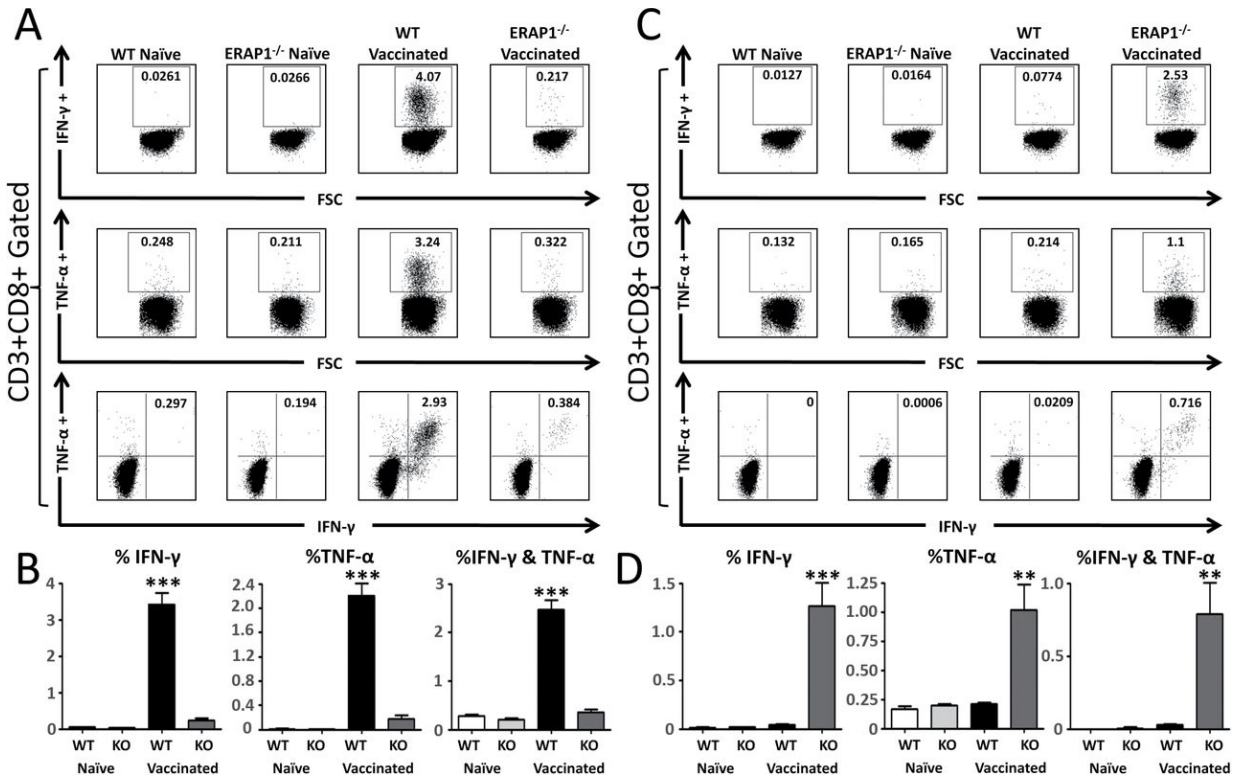

C56BL/6 mice (n = 8) or ERAP1$^{-/-}$ mice (n = 8) were immunized I.M. in the tibialis anterior with viral particles of Ad5-*C. difficile*-TA (1×10^{10}). At day 21, mice were sacrificed and splenocytes were harvested and stimulated for 6h at 37°C with a pool of peptides that responded in the WT mice only, the WT IDTAPs as described in Methods, (A and B), with a pool of peptides that responded in the ERAP1$^{-/-}$ mice only, the ERAP1$^{-/-}$ IDTAPs as described in Methods (C and D). (A) Representative example of IFN-γ-, TNF-α- or IFN-γ/TNF-α-producing splenic CD8+ T cells stimulated with the WT IDTAPs. (C) Representative example of IFN-γ-, TNF-α- or IFN-γ/TNF-α-producing splenic CD8+ T cells stimulated with the ERAP1$^{-/-}$ IDTAPs. Gates were set based on negative control (naIve) and placed consistently across

samples. (B) The total frequency of splenic CD8+ T cells expressing IFN-γ, TNF-α or IFN-γ/TNF-α stimulated with the WT IDTAPs. (D) The total frequency of splenic CD8+ T cells expressing IFN-γ, TNF-α or IFN-γ/TNF-α stimulated with the ERAP1$^{-/-}$ IDTAPs. The bars represent means ± SEM. Statistical analysis was completed using one-way ANOVA with a Student–Newman–Keuls *post hoc* test. A P value < 0.05 was statistically significant. ***P < 0.001, statistically significant from the other three groups of animals. **P < 0.01, statistically significant from the other groups of animals.

In vivo cytolytic activity of T lymphocytes against specific antigenic epitopes is dependent upon ERAP1 functions

As we have recently demonstrated, ERAP1 functions modulate the secretion of certain cytokines during innate immune responses, independent of its canonical role as an antigen-processing molecule.[171] To avoid these potentially confounding effects of ERAP1 and directly investigate if the T-cell activation observed in this study translates to a functional difference *in vivo*, we tested the role that ERAP1 may have in directing the *in vivo* cytolytic activity of T cells, using *in vivo* functional cytotoxic lysis assays.[267] Normal splenocytes were harvested, pulsed with the WT IDTAPs or the ERAP1$^{-/-}$ IDTAPs and differentially labeled with high or low concentration of the CFSE dye so as to allow us to track the survival of the two groups of differentially labeled splenocytes *in vivo* after administrations into syngenic Ad-TA-vaccinated WT or ERAP1$^{-/-}$ mice. In Ad5-TA-vaccinated WT mice splenocytes pulsed with WT IDTAPs were specifically killed compared with identical splenocytes pulsed with the ERAP1$^{-/-}$ IDTAPs (Chapter 2 Figure 4A). In contrast, adoptive transfer of ERAP1$^{-/-}$ splenocytes pulsed with either WT IDTAPs or ERAP1$^{-/-}$ IDTAPs into Ad-TA-vaccinated ERAP1$^{-/-}$ mice resulted in preferential killing of only splenocytes pulsed with ERAP1$^{-/-}$ IDTAPs (Figure 4B). We also noted that although ERAP1$^{-/-}$ T cells were able to generate potent cytokine secretion profiles, (Figure 3C) the cytolytic immune system of Ad5-TA-vaccinated ERAP1$^{-/-}$ animals did not kill cells loaded with ERAP1$^{-/-}$ IDTAPs as quickly or potently as the cytolytic immune system of Ad5-TA-vaccinated WT animals killed WT IDTAP-loaded cells (Figure 4B).

Figure 4: ERAP1 directs *in vivo* cytolytic activity of T lymphocytes against a specific set of antigens, and absence of ERAP1 directs *in vivo* cytolytic activity of T lymphocytes against a different, distinct set of antigens.

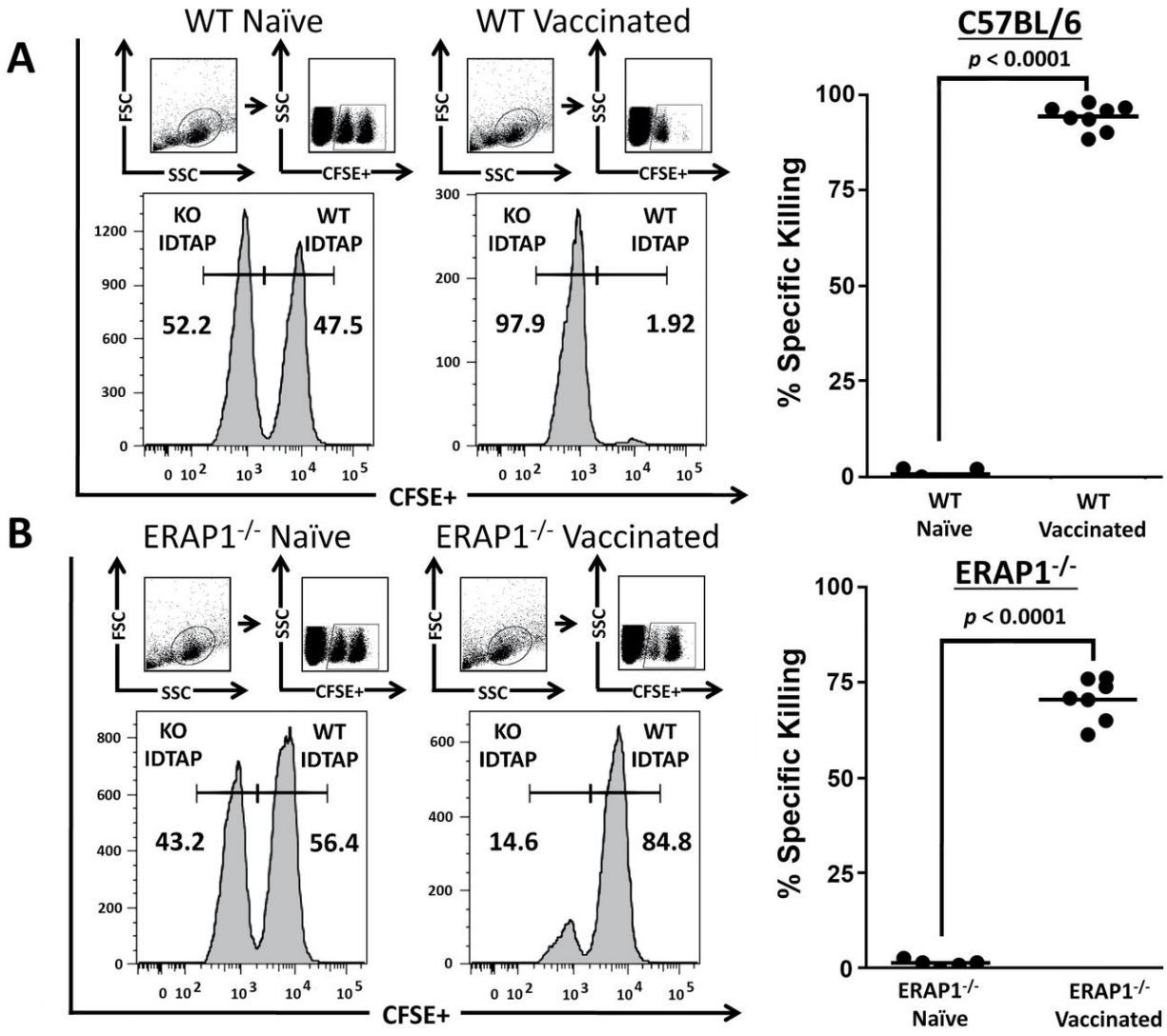

C56BL/6 mice (n = 8) or ERAP1$^{-/-}$ mice (n = 7) were immunized I.M. in the tibialis anterior with viral particles of Ad5-*C. difficile*-TA (1×10^{10}). At day 14, syngenic splenocytes were pulsed with either the pool of WT IDTAPs and stained with 10 μM (CFSE^{high}) or with the pool of ERAP1$^{-/-}$ IDTAPs and stained with 1 μM (CFSE^{low}), then transplanted into the

immunized mice, or corresponding naive animals (n = 5). Twenty-four hours after adoptive transfer, splenocytes were harvested and analyzed using an LSRII flow cytometer. (A) Representative examples of CFSE+ splenocytes from C57BL/6 mice and corresponding statistical analysis. (B) Representative examples of CFSE+ splenocytes from ERAP1$^{-/-}$ mice and corresponding statistical analysis. The percentage of CFSE+ cells was quantified using FlowJo software. % specific killing = 1 − [(% CFSE^{high}/% CFSE^{low})$_{immunized}$/(% CFSE^{high}/% CFSE^{low})$_{non\text{-}immunized}$].

ERAP1 functions are necessary to regulate the antigen-specific effector memory T-cell response in vivo

After an acute infection, antigen-specific memory T cells persist for long periods of time, *via* a cytokine-directed, antigen-independent mechanism.[268] To study if ERAP1 impacted long-term antigen-specific memory responses, we examined induction of memory CD8+ T cells after Ad-TA vaccinations of WT and ERAP1$^{-/-}$ mice. In addition, because of the important functional differences between the population of central and effector memory CD8+ T-cell development, we investigated the effects that ERAP1 had on T central memory (T_{CM}) and T effector memory (T_{EM}) cells.[269–271] Following immunization of WT or ERAP1$^{-/-}$ mice with Ad-TA, splenocytes were harvested and stimulated with TA peptides. Subsequently, the response of effector memory CD8+ T cells (CD3+, CD8+, CD62L−, CD127+ cells) was quantified by flow cytometry (Figure 5A). We observed that, TEM cells from Ad-TA-vaccinated WT mice had a potent and specific response to WT IDTAPs (Figure 5B). TEM from the vaccinated WT mice secreted significantly ($P < 0.001$) more IFN-γ and TNF-α in response to WT IDTAPs than TEM derived from Ad5-TA-vaccinated ERAP1−/− mice. The Ad5-TA WT derived TEM cells responded at a significantly greater level to the WT IDTAPs than to the ERAP1−/− IDTAPs ($P < 0.001$), demonstrating that ERAP1-mediated alterations in antigen-derived immunodominance (observed in effector T cells) also alters the activity of antigen-specific TEM cells.

In contrast, Ad5-TA-vaccinated ERAP1−/− mice generated a population of TEM cells that generated a significantly more potent response to the ERAP1−/− IDTAPs, than did TEM cells from WT mice exposed to these same IDTAPs ($P < 0.001$) (Figure 5C). Specifically, the

TEM from ERAP1−/− mice responded to the ERAP1−/− IDTAPs by secreting significantly more IFN-γ and TNF-α than they secreted in response to the WT IDTAPs. Because of our recent identification of ERAP1's effect on the cytokine response to innate immune stimulation, including changes in many important regulatory cytokines such as TNF-α and IL-12,[171] and because of the critical role of IL-12 in regulating the transition of memory T cells toward a T_{EM} phenotype, we also investigated if ERAP1 deficiency impacted on the phenotype of antigen-specific memory T cells induced following Ad-TA vaccination of WT or ERAP1$^{-/-}$ mice. Expression of IFN-γ, TNF-α or both cytokines in $CD8^+$ T cells was quantified, and from that population, the frequency of T_{CM} (CD62L+, CD127+) and T_{EM} (CD127+, CD62L−) CD8+ T cells were analyzed using flow cytometry as previously described.[272] Interestingly, following ERAP1$^{-/-}$ IDTAPs stimulation, we observed a significantly ($P < 0.001$) higher frequency of antigen-specific T_{EM} cell populations in Ad-TA-vaccinated ERAP1$^{-/-}$ mice, as compared with the number of similar cells generated in Ad-TA-vaccinated WT mice exposed to the WT IDTAPs (Chapter 2 Figure 6). Specifically, of the responsive antigen-specific CD8+ T cells secreting TNF-α, a significantly ($P < 0.001$) higher frequency of TEM CD8+ T cells were observed in Ad-TA-vaccinated ERAP1−/− mice compared with identically vaccinated WT mice (Figure 6A). The same trend was observed in TA antigen-specific CD8+ T splenocytes in that there were greater numbers of cells secreting IFN-γ (Figure 6B), and cells secreting both TNF-α and IFN-γ derived from Ad-TA-vaccinated ERAP1−/− mice as compared with identically vaccinated WT mice (Figure 6C). The antigen-specific CD8+ T cells that were positive for both TNF-α and IFN-γ also showed a significant ($P < 0.05$) increase in the percentage of TCM

(CD62L+, CD127+) cells in Ad-TA-vaccinated ERAP1−/− mice, as compared with identically vaccinated WT animals. Together, these results demonstrate that ERAP1 alters the quality and, interestingly, suppresses the quantity of the CD8+ memory T cells responding to specific, antigen-derived peptides.

Figure 5: ERAP1 directs cytokine secretion by T lymphocytes against a specific set of antigens, and absence of ERAP1 directs cytokine secretion by T lymphocytes against a different, distinct set of antigens.

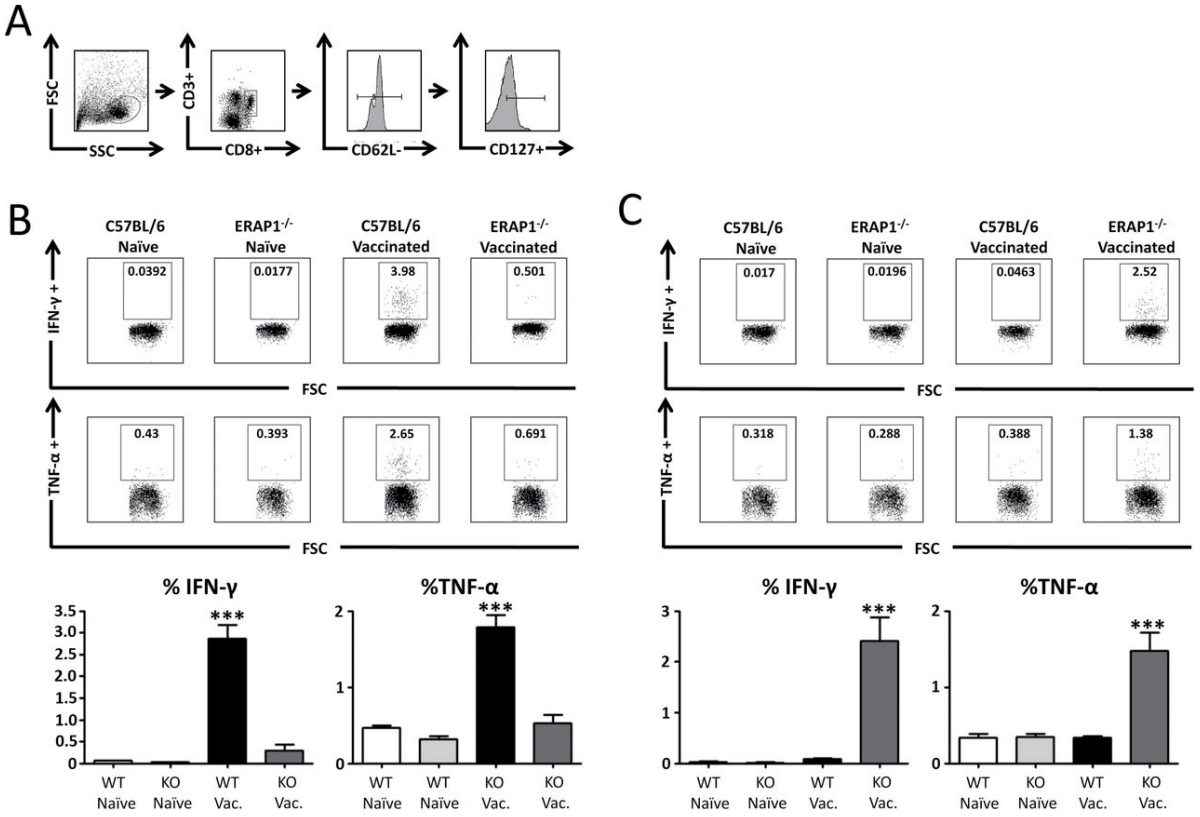

T effector memory cells directed at distinct sets of epitopes. C56BL/6 mice (n = 8) or ERAP1−/− mice (n = 8) were immunized I.M. in the tibialis anterior with viral particles of Ad5-C. difficile-TA (1×10^{10}). At day 21, mice were sacrificed and splenocytes were harvested and stimulated for 6h at 37°C with the labeled peptides. (A) Representative sample demonstrating our gating strategy. (B) Representative example of IFN-γ-, TNF-α-producing splenic CD8+ CD62L− CD127+ T cells stimulated with the WT IDTAP and percentage of IFN-γ-+, TNF-α+ TEM cells. (C) Representative example of IFN-γ-, TNF-α-producing splenic CD8+ CD62L− CD127+ T cells stimulated with the ERAP1−/− IDTAP and percentage of IFN-γ+, TNF-α+ TEM cells. The bars represent means ± SEM. ***P < 0.001, vs other groups of animals.

Figure 6: Deficiency of ERAP1 reprograms antigen-specific memory T cell toward an effector memory T-cell phenotype.

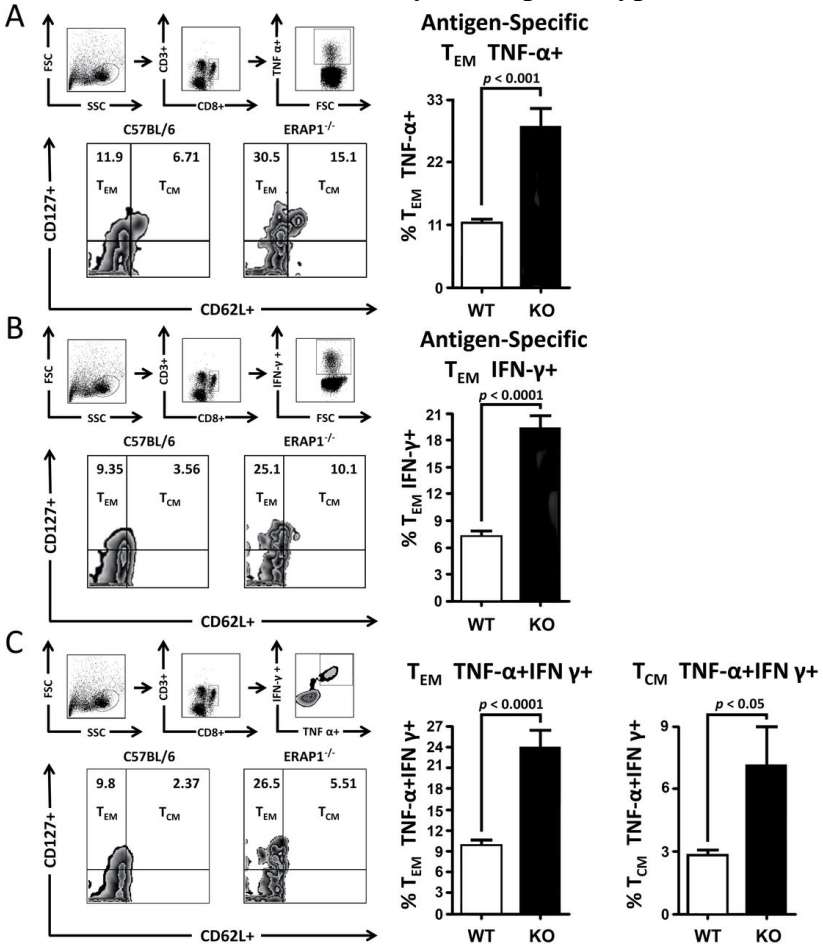

C56BL/6 mice (n = 8) or ERAP1−/− mice (n = 8) were immunized I.M. with viral particles of Ad5-C. difficile-TA (1×10^{10}). At day 21, mice were sacrificed and splenocytes were harvested and stimulated for 6h at 37°C with antigens. (A) Percentages of antigen-specific, TNF-α+ TEM and TCM shown. (B) Percentages of antigen-specific, IFN-γ+ TEM and TCM shown. (C) Percentages of antigen-specific, IFN-γ+ TNF-α+ double-positive TEM and TCM shown. The bars represent means ± SEM. Statistical analysis was completed using a two-tailed Student's t-test.

Discussion

Many genome-wide association studies have identified ERAP1 variants, that when present, increase the risk of several human autoimmune diseases.[15,16,38,43,126,273] It is also well documented that the aminopeptidase activity of ERAP1 has an important role in the antigen presentation component of adaptive immunity.[257] Because of ERAP1's role in antigen presentation it has been proposed that significant alterations in antigen presentation may be the mechanism underlying how single nucleotide polymorphisms (SNPs) in ERAP1 contribute as a risk factor for many autoimmune diseases.[13,274] Here, we have demonstrated that ERAP1 functions are not only important during the presentation of antigen-derived peptides, but these functions can also completely change which antigen-derived peptides ultimately become selected as immunodominant T-cell epitopes. Our results suggest that ERAP1 may do this by destroying epitopes that would otherwise become immunodominant in the absence of adequate ERAP1 functionality. By virtue of our use of classical peptide-pulsing experiments to stimulate splenocytes, we cannot discern if loss of ERAP1 functions may unmask effects of cross-presentation and/or the impact that cytosolic aminopeptidases may be having on the experimental results, a caveat that will require future studies to fully understand.

We further establish that ERAP1-mediated influences on T-cell functions are both qualitative and quantitative, by demonstrating that loss of ERAP1 function redirects CTL killing toward a different set of epitopes and increases the percent of antigen-specific memory T cells elicited by antigen exposure. In fact, our studies suggest that normal ERAP1 activity can act to suppress the numbers of T_{EM} cells that respond to a given antigen, as lack of normal ERAP1

activity allows for increased numbers of antigen-specific T_{EM} cells. Because T_{EM} cells have been implicated in autoimmunity,[275,276] this unique finding may shed light on why ERAP1 SNPs are associated with several autoimmune diseases, for example, by significantly altering the robustness and quality of CD8+ T-cell memory responses to antigenic proteins.

While it had been hypothesized that epitopes that are immunologically silent in WT adaptive immune responses may yet be important in generating CD8+ T-cell responses in ERAP1$^{-/-}$ backgrounds, it had not been directly demonstrated until our study.[147] We have now identified antigen-derived peptides that become immunodominant T-cell targets only in the absence of ERAP1 functions and further demonstrated that these epitopes are fully functional and capable of directing T-cell killing *in vivo*. These results confirm that ERAP1 is not essential to the process of immunodominant peptide selection and suggest that other factors such as dominant peptide suppression, the proteasome, TAP and MHC-I are sufficient to generate an immunodominant T-cell response. Despite the production of intact immunodominant peptide responses without ERAP1, the evolutionary conservation of ERAP1 suggests that ERAP1 must somehow enhance this process, providing for optimal induction of antigen-specific T-cell clones to a respective peptide target.

One reason for the evolutionary conservation of ERAP1 may be that for some antigens the absence of ERAP1 results in detrimental outcomes, such as diminished capability of the cellular arm of the adaptive immune response to kill pathogen-infected cells. Consistent with these notions, it has been demonstrated that ERAP1 is required to mount an effective immune response against *T. gondii*.[262] Alternatively, the immunodominant epitopes generated in the

absence of ERAP1 may be less potent, as our study demonstrates that although ERAP1$^{-/-}$ T cells were able to generate potent cytokine secretion profiles, ERAP1$^{-/-}$ animals did not kill cells loaded with ERAP1$^{-/-}$ IDTAPs as quickly or potently as WT animals killed WT IDTAP-loaded cells.

Evolutionary benefits may also explain why the presence of ERAP1 may eliminate certain peptides from the repertoire of presented epitopes, for example, to decrease the likelihood of generating immune responses to self-antigens. It has been demonstrated that certain pathogen-derived peptides with high homology to host peptides can break tolerance and result in CD8+ T-cell-mediated autoimmunity due to molecular mimicry.[277–279] Our data suggest that the presence of ERAP1 has the potential to 'over ride' immunodominant peptide selection so as to limit the number of homologous peptides presented to host T cells, by destroying immunodominant peptides that overlap between pathogen and host. ERAP1 may have evolved to eliminate certain problem epitopes or it may merely add a layer of complexity that must be overcome to generate self-mimicking epitopes. ERAP1's ability to specifically eliminate certain peptides could ultimately be functionally responsible for why the presence of specific ERAP1 alleles has been repeatedly associated with several autoimmune diseases, and specifically why ERAP1 has been shown to contribute risk to these diseases in an HLA-dependent manner.

In addition to demonstrating that ERAP1 alters the cytolytic activity of antigen-specific CD8+ T cells, we show an increased percentage of antigen-specific CD8+ T cells that express an effector memory (CD62L−, CD127+) phenotype in Ad-TA-vaccinated ERAP1$^{-/-}$ mice.T_{EM} cells have also been implicated in autoimmune diseases.[275,276,280,281] The increased frequency of

$CD8^+$ T_{EM} cells within the antigen-specific population of memory T cells in $ERAP1^{-/-}$ mice suggest that ERAP1 may be playing a role in autoimmunity by increasing the number of, or modifying the phenotype of memory T cells generated during an immune response to a degree that may contribute to increased autoimmune disease risk.

Our data demonstrating that ERAP1 suppresses T_{EM} responses appear counterintuitive relative to the known important role that ERAP1 plays during antigen generation and raises interesting questions about the evolutionary retention of ERAP1's functions with regard to T_{EM}. Our findings suggest that in the absence of ERAP1, greater percentages of memory T cells expressing the effector memory phenotype are generated, contrary to what might be expected of an important enzyme that facilitates CD8+ T-cell responses. However, memory T-cell expansion and contractions are tightly regulated by a network of positive and negative feedback loops.[282–284] Our data allow for the possibility that ERAP1 is involved in one of these regulatory mechanisms, affecting the number of T_{EM} cells elicited during an immune response. In this manner, the level of ERAP1 expression may act as a modulator, enhancing the effector function of T cells and slowing their progression into memory cells during an acute infection. Alternatively, ERAP1 may have important roles in other immune pathways, including the innate immune response, which may also significantly impact on the potency of downstream adaptive immune responses. For example, we recently demonstrated that there are major differences in cytokine responses to TLR stimulation in $ERAP1^{-/-}$ mice.[171] Therefore, future studies will have to discern if one of these mechanisms, a combination of these mechanisms, or none of these mechanisms are mediating this interesting effect on T-cell memory.

This study clarifies ERAP1's role in shaping immunodominance through creation and destruction of peptides *in vivo* and demonstrates the functional significance of ERAP1 in modulating T-cell killing based upon this role. However, we also confirm that ERAP1 is not necessary to establish an antigen-derived peptide as immunodominant. The work also expands upon ERAP1's roles in regulating some aspects of the adaptive immune system, beyond its known role in peptide processing and trimming for MHC-I display, by demonstrating that ERAP1 regulates the quantity of memory T cells with T_{EM} phenotype generated in response to an infection. These multiple functions of ERAP1 may play critical roles in the regulation of T-cell memory and may further explain the genetic link between ERAP1 and the seronegative spondyloarthropathies.

Chapter 3

Endoplasmic reticulum aminopeptidase-1 alleles associated with increased risk of Ankylosing Spondylitis reduce HLA-B*27 mediated presentation of multiple antigens

This chapter is adapted from an article published in Autoimmunity, Volume 46, Issue 8, Pp. 497-508 September 13, 2013.

Authors: David P.W. Rastall,* Sergey S. Seregin,* Irini Evnouchidou, Charles F. Aylsworth, Dionisia Quiroga, Ram P. Kamal, Sarah Godbehere-Roosa, Christopher F. Blum, Ian A. York, Efstratios Stratikos, and Andrea Amalfitano1 (*Authors contributed equally to this work)

Introduction

In chapter 2 we demonstrated the critical importance of ERAP1 in the process of antigen presentation. These data demonstrated that ERAP1 could completely reshape the immunodominant T-cell response to a given antigen, but did not shed light on how much allelic variation in humans could impact antigen presentation. This is critical as no humans are known to have a compete deletion of ERAP1. Instead the common human ERAP1 alleles vary at 5 key SNPs with alleles that have various collections of these 5 SNPs composing the vast majority of the population variance. Therefore, we wished to determine if those SNPs could impact antigen presentation within human cells.

As previously stated, AS has a strong genetic component, with nearly 90% of the risk for AS being attributable to hereditary factors.[285] As seen with many other autoimmune diseases, HLA-B*27 positivity is strongly correlated with AS development, with 90% of AS patients carrying this HLA allele. However, the presence of HLA-B*27 by itself is not causative, as only between one and five percent of individuals possessing HLA-B*27 alleles develop AS.[27] As the HLA-B*27 MHC class I allele is responsible for only 40–50% of all genetic susceptibility to AS, other genes are also involved in the pathogenesis of AS.[13,14,27] To identify these genes, several genome-wide association studies (GWAS) to identify other genetic risk loci that are associated with the development of AS have been carried out. Several large scale GWAS in various populations identified ERAP1 as the gene that contributed the most risk for development of AS, as well as identifying other candidate genes such as IL-23R, IL1R2, PTGER4, TBKBP1, CARD9, RUNX3, LTBR-TNFRSF1a, IL12B, EDIL3 and HAPLN1.[14,27,247] More recently, specific variants of ERAP1 have been identified to be responsible for ~26% of the total genetic

risk of AS, with HLA-B*27 and ERAP1 together comprising ~70% of the overall genetic risk for development of AS.[285,286] In HLA-B*27^{+} individuals, several ERAP1 SNPs, including rs30187 (K528R) and rs27044 (Q730E), are significantly associated with AS (Table 2).[27,285–288] In the HLA-B*27^{+} population, individuals that are homozygous for ERAP1_528K have the highest predisposition for AS. Furthermore, the most recent AS GWAS confirmed epistasis between HLA-B*27 and ERAP1 genes, revealing these ERAP1 alleles to be associated with AS risk only in HLA-B*27^{+} individuals, and not in HLA-B*27^{-} individuals.[13] This epistasis suggests that ERAP1 is directly interacting with HLA-B*27 in the pathogenesis of AS, in contrast to other AS susceptibility loci (e.g. IL23R, IL12B) that were shown to contribute risk to AS independently of HLA-B*27 status.[27]

Table 2 – ERAP1 Variants

SNP#	P value association with AS	Allele	349	528	575	725	730
		ERAP1 High	**M**	**K**	**D**	**R**	**Q**
		ERAP1 Low	**V**	**R**	**N**	**Q**	**E**
rs2287987	1.6×10^−4	M349V	**V**	**K**	**D**	**R**	**Q**
rs30187	**3.0×10^−6**	**K528R**	**M**	**R**	**D**	**R**	**Q**
rs10050860	1.1×10^−4	D575N	**M**	**K**	**N**	**R**	**Q**
rs17482078	2.3×10^−4	R725Q	**M**	**K**	**D**	**Q**	**Q**
rs27044	**1.0×10^−6**	**Q730E**	**M**	**K**	**D**	**R**	**E**
		HeLa (endogenous)	M/M (atg/atg)	K/R (aag/agg)	D/D (gac/gac)	R/R (cga/cga)	Q/E (caa/gaa)

Construction of plasmids, encoding for various ERAP1 alleles was performed as described in Materials and Methods. P value for association with AS is derived from recent GWAS studies on UK patients.[27] Amino acids positions, associated with high risk of AS are shown in grey. Endogenous ERAP1 alleles in our HeLa-Kb-B*27/47 resemble ERAP1_High, however, have heterogeneity at positions 528 and 730.

HLA-B*27 and ERAP1 are both central members of the antigen presentation pathway. The initial step in the processing of intracellular proteins occurs in the cytosol. Here, proteins are cleaved by the proteasome into 2–25 amino acid length peptides.[289] A small fraction (less than 1%)[253] of these peptides (those that are not completely degraded by the cytoplasmic proteases) are actively transported by the transporter associated with antigen processing (TAP) into the endoplasmic reticulum (ER) where ERAP1 and other ER-localized peptidases trim these peptides at their N-termini to either generate peptides of optimal size for loading onto MHC class I molecules, or alternatively degrade peptides to a size so small (below 8–9 amino acids) that they can no longer be efficiently loaded onto MHC class I molecules.[289–292]

ERAP1 is a central component of the antigen presentation pathway, and has been shown to be necessary for the generation of certain MHC class I presented peptides that can effect the ability to respond to specific diseases such as *Toxoplasma gondi*, and cancers such as cervical cancer.[262,293] The recently discovered genetic epistasis between HLA-B*27 and ERAP1 in AS, and their cooperative role in antigen presentation lends strength to the theory that AS is caused by aberrant antigen presentation. If aberrant antigen presentation is a factor in the pathogenesis of AS, one possibility is that in AS there is are novel peptides presented in AS patients relative to non-AS patients, which may lead to autoimmunity. The theory of "arthritogenic peptides" was strengthened by the observation that rats transgenic for human HLA-B*27 develop arthritis only in the presence of pathogens, but not in specific-pathogen-free environments.[134] Additionally these HLA-B*27 transgenic rats require T-cells to develop arthritis.[294] These observations led to the idea that arthritogenic peptides present in intracellular bacteria were being presented on

MHC class I, and potentially by mimicking endogenous epitopes, lead to activation of auto-reactive T-cells, However, CD8+ T-cells were not necessary for the development of the arthritic phenotype,[196] and recent work has suggested that Th17 cells may be involved in the inflammatory process, because CD4+ KIR3DL2+ T-cells are directly stimulated by HLA-B*27 homodimers present on the surface of HLA-B*27+ antigen presenting cells.[295]

Of the five ERAP1 SNPs originally linked to the AS by GWAS, all five have been shown to affect the biochemical function of ERAP1. M349V, K528R, R725Q and Q730E variants of ERAP1 directly affect trimming properties of ERAP1. For example, the Q730E and K528R variants have been shown to affect the activity and specificity of ERAP1 trimming[296] and K528R has been shown to affect ERAP1 preferences for substrate length.[251] The 725Q variant was shown to reduce peptide trimming (2), and in the additional presence of 349V, 528R, or 730Q the reduction of function in ERAP1 trimming caused by 725Q was further exagerated.[266] The D575N polymorphism is thought to play an important role in folding of ERAP1, and has been shown to directly affect peptide trimming by ERAP1 in the presence of the 349V polymorphism.[249,254]

In the following study, we have investigated the specific role that AS-associated variants of ERAP1 have upon HLA-B*27 antigen presentation. We have determined that the presence of a specific ERAP1 allele associated with an increased risk for development of AS (referred to here as ERAP1^{High}) mediates *reduced* presentation of both pathogen-derived and host-derived antigens onto HLA-B*27 in cultured cells, relative to a low AS risk ERAP1 variant (ERAP1^{Low}). These effects are consistent with *in vitro* biochemical assays for peptide catalysis, which

independently validated that the ERAP1^{High} variant has higher catalytic activity and is able to destroy HLA-B*27 epitopes more efficiently than the ERAP1^{Low} variant. Together, these findings suggest that a mechanism for AS induction may be due to global alterations in presentation of HLA-B*27 and HLA-B*27 destined-peptides by the presence of high-risk ERAP1 alleles, resulting in AS.

Results

Validation of an HLA-B*27 surface rescue system for use in AS studies

In this study, we have focused our investigation upon recombinant ERAP1 alleles containing a combination of amino acid substitutions associated with high and low AS risk, and refer to these as the ERAP1_High and ERAP1_Low alleles, respectively (Chapter 3 Table 1). Since there are at least five AS-linked SNPs[27] and the possible number of haplotypes is at least 32, we chose to focus our study on the two extreme haplotypes, even though these specific haplotypes do not represent all possible haplotypes found within the human population. This approach also evaluates possible synergism between SNPs, although it cannot deconvolute them. Importantly, the ERAP1_High allele (Genebank accession #NP_057526.3) is present in a significant number of humans.[297]

We next set out to evaluate the effect that the presence of various ERAP1 allelic variants has on HLA-B*27 antigen presentation in intact cells by using a previously described HeLa-K^b-B*27/47 surface rescue system (Figure 7).[146,296,298] HeLa-K^b-B*27/47 cells are HeLa cells that have been stably transduced with murine K^b, human HLA-B*27, and the herpes simplex virus TAP-blocker ICP47.[299] Using this system, only peptides containing an appropriate ER-localization signal can be substrates for ERAP-mediated loading onto HLA-B*27 molecules. Because this ER-localization signal cleaves peptides between two alanines, each peptide that did not already contain an N-terminal alanine, had one added as part of the ER-localization signal. This is not expected to effect ERAP1 trimming rates substantially because ERAP1 efficiently cleaves N-terminal alanines generating the correct substrates.[300] Of all HLA-B*27 subtypes, the

B*2705 allele has one of the most significant associations with AS,[116,301] and therefore this B*27 subtype was chosen for use in this system.

Figure 7: Model cell system for studying ERAP1 variants

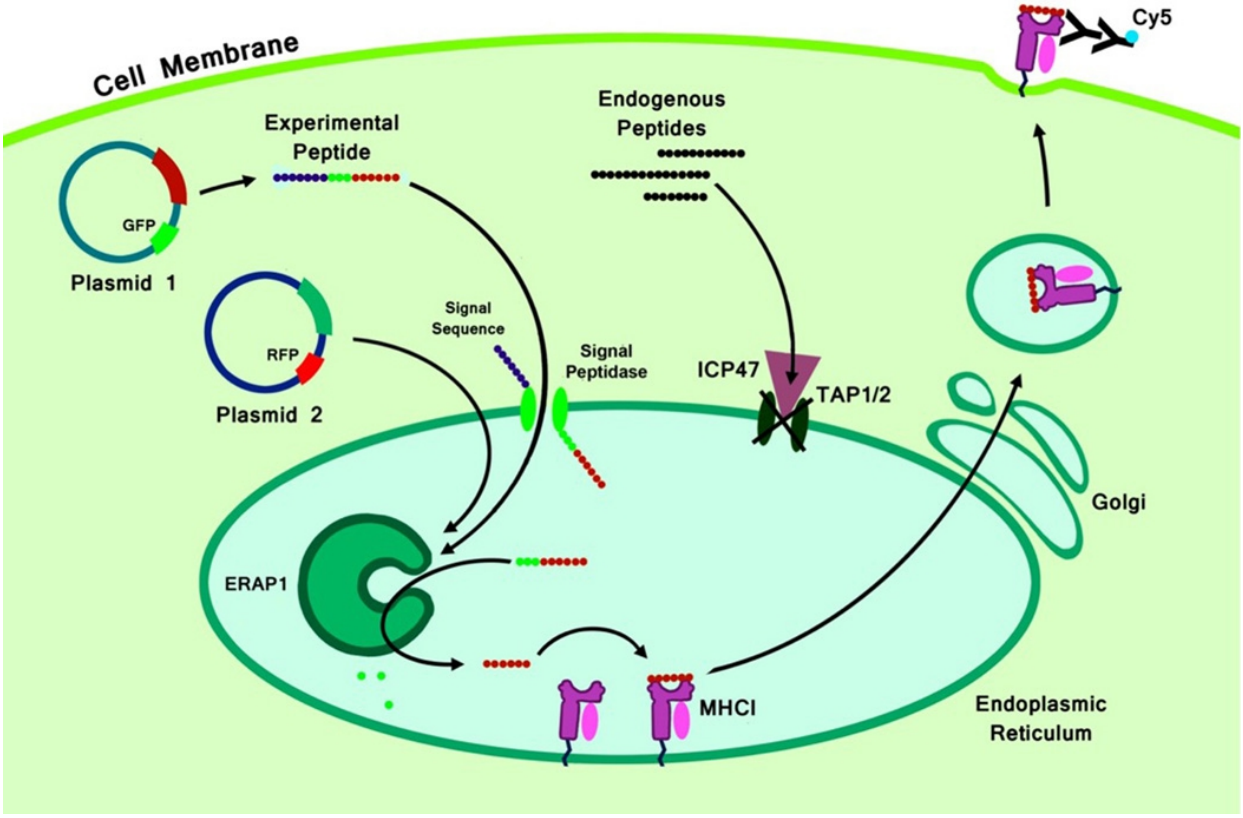

The initial critical step in the processing of intracellular proteins occurs in the cytosol. Proteins are cleaved by the proteasome into 2–25 aa peptides.[289] A fraction[302] of these peptides (those which were not degraded by the cytoplasmic proteases) is actively transported into the ER by TAP and trimmed at the N-terminus by aminopeptidase ERAP1[138,249,303,304] to generate peptides of optimal size for loading into MHC class I (8–10 aa). The MHC class I heavy chain first assembles with β2-microglobulin; this heterodimer is then assembled with 8–10 aa peptide.[305] Upon successful assembly, "mature" MHC I/peptide complexes are transported to the cell surface.[304] We have used HeLa cells stably expressing human HLA-B*2705 and TAP1/2 blocker (ICP47 protein), HeLa-K^b-B*27/47, to test the effect of ERAP1 allelic variants on HLA-B*27

antigen presentation in intact cells.[146,296,298] We used transient transfection with pTracer-CMV-GFP-peptide and pTracer-CMV-RFP-ERAP1 (one of the alleles). When transfected plasmid-derived peptide is delivered into ER (by means of ER-signal sequence from Ad2 E3gp19K protein, bypassing TAP blockage), surface HLA-B*27 (or other MHC class I) can be increased proportionally to the amounts of "mature" epitope available. By delivering N-extended HLA-B*27-specific peptide precursors to the ER and measuring surface expression of HLA-B*27, we can semi-quantitatively determine how much of the precursor was converted into "mature" HLA-B*27 epitope. Conversely, if a "mature" peptide is delivered, we can measure the rate of destruction of the peptide.

Figure 8: ERAP1 production by transfected cells

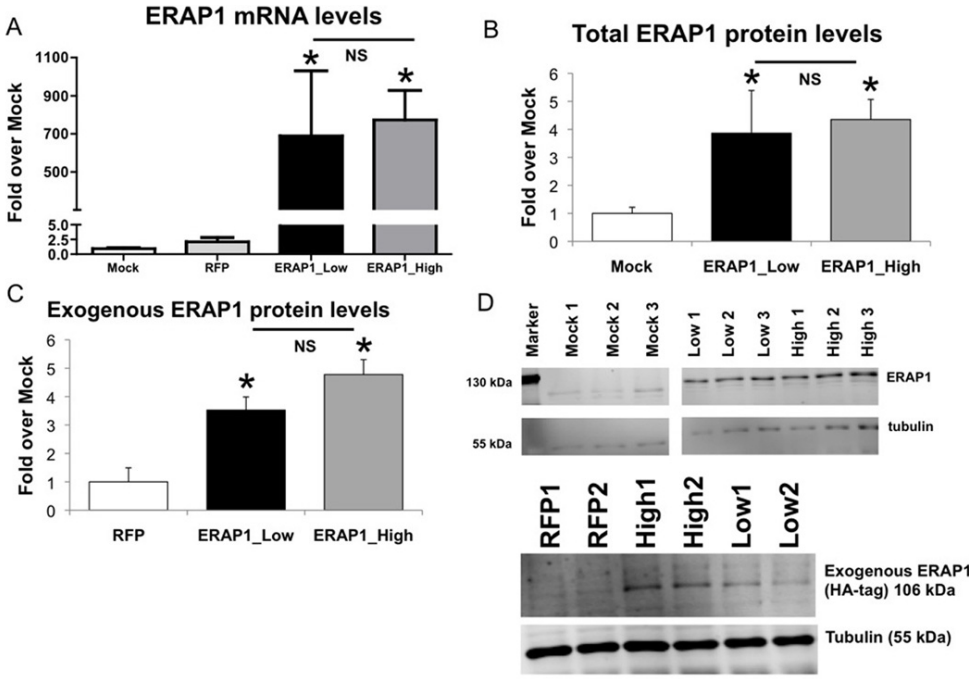

HeLa-K^{b}-B*27/47 cells were transiently transfected with plasmids expressing ERAP1_Low or ERAP1_High alleles (or no ERAP1). RNA and protein samples were harvested as described in Materials and Methods. Statistical analysis was completed using two-tailed Student's t-test, * - represent significant difference in ERAP1 levels as compared to control (mock or empty pTracer-RFP transfection), $p<0.05$; n=2 independent experiments performed. **(A)** Levels of ERAP1 mRNA are shown for each transfection group. About 700-fold induction in ERAP1 mRNA levels were noted for ERAP1_Low and ERAP1_High transfected cells, as compared to mock transfected cells. **(B)** Total ERAP1 levels were measured by Western blot. Significant ~3–4 fold induction in total ERAP1 protein levels were noted for ERAP1_Low and ERAP1_High transfected cells, as compared to mock transfected cells. **(C)** Exogenous ERAP1 levels were measured by Western blot with anti-HA-tag antibody. Significant exogenous ERAP1

levels were found in cells transfected with ERAP1_Low and ERAP1_High. **(D)** Representative Western blots for total ERAP1 (top) and exogenous ERAP1 (bottom) are shown. ERAP1 bands (106 kDa) and tubulin bands (55 kDa) are depicted.

HeLa-K^b-B*27/47 cells have reduced surface levels of HLA-B*27, as compared to HeLa-K^b-B*27 cells, as the presence of ICP-47 prevents transport of peptides into the ER. Without peptides being delivered to the ER, empty MHC class I molecules are retained in the ER and not subject to surface display.[146,298] Utilizing HeLa-K^b-B*27/47 and HeLa-K^b-B*27 cells and adenovirus vectors transducing ICP47, we further confirmed that nearly 80% of all HLA-B*27 molecules are retained in HeLa-K^b-B*27/47 cells as compared to HeLa-K^b-B*27 cells. This amount appears to be the maximal level of inhibition attainable, as the additional use of the ICP47 expressing adenovirus minimally decreased HLA-B*27 surface expression in HeLa-K^b-B*27/47 cells. We have also analyzed the amino acid composition of the endogenous ERAP1 alleles present in the genome of HeLa-Kb-B*27/47 cells, this analysis revealed heterogeneity at positions 528 and 730, but otherwise the endogenous ERAP1 alleles contain an identical amino acid sequence to the ERAP1_High allele (Table 2).

To further validate the system, we demonstrated that transfection of HeLa-Kb-B*27/47 with an ERAP1 expressing plasmid (pTracer-CMV-RFP-ERAP1) results in a significant increase in detectable ERAP1 transcription and expression within the cells (Figure 8A). Levels of ERAP1 transcription were measured by qRT-PCR, revealing a 500–1000 fold induction of ERAP1 mRNA levels in pTracer-CMV-RFP-ERAP1 transfected cells, while a minor ~2 fold induction of ERAP1 transcription occurred upon transfection with the control vector (Figure 8A). We also found a significant ~3–4 fold induction of ERAP1 protein expression in HeLa-Kb-B*27/47 cells, transfected with ERAP1_High (or Low) alleles, as compared to mock-transfected cells (Figure 8B, D).

ERAP1 alleles were designed to contain an HA-tag sequence at the C-termini (YPYDVPDYA). By using an HA-tagged antibody, we were able to measure the levels of exogenous ERAP1 expression derived from transfection in the HeLa-Kb-B*27/47 cells (Figure 8C, D). Importantly, we did not detect any significant differences in levels of ERAP1 transcription/expression when these cells were transfected with either the ERAP1_High or ERAP1_Low variant expressing plasmids, indicating that potential differences observed in the antigen presentation assay (see below) cannot be attributed to differences in ERAP1 allele specific levels of transcription, expression and/or stability.

Finally, we observed a minimal increase in TNFα release, representing a minimal inflammatory response, in HeLa-Kb-B*27/47 cells treated with the transfection reagent (mock transfection as compared to naïve, 48 hours post transfection), as well as moderate increases in cytokine/chemokine release in response to dsDNA (pTracer-CMV-RFP or pTracer-CMV-RFP-ERAP1 transfection). However, no additional increases in cytokine/chemokine levels were induced by ERAP1 expression.

An ERAP1 allele associated with increased risk of AS reduces surface expression of HLA-B*27 regardless of HLA-B*27 peptide utilized

HLA-B*27 restricted epitopes have been empirically found to be predominantly nonamers with an invariant arginine at position 2.[301] When signal-sequence containing versions of these peptides are delivered into the ER of HeLa-K^b-B*27/47 cells, surface HLA-B*27 (or other MHC class I) levels are increased proportionately to the amounts of "mature" epitope available for HLA-B*27 loading. To capitalize upon this system, we constructed plasmids that co-express RFP along with individual AS-associated ERAP1 alleles, each respectively containing up to five AS-correlated SNPs (Table 2).[25,285,306]

To determine if HLA-B*27 surface presentation was significantly altered due to the presence of ERAP1 allelic variants, we co-transfected Hela-K^b-B*27/47 cells with plasmids expressing various ERAP1 variants, together with plasmids expressing various signal sequence containing HLA-B*27-restricted peptides. By measuring surface expression of HLA-B*27 by flow cytometry we can semi-quantitatively compare how ERAP1 variants affect specific peptide loading onto HLA-B*27 molecules (Figure 8). We chose to investigate a variety of HLA-B*27 restricted peptides in our studies to determine if pathogen derived, or autologous peptides, (that have both been previously shown to correlate with AS) may show ERAP1 allele specific differences when processed for HLA-B*27 surface expression.[307–313] Transfection efficiencies were found to be high, with double positive cells averaging ~7.5% of the cells in each experiment.

In sum, we found that relative to the ERAP1_Low variant, the presence of ERAP1_High alleles generally reduced HLA-B*27 antigen presentation on the cell surface, (as measured by

HLA-B*27 mean fluorescent intensity (MFI)), regardless of which peptide was present for ER trimming (Chapter 3 Figure 3A, B). Increased HLA-B*27 surface expression (and by inference, antigen presentation) mediated by the presence of the ERAP1_Low allele was in fact independently observed for over 20 unique peptides tested in our studies, including both epitope precursors and mature epitope versions of each of these respective peptides (Figure 9A, B). Consistent with this, we further noted that this same phenomenon was observed when both N-extended (by 3 amino acids) peptides (Figure 9A) or the "mature" versions of these same respective peptides (Figure 9B) were expressed in the HeLa-K^b-B*27/47 cells. Although all peptides tested followed the same general trend, we noted that transfections with AGS_DRASFIKNL, ALE_ARKLLLDNL, APL_SRHHAFCFR, AQD_IRSSQNKL and AQA_KRVVINKDT and mature ARKLLLDNL showed the most dramatic differences in surface expression of HLA-B*27, differences that were also dependent upon whether the ERAP1_High or ERAP1_Low alleles were present in the HeLa-K^b-B*27/47 cells, (Figure 9 and Figure 10).

Specifically, pathogen derived peptides previously associated with AS pathogenesis (i.e.: *Chlamydia trachomatis* derived peptide: ALE_ARKLLLDNL or *Yersinia enterocolitica* derived peptides: AQD_IRSSVQNKL, AQA_KRVVINKDT) and peptides derived from self proteins previously noted in AS patients (AHS_VRYQCKNYY, AGS_DRASFIKNL, APL_SRHHAFCFR), and a control peptide (AED_RRYGPALSI) all showed similar ERAP1 dependent effects upon HLA-B*27 surface expression. These results confirm that the presence of the ERAP1_Low allele correlates with increased surface expression of HLA-B*27 antigens, regardless of the source (bacterial or autologous) or peptide composition of the antigen.

Figure 9: ERAP1_High reduces HLA-B*27 antigen presentation in intact cells as compared to ERAP1_Low for vast majority of HLA-B*27-restricted peptides.

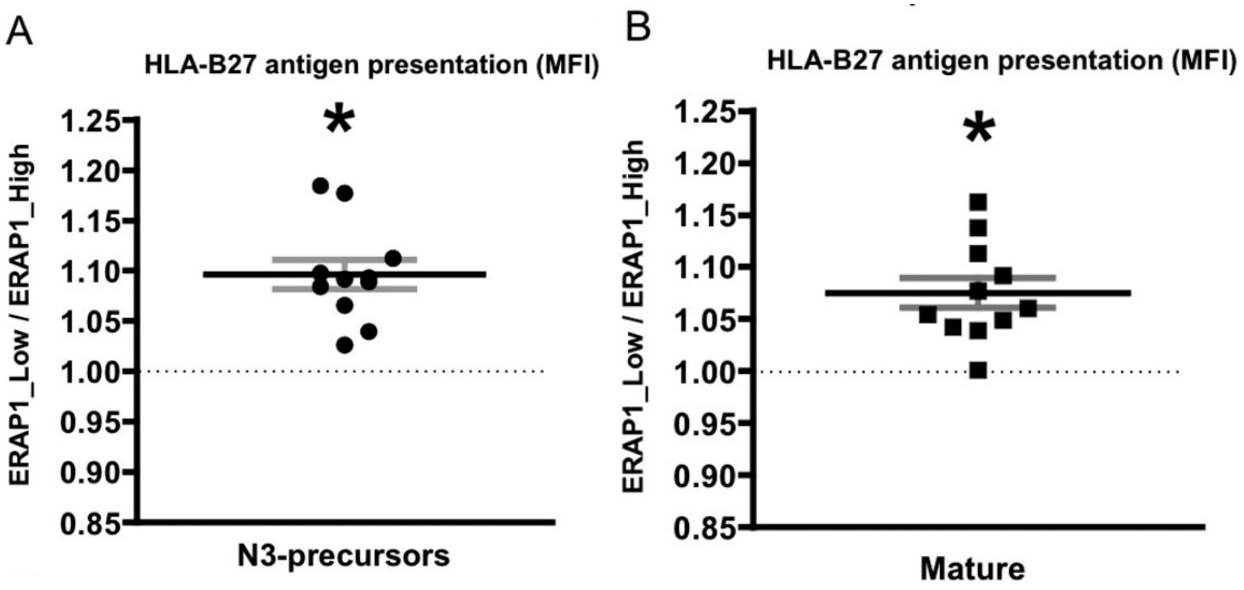

HeLa-K^b-B*27/47 cells were transiently transfected with plasmids expressing HLA-B*27-specific peptides (with ER-signal sequence) with GFP and either empty vector (control) or the indicated ERAP1 allele with RFP. At 48 hours post transfection surface HLA-B*27 surface expression on double-transfected (GFP^+RFP^+) was analyzed by flow cytometry using the ME-1 antibody. Peptides were transfected either as **(A)** N3-extended precursors or **(B)** "mature" epitopes. Ratio in mean fluorescent intensity (MFI) between ERAP1_Low and ERAP1_High variants is depicted. Combined graph is shown (n=11). Bars represent mean ± SEM. Statistical analysis was completed using one sample t-test [(mean ratio – 1)/SE)]; * - represent significant differences in HLA-B*27 surface expression mediated by ERAP1 polymorphism (i.e. fold ratio ERAP1_Low/ERAP1_High is significantly different from 1, dashed line), $p<0.05$.

Figure 10: Relative MHC-I expression for a given ERAP1 and a given peptide.

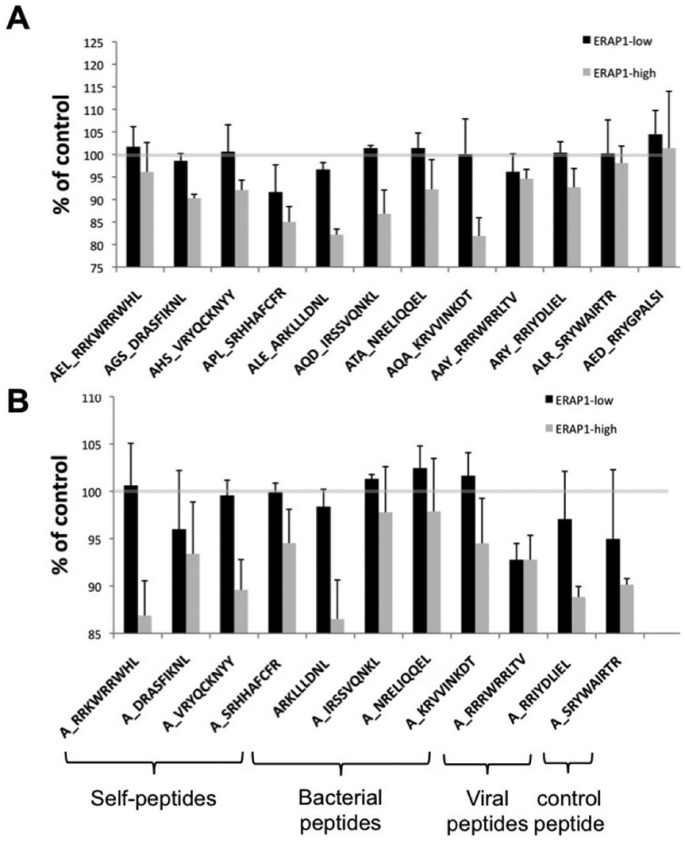

HeLa-K^b-B*27/47 cells were transiently transfected with plasmids expressing HLA-B*27-specific peptides (with ER-signal sequence) with GFP and either empty vector (control) or the indicated ERAP1 allele with RFP. At 48 hours post transfection surface HLA-B*27 surface expression on double-transfected (GFP^+RFP^+) was analyzed by flow cytometry. Peptides were transfected as N3-extended precursors **(A)** or as "mature" B*27 specific epitopes **(B)**, extended with Alanine on N-terminus for all peptides except ARKLLLDNL, which by coincidence already had N-terminal alanine. Mean fluorescent intensity (MFI), normalized to control (empty RFP vector, grey line, representing the level of endogenous antigen presentation) is shown. Combined graph is shown. Bars represent mean ± SEM.

The ERAP1_High variant more efficiently degrades B*27-specific epitopes below 9 amino acids in length, as compared to the ERAP1_Low variant

We have recently reported that ERAP1 variants differing by single SNPs can have significant differences in activity towards hydrolysis of the fluorogenic substrate L-AMC and 10-mer peptides.[296] Given the known ability of ERAP1 to destroy antigenic epitopes, one possible unifying interpretation for the results described above is that the ERAP1_High variant is relatively more efficient at degrading HLA-B*27 destined epitopes, decreasing the overall abundance of "loadable" HLA-B*27-specific 9 amino acid long peptides, and thereby resulting in decreased levels of HLA-B*27 surface expression. To investigate potential mechanistic differences between ERAP1 alleles ability to degrade antigenic epitopes, we purified the recombinant proteins and analyzed their *in vitro* enzymatic activity. The ERAP1_High variant had a significantly (at least 3-fold) increased rate of hydrolysis of the L-AMC substrate, a result that suggests that the ERAP1_High variant is more catalytically active relative to the low AS risk ERAP1 allele (Figure 11A). Given the lower levels of HLA-B*27 surface expression in cells transfected with ERAP1_High, we also tested if the recombinant enzyme could destroy an HLA-B*27 epitope *in vitro*. The purified ERAP1_High variant efficiently trimmed the B*27-specific epitope VRYQSKNYY, at a significantly higher ($p<0.0001$) rate compared to the ERAP1_Low variant, further suggesting that alleles containing these amino acid changes may be more efficient in destroying antigenic epitopes (Figure 11B).

Figure 11: Trimming of model substrates by ERAP1 variants

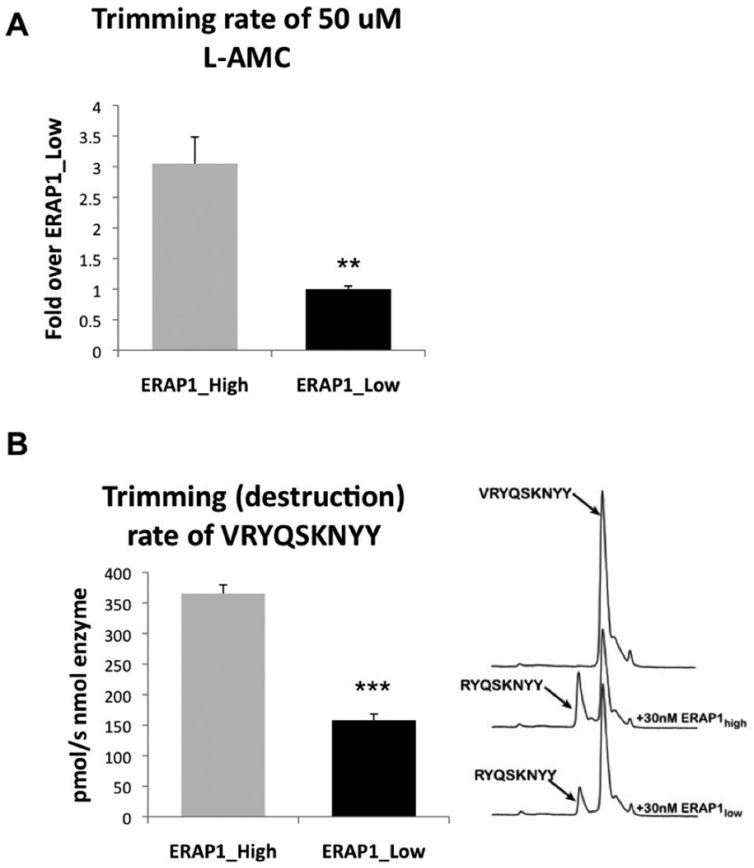

(A) Trimming of the model fluorogenic substrate L-AMC by purified ERAP1_Low and ERAP1_High alleles was performed. Statistical analysis was completed using two-tailed Student's t-test (** - indicates $p<0.001$). Two experiments performed, representative experiment shown. (B) Purified ERAP1_Low and ERAP1_High alleles (30 nM) were mixed with purified peptide VRYQSKNYY (50 μM) and N-terminal (V) trimming was measured by HPLC. HPLC traces and bar graph, showing intact and "degraded" peptides are shown. Statistical analysis was completed using two-tailed Student's t-test. *** - Indicate that ERAP1_High enzyme is able to trim VRYQSKNYY peptide with significantly higher efficiency as compared to ERAP1_Low, $p<0.0001$. Four independent experiments performed.

ERAP1 allele affects on surface expression of HLA complexes

To study possible differential effects that expression of ERAP1 alleles has on intact HLA complexes, as well HLA class I free heavy chain (FHC) complex presence at the cell surface, HeLa-Kb-B*27/47 cells were transfected with either the ERAP1_Low or ERAP1_High expression plasmids together with a control peptide (AED_RRYGPALSI), and at 48 hours post-transfection the cells were stained with ME1, HC10 or W6/32 antibodies. ME1 recognizes intact HLA-B*27 complexes on the cell surface,[288,314] HC10 recognizes HLA class I molecules not bound to peptide, including FHC and HLA-B*27 homodimers, on the cell surface,[288,314,315] while W6/32 recognizes all intact HLA-B, -A, –C, –E, –G complexes on the cell surface.[315]

As expected, staining with the W6/32 antibody was the most robust, with the majority of HLAs present at the surface of the transfected cells being HLA-B*27 (Figure 12A and Figure 12B). We also detected a significant amount of FHC formation in our system (HC10 staining), comprising up to 30% of all surface HLAs being detected regardless of whether the ERAP1_Low or the ERAP1_High alleles were being expressed in the transfected cells, (as well when only endogenous ERAP1 was present in control transfections), a result suggesting that overall rates of HLA-B*27 FHC formation do not seem to be influenced by the presence of different ERAP1 alleles (Figure 12B). It should be noted that we did not detect a significant difference in the amount of surface HLA-B*27 (detected by ME-1) using the B*27-specific control peptide (sequence: AED_RRYGPALSI), in pTracer-CMV-GFP, transfected cells, (Figure 12B), but did observe a difference in the surface HLA-B*27 for the other peptides tested (Figure 12).

Interestingly, although the differences were not significant, W6/32 staining trends to be higher in ERAP1_Low compared to ERAP1_High and the control plasmid transfected cells, while ME1 staining appears lower or unchanged for ERAP1_Low compared to ERAP1_High transfected cells. This may indirect suggest that ERAP1_Low variants are tailoring peptides more efficiently for presentation by non-B*27 HLA molecules as compared to ERAP1_High variants.

Finally, as shown on we did not detect any significant differences in levels of pro-inflammatory cytokines or chemokines being released by cells transfected with plasmids expressing control (empty RFP), the ERAP1_Low, or the ERAP1_High variants, suggesting that slight differences in FHC formation and antigen presentation observed in Figure 12A-B do not result in significant inflammatory responses in this system (Figure 13).

Figure 12: Overall abundance of MHC-I molecules on cell surface following transfection

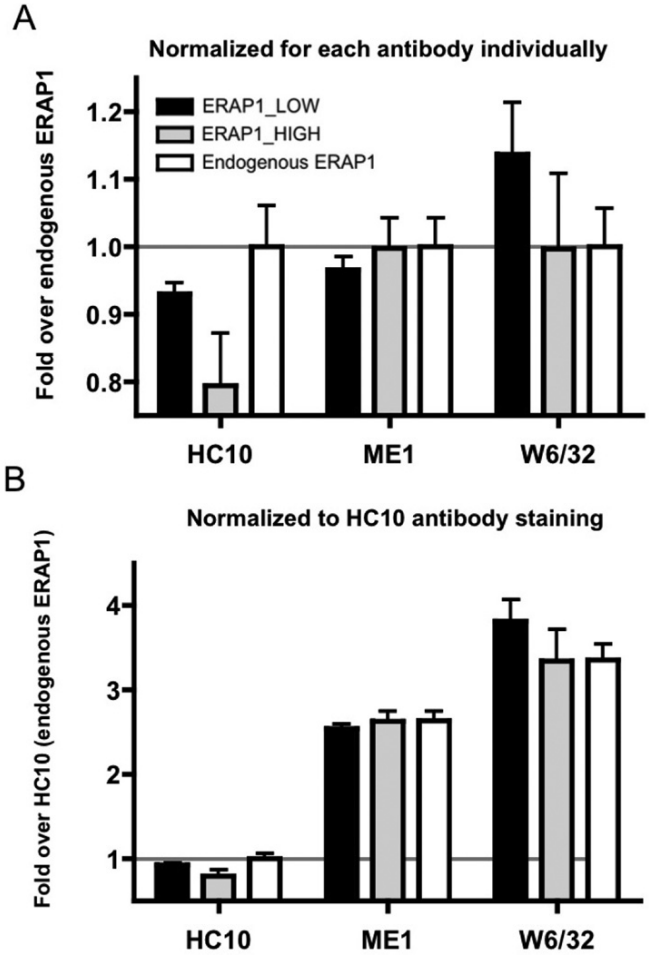

HeLa-K^b-B*27/47 cells were transfected with B*27-specific control peptide (sequence: AED_RRYGPALSI, in pTracer-CMV-GFP) and one of ERAP1-expressing plasmids (pTracer-CMV-RFP-ERAP1 or empty vector control, pTRacer-CMV-RFP) for 48 hours. Surface expression (MFI) of intact HLA-B, -A, -C, -E, -G was measured by staining with W6/32 antibody; surface expression of HLA-B*27 was measured by staining with ME1 antibody; surface expression of free heavy chain of HLA class I was measured by HC10 antibody. (A) MFI was normalized for each antibody individually (as fold over endogenous ERAP1), (B) MFI was normalized for HC10 antibody staining in endogenous ERAP1 setting.

Figure 13: Exogenous ERAP1 expression did not result in dramatic activation of pro-inflammatory cytokine/chemokines release.

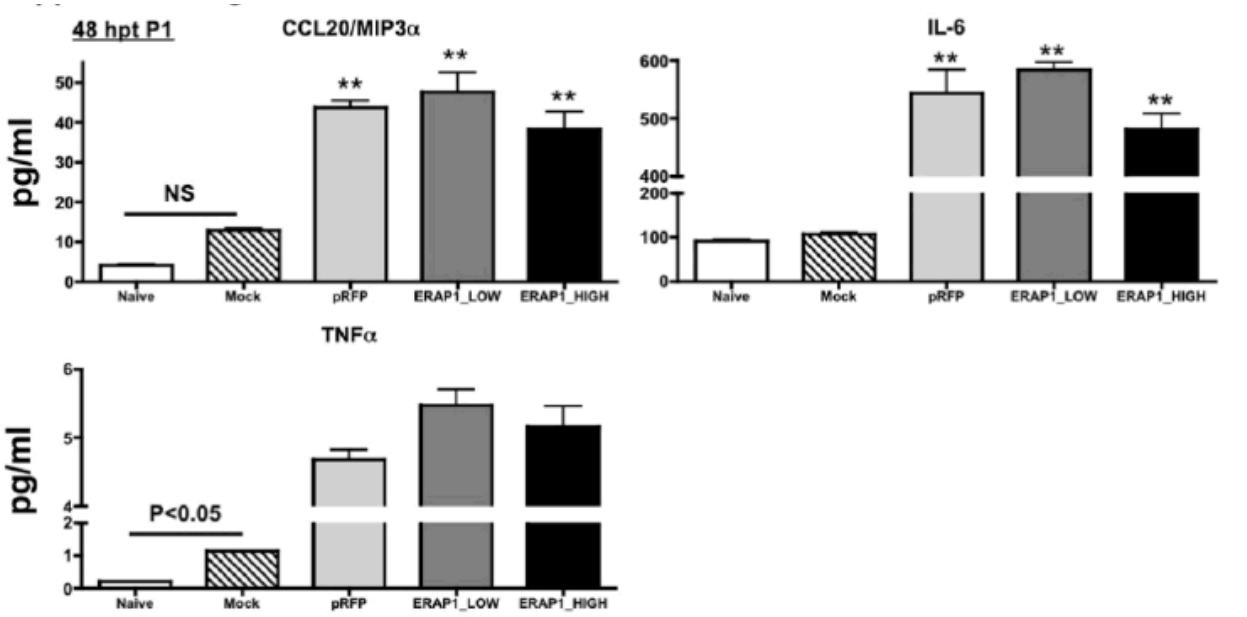

HeLa-Kb-B*27/47 cells were transiently transfected with plasmids expressing ERAP1_Low or ERAP1_High alleles (or no ERAP1). Mock (reagents only) transfected and non-transfected cells were also used. Media samples were collected at 48 hours post transfection and levels of MIP3, IL6 and TNF-α were determined as described in Materials and Methods. Bars represent mean ± SEM. Statistical analysis was completed using One Way ANOVA with a Student-Newman-Keuls post-hoc test: ** - indicate values, statistically different from Naïve and Mock groups, $p<0.01$ (plasmid dsDNA effect); no significant differences in ERAP1_Low and ERAP1_High transfected cells were found between each other and as compared to empty pTRacer-RFP transfection (no ERAP1 effect). Minimal effect of transfection reagent was found: small increases in TNF-α levels in Mock transfected cells as compared to naïve. One of two representative experiments is shown.

Discussion

In this study we investigated how in intact human cells, the over-expression of AS-specific ERAP1 alleles alters HLA-B*2705 subtype[307,308] surface expression in isolation, and upon presentation of HLA-B*27 specific peptides. We found that regardless of the source of the HLA-B*27-specific peptide (e.g. self-derived antigens, pathogen-derived antigen, and non-AS associated antigens), an ERAP1 allele associated with increased risk of AS consistently reduced overall HLA-B*27 surface expression levels (and by inference, antigen presentation) in intact cells as compared to cells expressing a low risk AS allele. Experiments utilizing both N3-extended peptide precursors and their shorter, or "mature" epitopes revealed the same overall results in our antigen presentation system, further verifying that the presence of high AS risk ERAP1 alleles results in globally reduced surface levels of HLA-B*27 (and HLA-B*27 antigen presentation) in intact cells regardless of antigenic peptide source or sequence. Enzymatic studies using purified ERAP1 proteins *in vitro* also demonstrated that high AS risk ERAP1 alleles trim HLA-B*27 epitopes more rapidly, and to a length that is below the length suitable for optimal loading onto the β2m/HLA-B*27 complex, as compared to the enzymatic properties of low AS risk ERAP1 alleles. Overall, the results are consistent with a model suggesting that the presence of high AS risk ERAP1 alleles may result in destruction of antigenic epitopes destined for HLA-B*27 loading, and also result in reduced surface expression of HLA-B*27 loaded peptide complexes.

These results are in agreement with a recent study by Evans et.al. in which the lower risk AS alleles ERAP1_528R and ERAP1_725Q appeared to have slower rates for enzymatic trimming of a model fluorogenic peptide, as compared to the reference allele.[316] Moreover, our

results and proposed model is in direct agreement with a recent study by Garcia-Medel et.al., where the authors found that ERAP1 alleles associated with low AS risk have diminished enzymatic activity and less efficient peptide trimming as compared to the high AS risk ERAP1 alleles, when the HLA-B*27:04-bound peptidome is analyzed.[317]

Our data shed light on the role that high AS risk ERAP1 alleles may have in the induction and pathogenesis of AS.[318] Because this model only allows for testing of a limited number of peptides, it cannot entirely rule out the arthritogenic peptide hypothesis for causation of AS, however, it does place limitations on the possible characteristics of such peptides should they be causative for AS. We show that all peptides we tested to date are degraded at a much faster rate by ERAP1_High than ERAP1_Low variants *in vitro*, a result consistent with the decreases in overall peptide presentation noted in intact human cells *in vivo*. This strongly suggests that if an arthritogenic peptide exists, it is one that is not easily degraded by ERAP1 (ie: to a size to small to load onto MHC class I).

It has also been suggested that the mere presence of HLA-B*27 homodimers on the cell surface may be activating Th17 CD4+ T-cells by activating the KIR3DL2 receptor.[295] This hypothesis is consistent with observations that arthritis in HLA-B*27+ rats requires T-cells, but not CD8+ T-cells.[196,294] Our data suggests that If ERAP1_High variants degrade peptides at a higher rate than ERAP_Low variants, that cells overexpressing the ERAP1_High variant may have more B*27 homodimers present on their surface, as compared to cells over-expressing the ERAP1_Low variant. However, surface staining for MHC class I using the HC10 antibody (detects MHC I molecules not associated with peptide) did not show a significant increase in surface staining in

the ERAP1_High variant transfected cellsv (Figure 12). Thus, if Th17 cells are the mechanism behind AS, our data suggests that ERAP1_High is not contributing to this phenomenon by increasing the amount of surface HLA-B*27 homodimers, but through a different mechanism. It has been observed that ERAP1 causes the shedding of certain cytokine receptors on the cell surface and it is possible that different ERAP1 alleles differentially affect the shedding of an important receptor on cells expressing B*27-homodimers that then affects the way that KIR3DL2-positive cells respond to them.[169,295] Future studies will be required to test these hypotheses.

Finally, our study raises the possibility that the SNPs that are low risk for AS, are contributing a protective effect by increasing the amount of non-B*27 HLA molecules presented on the cell surface. Though the results were not significant, Figure 12 demonstrates an increased trend in W6/32 staining in ERAP_Low variant expressing cells, and a decreased ME1 staining of these cells. This trend suggests that ERAP_Low may favor peptide trimming of non-B*27 HLA alleles. This could increase the amount of non-B*27 HLA Class I on the surface of cells, which could possibly confer a protective effect, potentially by altering the ratio of B*27 to non-B*27 present on the cell surface and thereby altering interactions with T cells or NK cells that are sensitive to surface expression levels of HLA molecules.

In summary, this report demonstrates that AS associated ERAP1 alleles differentially mediate levels of HLA-B*27 surface expression in cells processing a variety of HLA-B*27 destined epitopes. High AS risk ERAP1 alleles substantially reduce HLA-B*27 surface expression and antigen presentation of all tested peptides relative to low AS risk ERAP1 alleles. These findings suggest that the simultaneous presence of high AS risk ERAP1 alleles and HLA-

B*27 may increase the chances for exacerbations of inflammatory responses induced by lack of adequate levels of HLA-B*27 antigen complex surface expression. These alterations may also increased risk for abnormal interactions with the innate and adaptive arms of the immune response, with numerous consequences inclusive of an increased chance for development of auto-reactive T-cell clones. These possible mechanisms for ERAP1 dependent pathogenesis of AS will require further investigation.

Chapter 4

Mice expressing human ERAP1 variants associated with Ankylosing Spondylitis have significantly altered T-cell repertoires, NK cell functions, and in-utero mortality.

This chapter is adapted from an article submitted for publication.

Authors: David P.W. Rastall, Fadel Alyaqoub, Patrick O'Connell, Yuliya Pepelyayeva, Sarah Godbehere-Roosa, Cristiane Pereira-Hicks, Yasser Aldhamen, and Andrea Amalfitano

Introduction

Ankylosing Spondylitis (AS) is an autoimmune disease that causes inflammatory back pain and a progressive spinal ankylosis that can eventually lead to fusion of all bones in the spine and pelvis.[4] AS is one of the very few autoimmune diseases that are more common in men than women, and is highly heritable (~90%).[111] Over 90% of AS patients have specific MHC-I alleles present (including *HLA-B*27:05, B*27:02, B*13:02, B*40:01, B*40:02, B*47:01, B*51:01* and *B*57:01*),[14,28] however, only 5% of people harboring these MHC-I alleles develop the disease. As *HLA-B*27* alleles only contribute ~20% of the overall genetic risk for development of AS, other genes likely play a significant role in the genetic causation of AS.[28] These findings justified subsequent GWAS, which identified specific polymorphisms in the endoplasmic reticulum aminopeptidase 1(*ERAP1)* gene that were also highly associated with AS risk. After *HLA-B*, *ERAP1* has the strongest association of any gene with AS, and epistatic gene-gene interactions between MHC-I and ERAP1 further increased the risk for developing AS.[14,316] Interestingly, gene-gene interactions between *MHC-I* and *ERAP1* are also linked to other diseases in the same class as AS, including psoriasis,[16] and Behçet disease,[43] demonstrating that interactions between disease linked *ERAP1* and *MHC-I* alleles likely have global impacts on the immune system.

The confirmation of gene-gene interactions between *ERAP1* and *HLA-B* in GWAS of AS has led to the hypothesis that alterations in antigen presentation may be the primary cause for AS. *In vivo,* HLA and ERAP1 proteins directly interact to facilitate MHC-I antigen presentation.[139,319] The proclivity by which ERAP1 trims peptides can also predetermine the selection of peptides presented on MHC-I molecules.[147] The arthritogenic peptide hypothesis

proposes that a unique peptide presented due to the presence of specific ERAP1 and MHC-I variants cause autoimmune arthritis by recruiting auto-reactive CD8 T and/or NK cells to sites of inflammation in the spine and pelvis.[222]

Even small changes in antigen presentation can have a large impact on the immune response. For instance, in mice, the life-saving CD8 T-cell response to *Toxoplasma gondii* requires a single peptide epitope that is produced only in the presence of murine ERAP1.[262] Indeed, our lab and others have demonstrated that in the absence of ERAP1, a completely different set of peptides may be loaded onto MHC-I molecules, dramatically altering the immunodominant T-cell repertoires present in ERAP1 deficient animals.[262]

Having demonstrated that ERAP1 deficiency could completely alter the immunodominant peptidome, we next showed a similar effect was mediated by the presence of human disease-associated ERAP1 variants. For example, using *in vitro* biochemical assays we found that SNPs in ERAP1 affected their ability to process peptides, with each SNP trimming different peptides at different rates.[149,296] Furthermore, we demonstrated that the presence of all five AS-associated SNPs (associated with the highest risks for developing AS (an ERAP1 variant we refer to as ERAP1-High) in the ERAP1 protein had an additive effect, resulting in an ERAP1 protein having the fastest rate of peptide trimming, which likely resulted in over-trimming of peptides, and significant decreases in cell surface levels of MHC-I, including HLA-B*27.[149] It also appeared that ERAP1-High may have roles outside antigen presentation, as ERAP1-High expressing cells stimulated with an adenovirus, secreted increased amounts of IL-1β compared to identically treated cells expressing ERAP1-Low.[175] The converse was true for a human ERAP1 variant containing the five protective AS-risk SNPs (ERAP1-Low). ERAP1-Low had the slowest

rate of peptide trimming, and this correlated with increased antigen presentation on the surface of cells expressing ERAP1-Low.[149]

Although we confirmed that ERAP1 variants containing AS-associated SNPs trim peptides at different rates, and these changes correlate with surface expression of MHC-I, these results were obtained from biochemical assays and *ex vivo* based human tissue culture systems. To determine if AS associated ERAP1 variants also influence immune responses *in vivo*, we created two new strains of transgenic mice, one strain ubiquitously expressing the ERAP1-High variant, and a second expressing the ERAP1-Low variant.

Results

Generation of transgenic mice that express the ERAP1-High or the ERAP1-Low variant from the ROSA26 locus

To determine the physiological consequences of stable ERAP1-High expression on the immune system *in vivo*, we generated transgenic mice that ubiquitously express ERAP1-High, or ERAP1-Low (the protective control variant). *ERAP1-High* contains five disease-associated SNPs (**M**349V, **K**528R, **D**575N, **R**725Q, **Q**730E) and *ERAP1-Low* contains five protective SNPs (**V**349M, **R**528K, **N**575D, **Q**72R5, **E**730Q).[149,175] The location of these SNPs on a space-filling model of the ERAP1-High protein is shown in Figure 14A. To construct the respective mice, the ERAP1-High cDNA or the ERAP1-Low cDNA was subcloned into bacterial plasmids flanked by DNA homologous for the murine ROSA26 locus. These plasmids were co-injected into murine embryos along with zinc-finger-nucleases targeting double-stranded DNA breaks into the ROSA26 locus so that the *ERAP1* variants would be placed under transcriptional control of the ubiquitously expressed ROSA26 promoter after targeted recombination (Figure 14B).

After one round of embryo microinjections using the ERAP1-Low cDNA construct (300 embryos microinjected resulting in 74 pups), we identified two founder animals that transmitted the ERAP1-Low transgene to offspring. In stark contrast, generating the ERAP1-High transgenic mouse strain was extremely difficult, as over 900 embryonic microinjections were required, resulting in only 89 pups, before a single ERAP1-High transgenic (female) founder mouse was identified.

Unlike ERAP1-Low, transmission of the ERAP1-High transgene from generation to generation was remarkably low, and after several generations, it became apparent that the ERAP1-High transgene was only being transmitted to female mice. To control for the small

possibility that the zinc-finger nucleases simultaneously damaged DNA on the X chromosome, female ERAP1-High transgenic mice were backcrossed 5 times onto the C57BL/6 background, but still no male carriers of the ERAP1-High transgene were identified. To formally confirm that the presence of ERAP1-High negatively impacted male viability, we crossed female ERAP1-High mice with male WT (C57BL/6) mice and recorded the number and genotypes of all offspring derived from these breedings (Figure 15A). Of the 149 offspring derived from these crosses, no male ERAP1-High variant mice were identified to be among the surviving offspring ($p<0.0001$) (Figure 15A). Importantly, this effect was unique to ERAP1-High, as the transmission of the ERAP1-Low transgene in mice followed simple Mendelian genetics (Figure 15B). The loss of male ERAP1-High offspring significantly reduced the litter sizes derived from the breeding of female ERAP1-High mice ()$p<0.0001$) (Figure 15C). This decreased litter size was found to be due to a unique effect of ERAP1-High on only male offspring and was not due to a decrease in maternal fitness, as there was no impact on the numbers of female mice derived from these same crossings (Figure 15D).

Our prior publications demonstrate that ERAP1 impacts NK cell activation and development[171] and that ERAP1-High can significantly alter the peptides presented on surface MHC-I molecules.[149] Previous reports also demonstrated that peptides presented on MHC-I can play a critical role in early fetal development and survival by inhibition of maternal uterine NK cells.[320] Inhibition of these cells results in failure of the spiral arteries and spontaneous termination of the fetus.[320] These findings suggest that the decreased fitness of male ERAP1-High mice may be due to the presence of aberrant peptides loaded onto MHC-I. To determine if removing MHC-I expression on the surface of cells would rescue ERAP1-High male mice, we

crossed ERAP1-High female mice that were homozygous for the homozygous β2-microglobulin knockout allele with homozygous β2-microglobulin knockout (β2m-/-) male mice. β2m-/- mice display no MHC-I on the surface of cells but generate a normal frequency of male pups after breeding (data not shown). Of 25 offspring derived from these breedings, no male β2m-/-/ERAP1-High+/- pups were ever detected in surviving offspring (Figure 15E). This suggests that ERAP1-High is decreasing male fitness independent of the presence of MHC-I, or fetal antigen presentation. These results confirm that ERAP1-High has unique biological significance and suggest that ERAP1-High has a dominant gain-of-function mutation that causes in utero and perinatal lethality to male mice inheriting the transgene. As a consequence of this finding, all further studies described were performed using only female mice.

To further verify expression of ERAP1-High and ERAP1-Low in the respective transgenic mouse strains, we developed ERAP1-High- and ERAP1-Low-specific primer pairs, and performed quantitative RT-PCR on cDNA derived from liver tissues. We confirmed that ERAP1-High mRNA was only expressed in mice transgenic for ERAP1-High (Figure 14C), and that ERAP1-Low mRNA was only expressed in mice transgenic for ERAP1-Low (Figure 14D). We next compared the relative expression levels of ERAP1-High to ERAP1-Low mRNA using primers specific for human ERAP1, and confirmed that there were no significant differences in their expression levels when comparing the two strains of transgenic animals (Figure 14E). Finally, to compare the expression level of the transgenic human ERAP1 to the expression level of endogenous murine ERAP1 (mERAP1), we crossed ERAP1-High or ERAP1-Low mice with mERAP1-/- mice and used a generic ERAP1 primer set that binds to regions conserved between the mERAP1, ERAP1-High and ERAP1-Low mRNAs. Expression of ERAP1-High and ERAP1-

Low directed by the ROSA26 locus resulted in an approximately ten-fold lower level of expression than endogenous mERAP1 (Figure 14F), a result that parallels prior studies using the ROSA26 locus in similar strategies.[321,322] We also performed each of these analyses on additional tissues derived from brain (ectoderm), liver, thymus (endoderm), and skeletal muscle tissues (mesoderm). Results from liver are shown (Figure 14C-F) and did not differ significantly from other tissues (Supplemental Figure 15). We also analyzed by flow cytometry splenocytes derived from the two strains of mice, and confirmed that the mice were grossly immunologically intact, with both strains having an equivalent percentage of CD4 T-cells, CD8 T-cells, and NK cells as compared to WT mice (Figure 14G-I).

Figure 14: Generation of ERAP1-High variant and ERAP1-Low variant Mice.

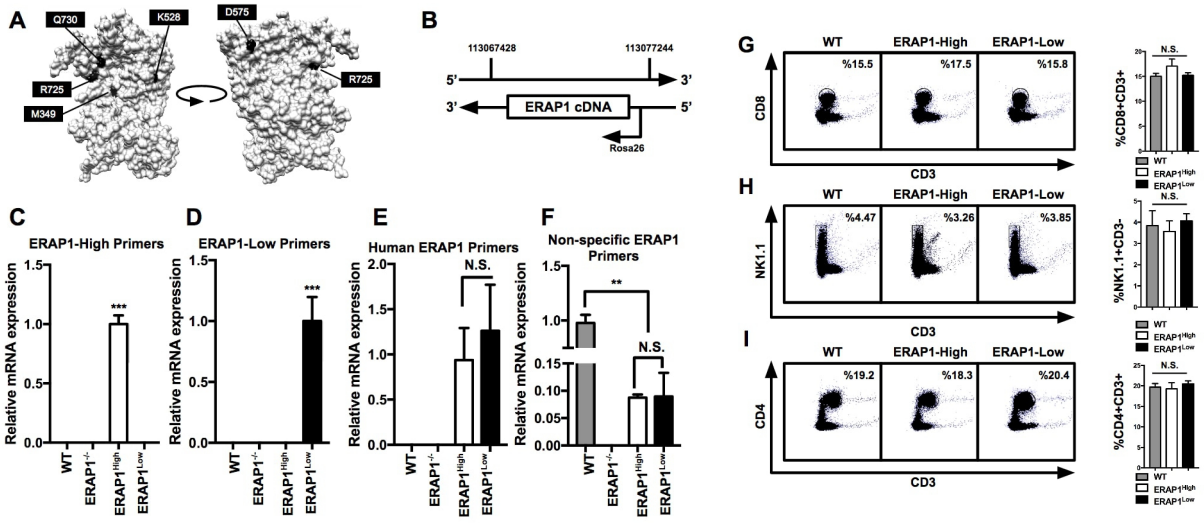

5 SNPs in ERAP1 were described to have an association with AS[25] and subsequently confirmed in vitro to have altered enzymatic activity and HLA-B27-restricted antigen presentation.[149] We used a zinc-finger-nuclease microinjection technique to generate a strain of mice expressing a human ERAP1 allele associated with increased risk for developing AS, and another with a decreased risk into the murine rosa26 locus. **A)** The location of the 5 SNPs on a space-filling model of human ERAP1. **B)** a schematic showing the human ERAP1 gene inserted into the murine Rosa26 locus to be driven by the endogenous Rosa26 promoter on chromosome 6. **C)** qPCR was used to confirm ERAP1-High expression using ERAP-High-specific primers. **D)** qPCR was used to confirm ERAP1-Low expression using ERAP-Low-specific primers. **E)** qPCR was used to compare relative expression of ERAP1-High and ERAP1-Low mRNA derived from liver tissue, using human ERAP1 primers and they were found to be equivalent. **F)** qPCR was used to compare relative expression of ERAP1-High and ERAP1-Low mRNA with endogenous murine ERAP1 primers that overlapped a conserved region. ERAP1-High and

ERAP1-Low mRNA was expressed many fold less than endogenous murine ERAP1. Flow cytometry was performed on splenocytes harvested from the indicated genotypes of mice and confirmed that the immune system was grossly intact, with each strain of mice having equal amounts of CD8+ T-cells **(G)**, NK cells **(H)**, and CD4 T-cells **(I)**. **J)** qPCR was used to compare relative expression of ERAP1-High and ERAP1-Low mRNA from in various tissues (derived from different germ layers) and they were found to be equivalent. Bars represent the relative mRNA expression normalized to GAPDH ± SEM. *** $p<0.001$ compared to all other groups. ** $p<0.01$. The figure is representative of two separate experiments.

Figure 15: ERAP1-High is lethal in male mice in an MHC-I-independent mechanism.

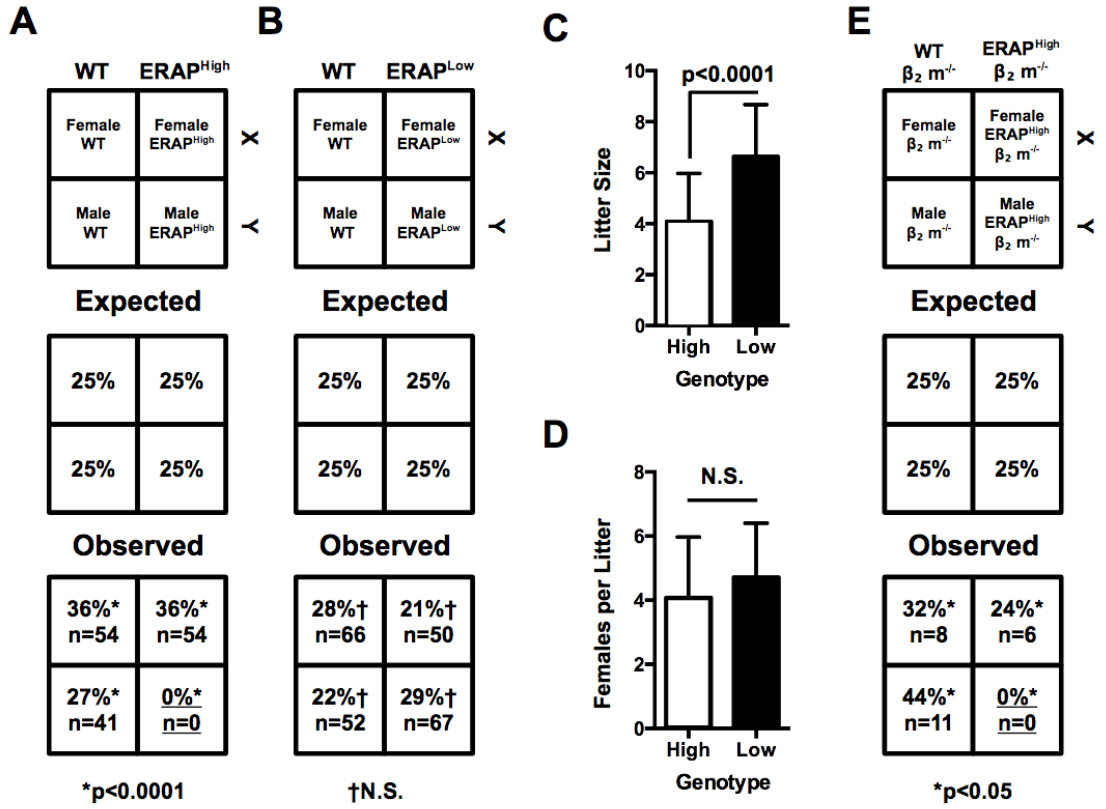

A) ERAP1Hgih+/- females were crossed with WT males. The expected and observed results of 41 crosses are shown. No male mice with ERAP1-High were born. **B)** A control cross was performed with ERAP1Low+/- females and WT males. The expected distribution of genotypes was observed. **C)** The litter sizes of ERAP1-High mice were reduced, but the number of females per litter was unaffected. **D)** To determine if ERAP1-High was lethal in males as a result of antigen presentation, ERAP1-High+/-/β2m-/- females were crossed with β2m-/- males 8 times. The removal of surface MHC-I by the cross failed to rescue the male ERAP1-High pups. N represents the number of offspring with the given genotype. Significance was determined by a chi squared test with $p<0.05$ deemed significant.

Expression of the ERAP1-High variant decreases surface levels of MHC-I in vivo.

The sum of available peptides derived from endogenous protein breakdown positively correlates with the amount of MHC-I present on the cell surface,[319,323] which in turn shapes the development and function of T cells[323] and NK cells.[151] Using an in vitro system, we previously demonstrated that ERAP1-High had increased enzymatic activity, over-trimmed peptides, and decreased the surface expression of MHC-I on the surface of human cells.[149] Therefore, we investigated whether or not ERAP1-High would have similar effects *in vivo*. We measured the surface level of murine MHC-I (H2-Kb) on a variety of immune cell types including CD8 T-cells (Figure 16A), NK cells (Figure 16B), and CD4 T-cells (Figure 16C) derived from ERAP1-High and ERAP1-Low mice, with and without the addition of interferon γ (IFN-γ), which increases surface expression of MHC-I.[324] While there were no significant differences detected at baseline, when cells were stimulated with IFN-γ, CD4 T-cells and CD8 T-cells derived from ERAP1-High mice had a subtle, but significant decrease in their MHC-I surface expression levels (Figure 16A & 16C). We hypothesized that differences mediated by ERAP1-High may be partially masked by endogenous murine ERAP1 (mERAP1), especially because ERAP1-High was expressed at a lower level than mERAP1 (Figure 14F). To determine if mERAP1 was masking the effect of ERAP1-High, we crossed ERAP1-High and ERAP1-Low mice onto the mERAP1$^{-/-}$ background and repeated the study. Without the interference of endogenous mERAP1, the presence of ERAP1-High correlated with significant decreases of MHC-I expression on CD8 T-cells (Chapter 4 Fig. 3D-E), NK cells (Chapter 4 Fig. 3F-G), and CD4 T-cells (Figure 16H-I) compared to these same cells derived from similarly treated ERAP1-Low and control (mERAP1$^{-/-}$) mice.

Figure 16: ERAP1-High significantly reduces MHC-I on the surface of cells.

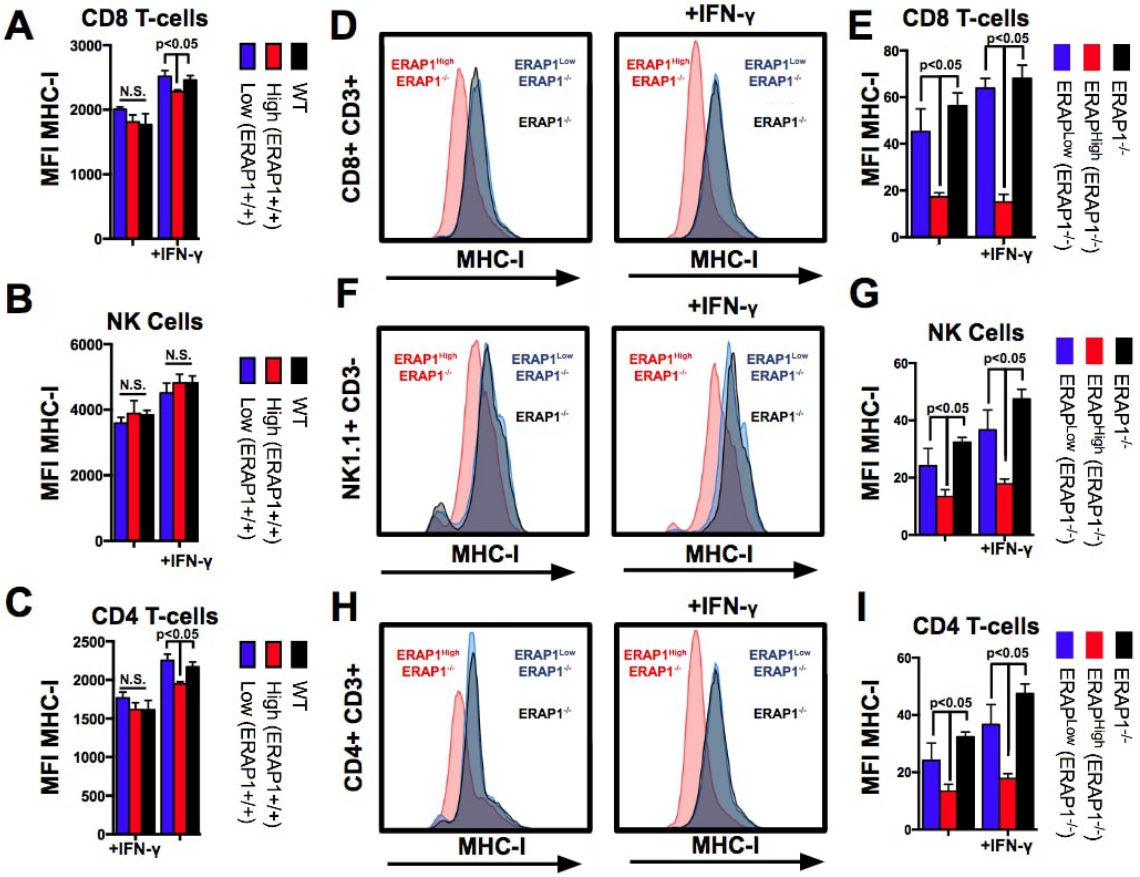

Splenocytes from the indicated genotypes of mice were harvested as described in methods. They were then activated with 0.1µg/mL IFNγ or 0µg/mL IFNγ for 2 hours, stained and analyzed with flow cytometry. A subtle, but significant reduction in surface MHC-I was observed in CD8+ T-cells **(A)**, NK cells **(B)**, CD4+ T-cell **(C)** derived from ERAP1-High mice when treated with IFNγ compared to other groups. To remove the potential masking effect of endogenous murine ERAP1 (mERAP1), ERAP1-High and ERAP1-Low mice were crossed with mERAP1-/- mice. On the mERAP1-/- background, ERAP1-High significantly reduced MHC-I surface expression in CD8+ T-cells **(D-E)**, NK cells **(F-G)**, CD4+ T-cell **(H-I)** with and without IFNγ compared to ERAP1-Low or no ERAP.

The presence of the ERAP1-High alters immunodominant T-cell adaptive immune responses in vivo.

Immunodominance is a critical phenomenon in adaptive immunity and governs the effectiveness of adaptive immune responses against intracellular bacteria,[262] viral infections[325] and cancer.[326] Moreover, patterns of T-cell immunodominance have also been linked to risk for developing autoimmune diseases that are associated with ERAP1 polymorphisms.[126,327] We previously demonstrated that the presence of ERAP1 completely reshapes the immunodominant T-cell response to model antigens such as the *Clostridium difficile* toxin A (TA).[148] We therefore wished to determine if ERAP1-High and/or ERAP1-Low would similarly reshape the immune response to antigens such as TA. To identify peptides that may be differentially processed by ERAP1-High and ERAP1-Low, we performed a pilot study by immunizing mice with an adenovirus expressing TA (Ad-TA) and an adenovirus expressing HIV-Gag (Ad-Gag) as previously described.[148] Fourteen days after immunization, splenocytes from the immunized animals were exposed to a 15-mer overlapping peptide library (peptides overlapping by five amino acids) that spanned the entire TA and Gag proteins, and the production of IFN-γ to each peptide was measured using IFN-γ ELISPOT. From the 208 peptides tested, 5 generated a strong T-cell response (Figure 18A-B) in all strains of mice evaluated. Two of the peptides (ALTSYKIINGKHFYF and VNGSRYYFDTDTAIA) generated an equally strong response independent of the presence of ERAP1-High or ERAP1-Low and serve as an internal control. Three peptides (TGYTIINGKHFYFNT, EAMSQVTNSATIMMQ, and YTSINGKHFYFNTDG) generated significantly reduced T-cell responses in ERAP1-High mice as compared to ERAP1-Low and WT control animals (Figure 18A), demonstrating that ERAP1-High can selectively remove epitopes

from the immunodominant T-cell response, even at a low expression level relative to mERAP1. These differences mediated by ERAP1-High also appear to be genetically dominant, as they occur in the presence of mERAP1, effectively "overwriting"epitopes normally presented via MHC-I in WT mice (Figure 18A). We repeated the studies in the absence of mERAP1 and found that the mere presence of ERAP1-High alone significantly altered the T-cell responses to a variety of peptides in the library (Figure 17). One peptide (AAIHLCTINNDKYYF) had an unchanged, but strong response in all mice (Figure 18D), and serves as a useful internal control. Similar to results on the mERAP+/+ background, T-cell responses to several peptides were greatly diminished in ERAP1-High/mERAP1$^{-/-}$ mice (Figure 18C), demonstrating again that the usual T-cell immune responses to these peptides are abrogated in the presence of ERAP1-High, and not ERAP1-Low. Surprisingly, several additional peptides now generated T-cell immune responses in splenocytes derived from the ERAP1-High/mERAP1$^{-/-}$ mice (Figure 18E). Importantly, no such unique peptides were identified when splenocytes from ERAP1-Low mice were similarly evaluated, suggesting that ERAP1-Low shares some overlapping trimming specificity with murine ERAP1. Finally two peptides generated decreased T-cell responses in the presence of either ERAP1-High or ERAP1-Low (Figure 18F). In our previous work we demonstrated that these same peptides also failed to elicit T-cell responses in the presence of the mERAP1 protein,[148] and were only immunogenic in the absence of mERAP1. Because they are removed from the immunodominant T-cell response by ERAP1-High, ERAP1-Low, and mERAP1, they may belong to a set of peptides destroyed by many, or all forms of ERAP1.

The presence of these same human ERAP1 variants did not significantly impact the humoral arm of the adaptive immune response of the mice, as an ELISA measuring total Ig

responses to the TA and Gag peptides demonstrated no significant difference in the quantity or specificities of these antibody responses [Data not shown].

Figure 17: ERAP1-High significantly alters the immunodominant profile to exogenous antigens.

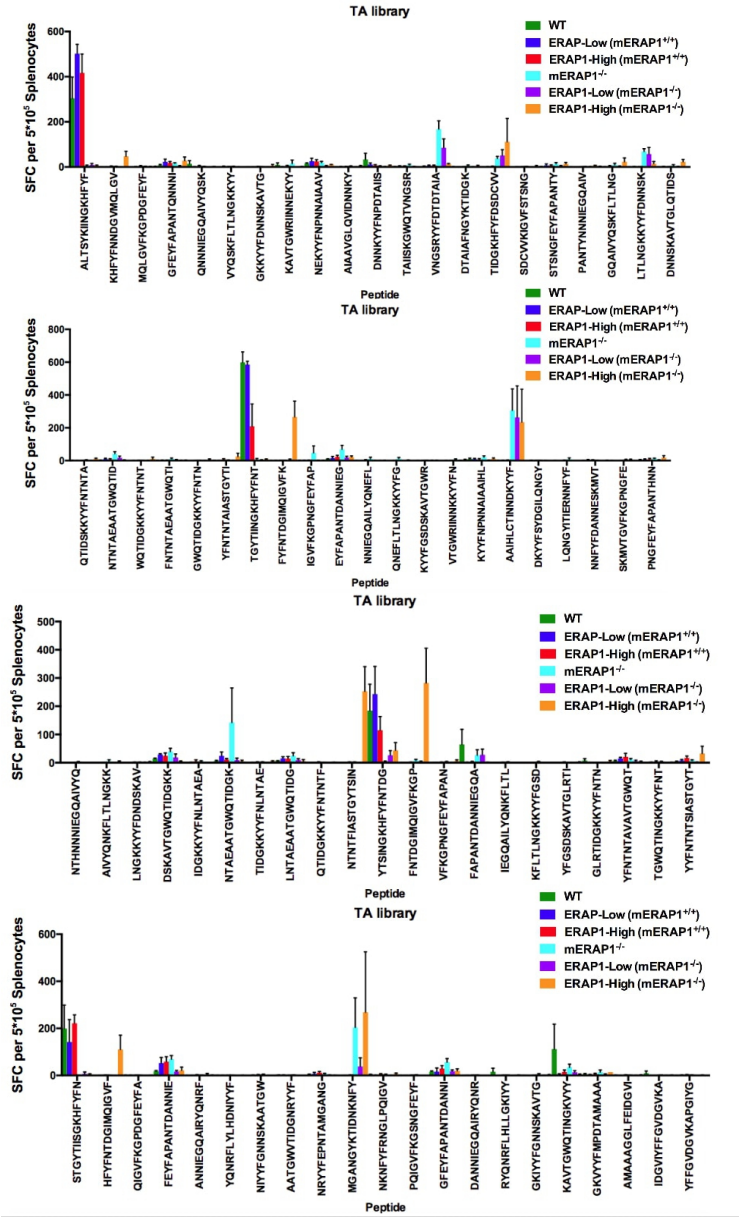

Mice were immunized I.M. in the tibialis anterior with Ad5-*Clostridium difficile*-TA as described in Methods. At day 14, mice were sacrificed and splenocytes were harvested and stimulated with 2 μg per well of the listed 15-mer peptides. Splenocytes were then analyzed for IFN-γ production using IFN-γ ELISpot. Total library shown.

Figure 18: ERAP1-High significantly alters the immunodominant profile to exogenous antigens.

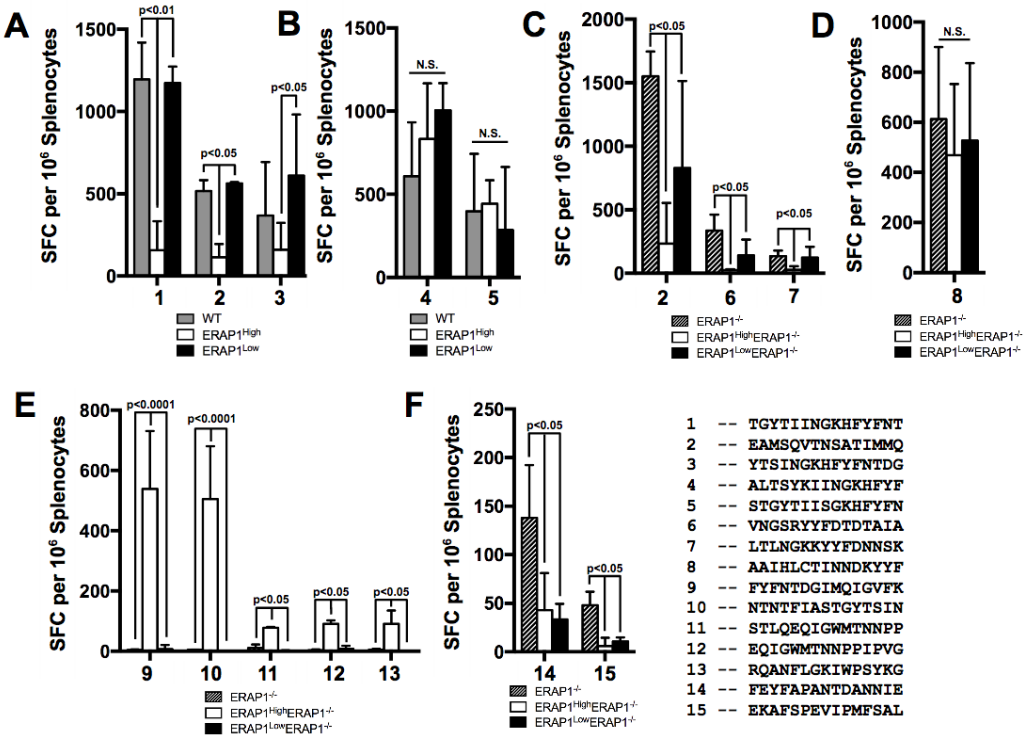

Mice were immunized I.M. in the tibialis anterior with Ad5-*Clostridium difficile*-TA and Ad5-HIV-Gag as described in Methods. At day 14, mice were sacrificed and splenocytes were harvested and stimulated with 2 μg per well of the listed 15-mer peptides. Splenocytes were then analyzed for IFN-γ production using IFN-γ ELISpot. From the 84 and 121 peptide libraries, the peptides that generated a strong response (100 or more spots) and showed an average of at least 100 less spots in the other strain of mouse were selected and repeated. **A)** Peptides that were significantly different between ERAP1-High and ERAP1-Low. **B)** Peptides that were strong responders but not significantly different between ERAP1-High and ERAP1-Low variant. All responding peptides that were different were reduced in ERAP1-High compared to ERAP1-Low variant and WT mice. To remove the effect of endogenous murine ERAP1, the experiment was

repeated in mERAP1-/-, ERAP1-High/mERAP1-/-, and ERAP1-Low/mERAP1-/- mice. **C)** Peptides that had significantly less T-cell response in ERAP1-High/ERAP1-/- compared to ERAP1-Low/ERAP1-/-. **D)** Peptides that were strong responders but not significantly different between ERAP1-High/ERAP1-/- and ERAP1-Low variant/ERAP1-/-. **E)** Peptides that only generated T-cell response in ERAP1-High/ERAP1-/-. **F)** Peptides that were significantly reduced by both ERAP1-High and ERAP-Low on the ERAP1-/- background. Bars represent the mean number of spot-forming cells per 10^6 splenocytes ± SEM. Below are representative wells. A *P* value < 0.05 was statistically significant. The figure is representative of two separate experiments.

Presence of ERAP1-High correlates with decreased NKG2D expression on CD8 T-cells and NK cells.

In addition to its usual role in fostering adaptive immune responses via antigen presentation, the presence or absence of antigen loaded MHC-I molecules can also impact the development[151] and activation[328] of NK cells. We previously demonstrated that following innate stimulations, NK cells derived from mERAP1$^{-/-}$ mice had increased NK cell activation levels (CD69 expression) as compared to NK cells derived from WT mice.[18] To determine if ERAP1-High or ERAP1-Low altered activation or phenotypes of NK cells at baseline (without immune stimulation) we harvested splenocytes from WT, mERAP1$^{-/-}$, ERAP1-High, ERAP1-Low, ERAP1-High/mERAP1$^{-/-}$, and ERAP1-Low/mERAP1$^{-/-}$ mice and phenotyped these cells with CD3, NK1.1, CD94, Ly49D, CD69, CD107a, and NKG2D fluorescent antibodies. CD3- NK1.1+ cells derived from all these strains of mice demonstrated similar expression levels of CD94, Ly49D, CD107a, and CD69 [Data not shown]. Interestingly, mERAP1$^{-/-}$ mice lacked expression of NKG2D on their NK cells (Figure 19A-B). ERAP1-High/mERAP1$^{-/-}$ mice also lacked NKG2D from the surface of their NK cells, although WT and ERAP1-Low/mERAP1$^{-/-}$ mice had normal surface expression levels of NKG2D (Figure 19A-B). These surprising results demonstrate that deficiency of ERAP1 results in an almost complete loss of NKG2D expression on NK cells, and that the presence of ERAP1-Low (but not ERAP1-High) restores NKG2D surface expression to NK cells. ERAP1-High mice have normal levels of NKG2D expression when on the mERAP1+/+ background (Figure 19C).

NKG2D is a constitutively expressed activating receptor on NK cells and CD8 T-cells in mice.[329] Similar to NK cells, CD8+ CD3+ cells derived from both mERAP1$^{-/-}$ and ERAP1-

High/mERAP1$^{-/-}$ animals had no surface NKG2D expression (Figure 19D-E), while NKG2D expression was preserved in ERAP1-High/mERAP1+/+ mice (Figure 19F).

Figure 19: ERAP regulates NKG2D expression on NK cells and CD8 T-cells.

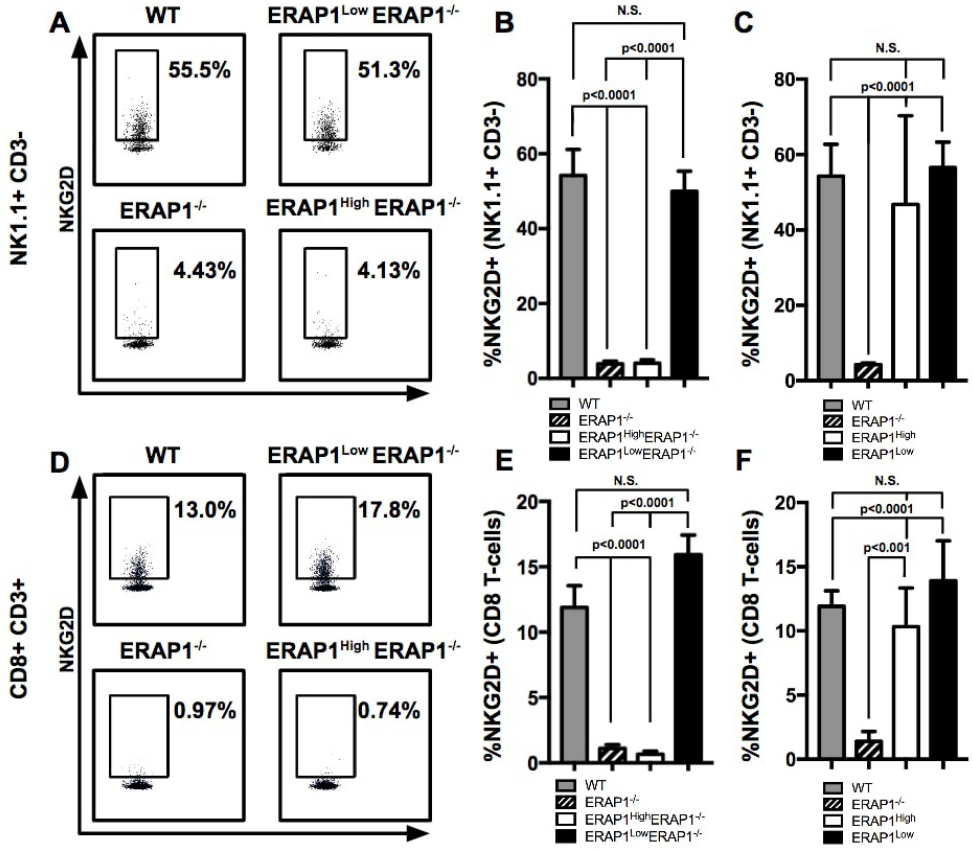

NK cells were isolated from WT, ERAP1-/-, ERAP1-High/ERAP1-/- and ERAP1-Low/ERAP1-/- mice and surface NKG2D was measured by flow cytometry. **(A)** Representative image of NKG2D on NK1.1+ CD3- splenocytes from WT, ERAP1-/-, ERAP1-High/ERAP1-/- and ERAP1-Low/ERAP1-/- mice. **(B)** %NKG2D on NK1.1+ CD3- splenocytes demonstrates a complete loss of NKG2D on NK cells from ERAP1-/- and ERAP1-High ERAP1-/-. **(C)** Representative image of NKG2D on CD8+ CD3+ splenocytes from WT, ERAP1-/-, ERAP1-High/ERAP1-/- and ERAP1-Low/ERAP1-/- mice. **(D)** %NKG2D on CD8+ CD3+ splenocytes demonstrates a complete loss of NKG2D on NK cells from ERAP1-/- and ERAP1-High ERAP1-/-. Murine ERAP1 blocked the effect of ERAP1-High on NKG2D in NK cells **(E)** and

CD8 T-cells **(F)**. CD4+ CD3+ T-cells were also examined in all genotypes and found to not express a significant amount of NKG2D in any genotype (Data not shown).

mERAP1$^{-/-}$ and human ERAP1 variant expressing mice have altered NK mediated killing of MHC-I-deficient cells.

We next determined if mERAP1 had a direct, intrinsic effect on NK cell killing capabilities, and if ERAP1-High and ERAP1-Low may alter this effect. Utilizing an *ex vivo* killing assay, NK cells derived from mERAP1$^{-/-}$ mice killed more RMA-s target cells (MHC-I deficient) than NK cells derived from WT mice (Figure 20A). This is the first report demonstrating that ERAP1 intrinsically impacts NK cell killing functions. NK cells from WT, ERAP1-High, and ERAP1-Low variant mice were similarly analyzed. NK cells from ERAP1-High mice had similar levels of RMA-s cell killing as NK cells derived from WT mice (Figure 20B). Surprisingly, NK cells derived from ERAP1-Low mice killed significantly more target cells than NK cells derived from ERAP1-High mice, or WT mice (Figure 20B).

As the differences in NKG2D and MHC-I expression levels mediated by ERAP1-High were observed only in the mERAP1$^{-/-}$ background, we repeated this experiment utilizing NK cells derived from ERAP1-High/ERAP1$^{-/-}$, and ERAP1-Low/ERAP1$^{-/-}$ mice. Again, the presence of ERAP1-Low in NK cells significantly increased their capacity to kill target cells, while the presence of ERAP1-High did not (Figure 20C). Compared to ERAP1$^{-/-}$, ERAP1-Low/ERAP1$^{-/-}$ NK cells appeared to kill more target cells, suggesting that ERAP1-Low increases NK killing capacities via a mechanism independent of antigen presentation or NKG2D signaling.

Figure 20: ERAP1 regulates NK cell killing.

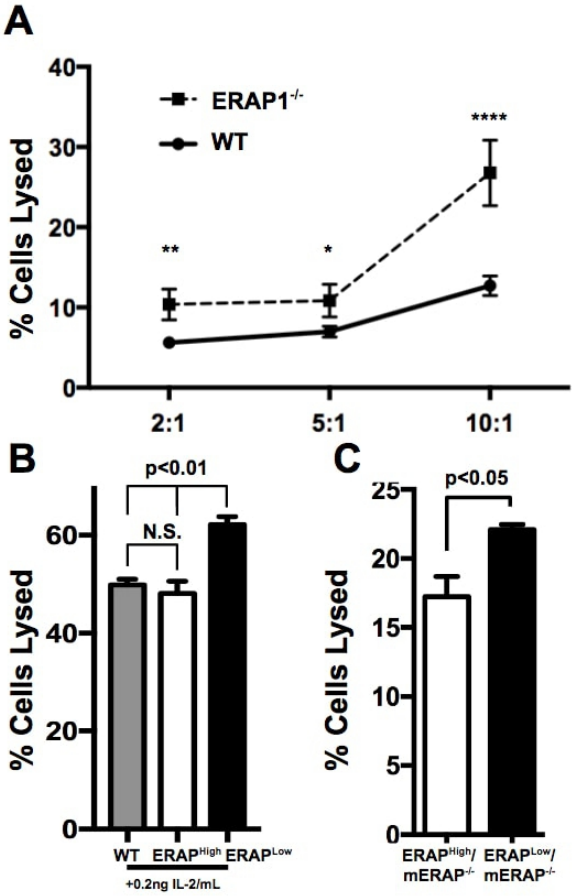

NK cells were isolated from WT and ERAP1-/- mice and incubated with RMA-s target cells at the indicated effector to target (E:T) ratios for 48 hours. **A)** At all E:T ratios NK cells derived from ERAP1 deficient mice demonstrated increased killing. **B)** To test the effect of disease-associated ERAP1 variants, NK cells were isolated from ERAP1-High, ERAP1-Low, or WT mice and NK killing assay performed as described in methods. Surprisingly, ERAP1-Low had higher killing than ERAP1-High or mERAP1. **C)** To determine if mERAP1 or IL-2 were impacting the effect of ERAP1-Low on NK cells, we performed the killing assay with NK cells derived from ERAP1-High/mERAP1-/- and ERAP1-Low/mERAP1-/- mice and observed that ERAP1-Low still mediated increased killing.

Discussion

The correlation of the presence of specific HLA-B27 variants with AS susceptibility has been known for over 40 years. The association of these variants with AS remains one of the strongest associations in any complex genetic disorder, with an odds ratio of up to 170.[116] However, *HLA-B*27*, contributes only ~20% to the overall genetic burden of AS, leaving ~70% of the heritable risk for AS unexplained.[14,111,117,118] When GWAS were conducted to identify the remaining genetic risk factors, they identified ERAP1 as the gene with the strongest association for AS after HLA-B27 and found that the two genes interacted to further increase the odds for developing AS.[14,316] Unfortunately, GWAS can only correlate the presence or absence of SNPs with disease susceptibilities. Additional extensive studies are always required to ascribe biological significance to the genetic regions or specific gene variants identified in GWAS.

While we and others have utilized in vitro and ex vivo systems to identify biological impacts of AS associated ERAP1 variants,[149,175,296] here we demonstrate for the first time the systemic effects that AS-associated ERAP1 polymorphisms can have, using transgenic animal models. The work presented here is the first evidence that the expression of specific, AS-associated human ERAP1 variants can significantly impact several aspects of mammalian biology, including in utero survival, the innate immune system, and the adaptive immune system.

Relative to impacts on the adaptive immune system, our results found that the immunodominant CD8+ T-cell repertoire to exogenous antigens in animals could be significantly altered dependent upon the presence or absence of specific, AS-associated ERAP1 variants. Furthermore, the changes in immunodominance mediated by the presence of the

ERAP1-High variant were profound, and ERAP1-High had as much of an impact on the presentation of specific peptides as the differences between two HLA molecules.[319,330] Introduction of ERAP1-Low into the C57BL/6 mouse had almost no change on which peptides derived from an exogenous antigen became immunodominant (Figure 19). The presence of ERAP1-High was also able to overwrite the impact that endogenous murine ERAP1 had on immune-dominant antigen selection, effectively ablating T-cell responses to specific peptides normally destined to generate an immunodominant T-cell response. We have previously shown that the ERAP1-High variant has an abnormally high enzymatic activity and is able to over-trim peptides, potentially destroying a unique set of peptide epitopes prior to their loading onto MHC-I. Therefore it is likely that the presence of ERAP1-High in mice also removes otherwise immunodominant epitopes by destroying these peptides before they can be loaded onto MHC-I.[149] Furthermore, this unique property of ERAP1-High appears to be globally impactful, since the presence of ERAP1-High correlates with a reduction in the overall surface levels of MHC-I on a variety of cell types in vivo; results consistent with our earlier ex vivo work.[149] The presence of ERAP1-High also generated a unique set of immunodominant epitopes derived from exogenously provided antigens, furthering the potential impact this AS-associated variant may have on adaptive immune responses.

Abnormalities in the innate immune system, and in particular, NK cells, have been demonstrated in patients with AS.[171,175,331,332] Specifically, it has been shown that AS patients have higher numbers of circulating NK cells, and that NK cells from AS patients express a higher percent of CD56, and CD16.[228,331,332] The theory that NK cells may be involved in AS was strengthened by the observation that certain variants of HLA-B*27 form homodimers that can

activate the inhibitory receptor KIR3DL1 on NK cells.[227] Our prior *ex vivo* work demonstrated that ERAP1 can also impact NK cells, as NK cells from mERAP1$^{-/-}$ mice had higher frequencies of terminally matured NK cells, as well as higher frequencies of licensed NK cells and more active NK cells following TLR stimulation.[171]

In this report we confirmed that the presence or absence of mERAP1 can significantly impact NK cell killing, and further demonstrated that AS-associated polymorphisms in ERAP1 can also have an impact on these functionalities. To investigate how ERAP1 may be further altering the phenotype of NK cells, we measured the surface levels of several NK receptors and found only the levels of NKG2D were altered. Specifically, loss of *mERAP1* resulted in complete lack of NKG2D on the surface of NK cells and CD8 T-cells (Figure 26). The presence of ERAP1-Low restored the surface level of NKG2D to mERAP1$^{-/-}$ mice while the presence of ERAP1-High did not. This suggests that a loss-of-function mutation in ERAP1-High may impact the NKG2D pathway.

The discovery of a role for ERAP1 in the NKG2D pathway is significant because NKG2D itself has been directly implicated in autoimmune diseases in mice[333] and humans,[334] and is also associated with AS via its ligand, MICA. MICA activates NK and CD8 T-cells via its interaction with NKG2D, and polymorphisms in MICA are also associated with early-onset AS.[335,336] Interestingly, mice constitutively expressing MICA have decreased NKG2D surface levels on their NK cells,[337] and human NK cells stimulated for long periods with MICA also have decreased NKG2D surface levels.[338] Therefore, it is possible that NKG2D may become over-stimulated in mERAP1$^{-/-}$ and ERAP1-High /mERAP1$^{-/-}$ mice due to the propensity of these mice to have exaggerated innate immune system responses to known innate immune system

agonists.[171,175]

This would also support findings in AS patients, since the MICA polymorphism associated with early-onset AS mediates increased activation of NKG2D.[336] However, these possibilities become somewhat clouded by our additional finding that the presence of ERAP1-Low increases NK-mediated killing. This surprising result suggests that ERAP1-Low increases NK-mediated killing of MHC-I deficient cells via a mechanism outside antigen presentation and NKG2D signaling. Future studies will be necessary to fully understand the impact that AS-associated ERAP1 variants have on NK cell biology.

Another unexpected result of this work was the observation that the presence of ERAP1-High is lethal to male mice. There are few dominant lethal alleles, and even fewer that selectively kill one sex.[339] Furthermore, to our knowledge there are no dominant lethal sex-linked alleles located on an autosome (as opposed to a sex chromosome).[339] It is interesting that we observed this sex-specific effect of ERAP1-High, as AS is one of the few autoimmune diseases more common in men than in women.[4,111] The mechanism behind this phenotype remains unclear. One potential explanation is that unique antigens derived from proteins on the Y chromosome are being differentially trimmed by ERAP1-High and therefore are only presented in ERAP1-High male fetuses.[320] However, because the ERAP1-High male lethal phenotype persisted despite extensive backcrossing onto a $\beta 2m^{-/-}$ background, it seems that ERAP1-High acts as a dominant lethal allele independent of its role in antigen presentation. Possibly, the ERAP1-High protein acts in a dominant-negative fashion relative to a critical protein expressed from the murine X chromosome. Interestingly, direct interaction between ERAP1 and RBMX (RNA-binding motif gene, X chromosome) has been observed[340]. Possibly ERAP1-High is

binding enough RBMX in male mice so as to significantly inhibit the RNA-splicing functions of RMBX, causing embryonic lethality. The future study of these findings may help better understand the reported association of ERAP1 variants in preeclampsia and gestational disease.[127]

Beyond the role of ERAP1 and its variants in susceptibility to various diseases, this work is also important for the field of antigen presentation as a whole. Our results demonstrate that the presence or absence of specific ERAP1 variants can alter antigen presentation drastically *in vivo*. Much work has been done to predict which peptides will become immunodominant epitopes, especially for vaccine development, cancer immunotherapy, and precision medicine.[341–343] The majority of these efforts have focused exclusively on using specific MHC-I peptide binding and presentation models to attempt to predict the ultimate immunodominant CD8 T-cell responses to a given antigen.[341,343] Although these predictions work well in syngeneic animal models, they seem to have hit an upper range of accuracy (between 70-80%) when applied to predictions of human immunodominant immune responses.[343,344] These realities prompted the creation of multiple strains of HLA-humanized mice to help predict human immunodominant epitopes for vaccine development, but these mice also did not accurately predict which epitopes eventually became immunodominant when human studies were attempted.[345] Based on the work presented here, we suggest that the plateau in human applications of these predictive models may be overcome by also considering the presence or absence of specific human ERAP1 alleles in the respective model systems.

In this work, the presence or absence of specific ERAP1 variants also appeared to be mediated by several mechanisms. Our results uncovered a mix of dominant and recessive

phenotypes when the ERAP1-High or ERAP1-Low variants were expressed in mice. For example, the male-lethal phenotype (Figure 15) and the destruction of various antigen-derived epitopes (Figure 18A) appeared to be genetically dominant, as these phenotypes were observed in mice regardless of the presence of mERAP1. In contrast, ERAP1-High decreased the surface expression of MHC-I on the surface of cells (Figure 16) and the loss of surface NKG2D (Figure 20), only in the mERAP1$^{-/-}$ background, suggesting that these ERAP1-High dependent phenotypes are genetically recessive.

The presence or absence of the ERAP1-Low variant also mediated intriguing phenotypes in both dominant and recessive fashions. ERAP1-Low dependent increases in the NK mediated killing of MHC-I deficient cells occurred regardless of the presence or absence of mERAP1. In contrast, the effect of ERAP1-Low on presented antigens was recessive, as it was only apparent with the removal of murine ERAP1 (Figure 17F).

Overall, these studies demonstrate that human ERAP1 variants identified by GWAS as important, relative to AS and other auto-immune disease susceptibilities, can be demonstrated to have major impacts on antigen presentation, overall MHC-I abundance, T-cell immunodominance, NK cell functions *in vivo*, as well as overall male survival. The results here translate genetic associations made from GWAS into a better understanding of the complex biological role these ERAP1 variants have within a living organism.

Chapter 5

ERAP1 modifies risk for developing spinal ankylosis and osteoporosis

This chapter is adapted from an article that is being submitted for publication.

Authors: David P.W. Rastall, Yuliya Pepelyayeva, Sandra Raehtz, Patrick O'Connell, Fraser L. Collins, Sarah Godbehere-Roosa, Cristiane Pereira-Hicks, Laura R. McCabe, Andrea Amalfitano

Introduction

Ankylosing Spondylitis (AS) is an autoimmune disease that causes inflammation, sporadic bony fusion of vertebral joints, and osteoporosis.[4,48] Most forms of arthritis have a late onset and predominantly involve the joints of the peripheral skeleton. AS is fundamentally different. AS affects young people (mean age 26),[47] and the arthritis begins in the axial skeleton, and affects the peripheral skeleton in less than 35% of cases.[51,52] AS is defined by its hallmark feature, spinal ankylosis. Bridging calcifications form between adjacent bones and those bones fuse. Ankylosis can occur between two vertebrae, between a lumbar vertebra and the sacrum, or between the sacrum and the ilium. In all cases the first finding on radiology is a loss of bone. Between two vertebra bone loss is seen at the superior and inferior endplates (termed the shiny corner sign) and at the sacroiliac joint bone loss is seen as an initial widening of the joint with prominent erosions on the iliac side of the joint.[346] Paradoxically, following this period of bone loss, abnormal bone forms at the affected joints until they fuse completely. In the spine this can be observed as bridging syndesmophytes, calcifications of the anterior longitudinal ligament, and intervertebral Anderson lesions. Importantly, these observations have been made via radiology, so it is unknown if any abnormal cells are present, or how the fusion progresses within the joint space that is not easily visualized on radiography. While excess bone is deposited along the joints of the axial skeleton, osteoporosis begins within the same bones. The phenomenon of cortical thickening and syndesmophyte formation masks underlying osteoporosis of the trabecular bone on radiograph, making detection of osteoporosis in AS patients difficult and explaining why this feature was only recognized once more advanced imaging became accessible. AS patients have been shown to lose trabecular bone and have decreased bone

mineral density (BMD) in their lumbar spine, radius and femoral neck.[10] This finding is very significant as the excess bone deposition along the outside of the axial skeleton, coupled with osteoporosis explains the high spinal fracture risk associated with AS.[347]

AS is a highly heritable disorder. Over 40 years ago HLA-B*27 became the first gene associated with AS and suggested that MHC-I antigen-presentation may be involved with the disease.[23,24,348] Subsequent genetic studies confirmed that multiple HLA-B alleles are associated with AS, and identified an association between AS and alleles of *ERAP1*, another antigen-presentation gene.[14,316] After HLA-B, ERAP1 alleles have the strongest association with AS and gene-gene interactions between ERAP1 and HLA-B further increase the risk for developing AS.[14,316] ERAP1 and MHC-I are the two core elements of the mammalian antigen presentation pathway that determine which peptides are presented on all nucleated cells.[249,319] ERAP1 trims peptides for loading into the peptide-binding groove in HLA, and after HLA is loaded with peptide it associates with beta-2-microglobulin (β2m) and relocates to the cell's surface.[319] ERAP1 is critical in this pathway, as we and others have shown that the presence or absence of ERAP1 can completely alter which peptides are loaded onto MHC1 molecules, and in turn direct the adaptive immune system.[148,249] For these reasons, many have hypothesized that antigen presentation in and of itself may play a central role in the pathogenesis of AS.[14,316,349] This theory is further supported by the observation that while most HLA-B*27 MHC-I alleles are associated with AS, the two HLA-B27 alleles that are protective (HLA-B*27:09 and HLA-B*27:06) differ only in 1-2 amino acid residues located at the peptide-binding groove, and therefore only in the peptides they bind.[117,118] Despite the mountain of genetic evidence that implicates antigen-

presentation as the cause of AS, no link between MHC-I antigen presentation and bone regulation has been shown. This is the major limitation with the antigen-presentation theory of AS.

To address this limitation we wished to study the effect of ERAP1 on bone homeostasis. We previously showed that ERAP1$^{-/-}$ mice develop exaggerated inflammatory responses in response to immune adjuvants. For instance in response to adenoviruses and TLR activators, ERAP1$^{-/-}$ mice produced increased levels of TNF-α, IL-6, and IL-17.[171] All of these cytokines were found increased in AS patients and play important roles in arthritis.[59,350] TNF-α and IL-6 increase bone resorption by increasing osteoclast differentiation and activity,[351,352] while IL-17 may promote inflammation at the enthesitis, where bones connect to ligaments.[191] Because the ERAP1$^{-/-}$ mice mimicked the pro-inflammatory cytokine changes observed in AS, we believed that they may also have alterations in their bones.

To investigate if ERAP1 had a significant role in bone homeostasis, we investigated the skeletal system in ERAP1$^{-/-}$ animals. In this study we demonstrate that ERAP1$^{-/-}$ mice develop ankylosis in their axial skeleton and osteoporosis. Additionally complete disruption of antigen presentation by removal of β_2 microglobulin (β2m) resulted in development of a similar level of spinal ankylosis, and an even more profound systemic osteoporosis. ERAP1$^{-/-}$ mice will serve as a model to study therapeutics for prevention of bone fusion, osteoporosis, and other features of AS.

Results

Loss of ERAP1 results in spinal ankylosis, in the absence of peripheral arthritis.

Previous reports in rodent models of AS have primarily duplicated secondary/associated features of the disease including colitis, uveitis, aortitis, enthesitis, and peripheral arthritis, but not spinal ankylosis.[191,192,207] Pathology in the axial skeleton of these models, when present, was less frequent, less severe, and occurred secondary to severe arthritis in the feet.[191,192,207,353–355] We therefore began our studies by aging and monitoring ERAP1$^{-/-}$ mice for signs of peripheral arthritis as previously described.[207,355] Alongside ERAP1$^{-/-}$ mice, we chose to age and monitor several other genotypes for peripheral arthritis, including HLA-B*27:05/B2m$^{-/-}$ mice that had been previously described to develop arthritis in their hind feet, and were included as a positive control.[207,355] Despite this effort, we observed no convincing evidence of peripheral arthritis in WT mice (n=39), ERAP1$^{-/-}$ mice (n=42), B2m$^{-/-}$ mice (n=26), HLA-B*27:05/B2m$^{-/-}$ mice (n=53), or HLA-B27/B2m$^{-/-}$/ERAP1$^{-/-}$ mice (n=21). Of the 181 animals, only four developed foot inflammation and there was no correlation with genotype or sex (Data not shown). To assure ourselves that we weren't overlooking evidence of subclinical inflammation that may non-the-less impact the bones of the feet, we harvested the paws of WT, ERAP1$^{-/-}$, B2m$^{-/-}$ mice and analyzed them using micro computed tomography (μCT). Again, no significant differences were observed in the various strains of animals analyzed (Data not shown). This finding is contradictory to previous reports that HLA-B*27:05/B2m$^{-/-}$ mice spontaneously develop peripheral arthritis.[206,207] However, the previous reports found that the mice only developed arthritis when transferred from their specific pathogen free (SPF) facility to a non-SPF facility,[207]

suggesting that the differences in our findings may be attributable to differences in environment or to subtle strain specific genetic background differences.

Peripheral arthritis is only present in ~35% of AS patients,[51,52] and frequently only at older ages, while spinal ankylosis is the hallmark feature of AS.[4] Therefore, we wished to determine if ERAP1$^{-/-}$ mice develop spinal ankylosis. Mice were sacrificed at 14, 37, and 80 weeks and a μCT analysis of their bones was performed. MCT scans were reconstructed in MicroView software and 2D slices and 3D isosurfaces were analyzed and scored for features of spinal ankylosis including vertebral fusion, calcification of the anterior longitudinal ligament, and sacroiliac erosions. Bridging syndesmophytes and fusions were observed most frequently at the L6/Sacrum intervertebral joint, and were scored using a system that quantifies the severity of bridging syndesmophytes present at a respective joint. Scores were assigned to each joint analyzed in a respective animal as described in chapter 5 Figure 1A. Our results confirmed that ERAP1$^{-/-}$ mice develop a previously unreported propensity to spontaneously develop bony ossifications between their sacral and vertebral joints. Furthermore, similar to the highly unpredictable and sporadic formation of spinal fusions in AS, the age at which spinal ankylosis occurred appeared to be highly variable and sporadic (Figure 21B&C). Importantly, all ERAP1$^{-/-}$ mice had evidence of significant spinal ankylosis by 80 weeks of age (Figure 21C). Notably, of the 41 similarly evaluated WT mice, only one was observed to have a single, unilateral fusion of one vertebrae, the remaining WT animals had no evidence of ankylosis at these joints.

In addition to these findings, several other bony abnormalities were observed among the ERAP1$^{-/-}$ group as compared to WT mice. In the final stages of vertebral fusion in AS, the anterior longitudinal ligament (ALL) calcifies forming a smooth surface between vertebrae.[55] In

the severe cases in the aged (80-week old) ERAP1$^{-/-}$ mice calcification of the ALL was observed (Figure 21D). In AS erosions at the ilia side of the SI joint typically precede the onset of SI fusion.[55] Similar lesions were observed in the 80-week old ERAP1$^{-/-}$ mice, with prominent erosions along the iliac surface of the SI joint (Figure 21E). To differentiate this from any age-related changes, this was quantified as described in the figure and the result demonstrates that ERAP1$^{-/-}$ mice developed significantly ($p<0.05$) more erosions than WT mice (Figure 21F).

Figure 21: Loss of ERAP1 results in spinal ankylosis.

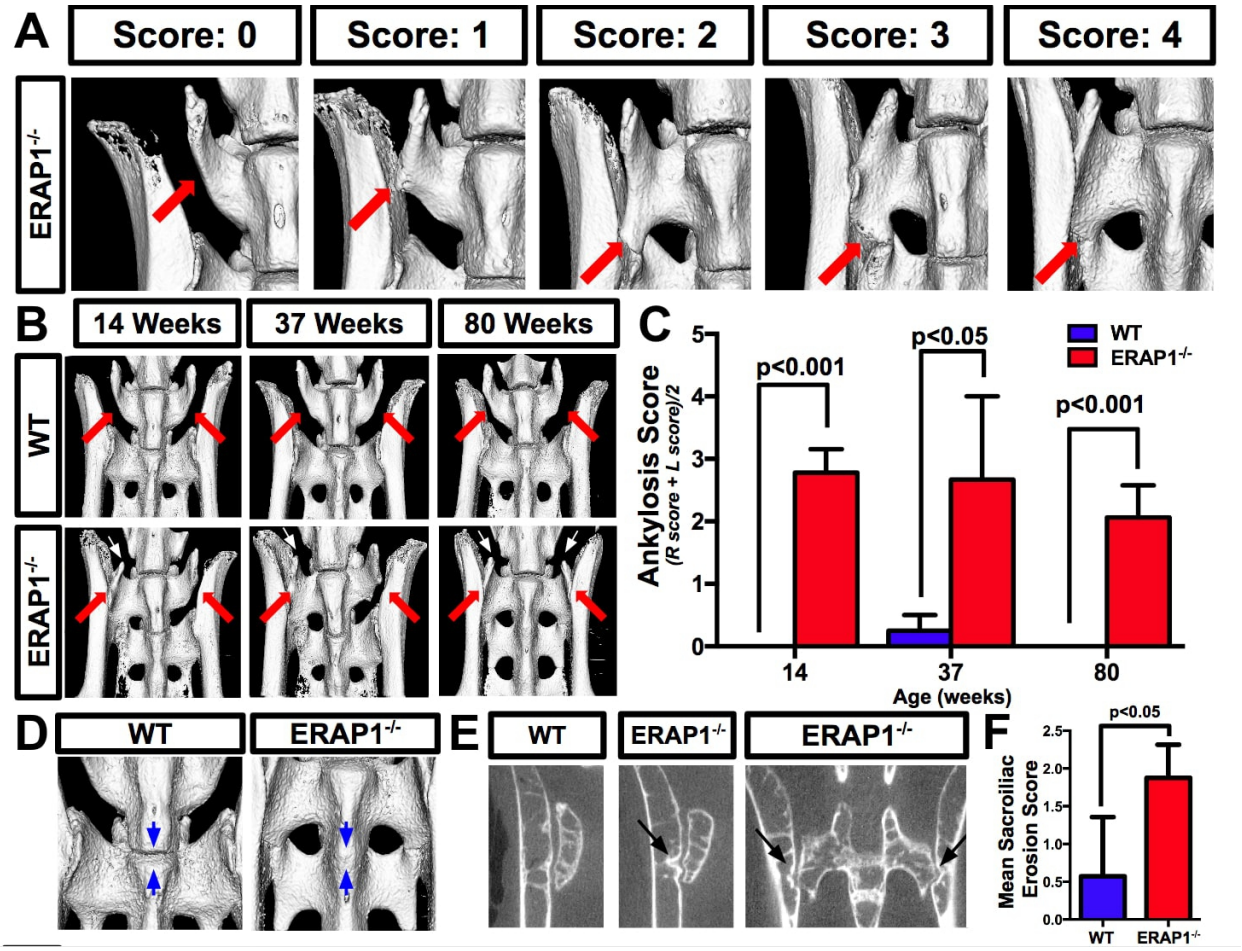

The spine and ilia were harvested from 80 week old ERAP1-/- and WT mice and analyzed with µCT and H&E. **A)** Scoring system with representative images of each score (from ERAP1-/- animals). R/L sides were scored separately 0-4, then the scores were averaged. A 0 represented WT morphology of L6; a 1 represented the beginning of a syndesmophyte growing from L6; a 2 represented a syndesmophyte that exceeded 3mm in length and crossed the joint; a 3 represented a bridging syndesmophyte that had not yet fully fused; and a 4 represented a fully fused joint. **B)** Representative isosurfaces of ERAP1-/- and WT mice demonstrating spinal ankylosis and unilateral or bilateral fusion of the L6 vertebra to the sacrum in ERAP1-/- mice.

Bold red arrows indicate the L6 vertebra. Fine white arrows indicate remnants of the transverse process of L6, which is rotated during fusion. Isosurfaces are oriented with the anterior surface of the spine facing out and the caudal spine at the top of the image. **C)** Graph representing mean score of all WT (n=24) and ERAP1-/- (n=28) mice by age. **D)** Representative images demonstrating that the anterior longitudinal ligament is calcified in some of the ERAP1-/- animals similar to in patients with advanced AS. Blue arrows indicate the location of the anterior longitudinal ligament as it traverses L6 to S1. **E)** Representative 2D radiograph demonstrating erosions at the sacroiliac (SI) joint similar to SI erosions observed in AS. **F)** SI joints were assessed and scored for erosions. A 0 represented a smooth joint. A 1 represented a joint with mild erosions. A 2 represented erosions >1mm or >3 erosions in one joint. Both SI joints were scored separately and summed.

Osteoporosis progresses uniformly, and precedes ankylosis, throughout the lives of ERAP1$^{-/-}$ mice.

In AS osteoporosis paradoxically develops alongside ectopic bone formation.[347,356] AS patients have decreased bone mineral density (BMD), and bone mineral content (BMC) in the trabecular space of their spines, femurs, and radii,[10,74,75] as well as overall decreases in the trabecular thickness of the spine.[76] The combination of rigidity from fused joints alongside osteoporosis predisposes AS patients to a significant risk for pathologic fractures of the spine and neurologic sequelae.[4,10,347,356] Using μCT and Microview software we deployed quantitative micromorphometry to determine if ERAP1$^{-/-}$ mice also mimicked these important clinical features of AS. We chose to start the study using 14-week old animals, as at this age the spines have fully mineralized. Six quantitative, objective measures of trabecular bone loss were taken including bone mineral volume (BV/TV%), bone mineral density (BMD), bone mineral content (BMC), trabecular number (Tb. N.), trabecular thickness (Tb. Th.), and trabecular spacing (Tb. Sp.) as described in figure 2 and methods. Importantly, when analyzing S1 and L6, the entire trabecular compartment of the vertebral bodies was measured, and did not significantly vary in total volume between groups, so the BMD and BMC were not artificially skewed by changes in volume. Similar to AS patients,[10] ERAP1$^{-/-}$ mice developed osteoporosis in their sacrum (Figure 22A-B), vertebrae (Figure 22C-D), and femur (Figure 22E-F). ERAP1$^{-/-}$ mice had significantly decreased trabecular BV/TV, decreased BMC, decreased Tb. Th., and increased Tb. Sp. in the sacrum (Figure 22A-B), spine (Figure 22C-D), and femur (Figure 22E-F). Interestingly, the phenotype appeared to be the most pronounced in the sacrum and least pronounced in the long bones.

Next we performed a time-course to track the development of osteoporosis as a function of time. We chose to start the time-course using young mice (ie: 5 weeks of age), as murine bones have typically not yet completely mineralized at this age. We took the same six measurements of the trabecular bone density in the sacrum, the L6 vertebrae, and the femur at the indicated ages. Surprisingly, young ERAP1$^{-/-}$ mice already had a slight, but significant decreased in their BMC and Tb. Th. in their sacra as compared to age-matched WT mice (Figure 23A). By 14 weeks of age, the bones of all mice have completed mineralization. At this age of skeletal maturity, ERAP1$^{-/-}$ mice had significantly reduced BMV, BMD, BMC, Tb. N., and Tb. Th. and significantly increased Tb. Sp. as compared to identical studies and analyses performed in age- and sex-matched WT mice (Figure 23A). As expected, a decrease in overall bone content of the sacrum was observed to occur in WT mice as they aged beyond 14 weeks, a finding that is consistent with previously published reports in healthy mice.[357] Despite this natural decrease, the abnormally decreased bone density noted in ERAP1$^{-/-}$ mice continued to be significantly different than those noted in age-matched WT mice from 14 weeks onward (Figure 23A). The results were most pronounced at the highest ages of the animals, [Fig 22] as ERAP1$^{-/-}$ mice had significantly decreased trabecular BV/TV, decreased BMC, decreased Tb. Th., and increased Tb. Sp. in the sacrum (Figure 22A-B), spine (Figure 22C-D), and femur (Figure 22E-F).

Figure 22: Osteoporosis is present in spines and long bones of ERAP1-/- mice.

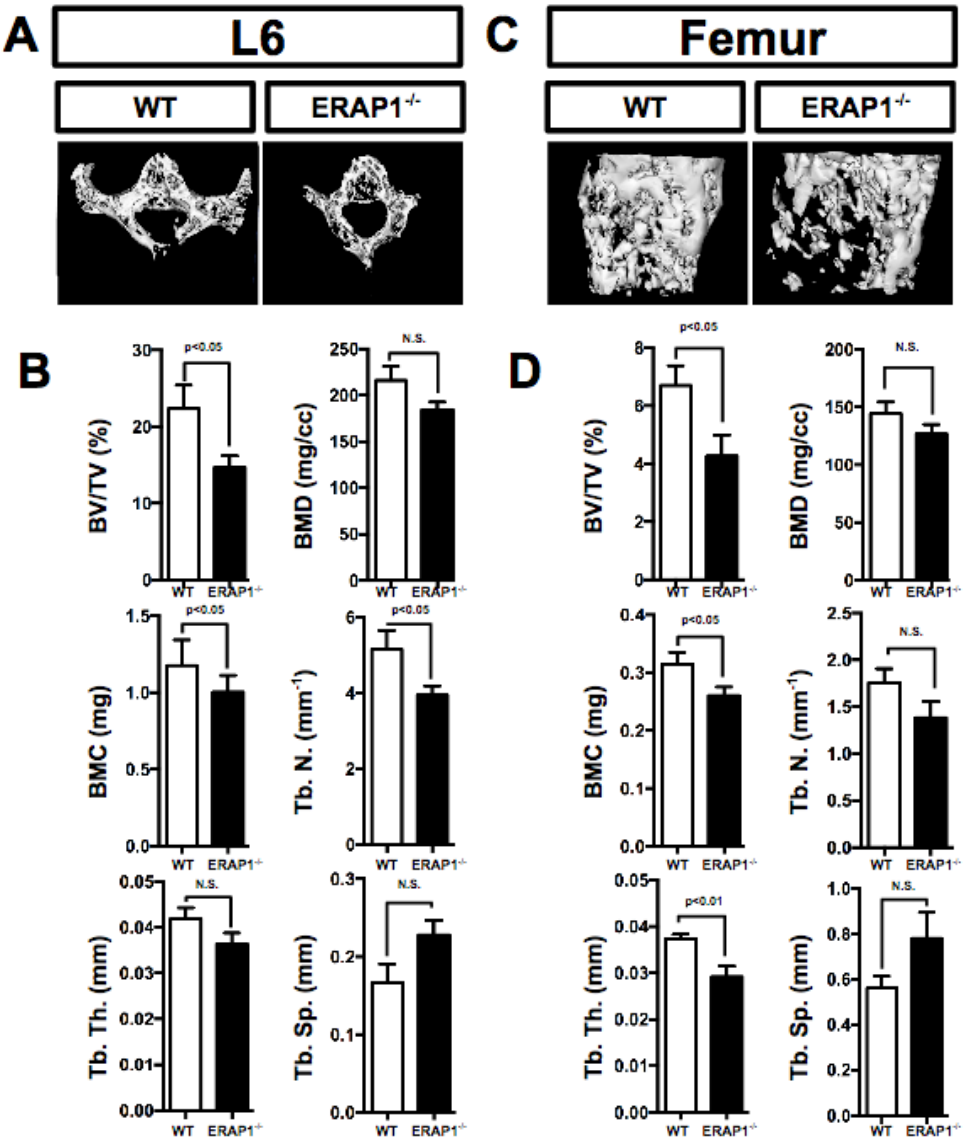

ERAP1-/- and WT mice were sacrificed at 80 weeks of age and analyzed with µCT. **(A)** Representative isosurfaces of trabecular space in L6 vertebrae. **(B)** Micromorphometry of trabecular bone in L6 vertebra was analyzed with Microview software and bone volume fraction (BV/TV%), bone mineral density (BMD), bone mineral content (BMC), trabecular number, trabecular thickness, and trabecular spacing were calculated. **(C)** Representative isosurfaces of trabecular space in femur. **(D)** Micromorphometry of trabecular bone in femur was analyzed with

Microview software and BV/TV%, BMD, BMC, trabecular number, trabecular thickness, and trabecular spacing were calculated. p value calculated by student's t-test. SEM shown.

Figure 23: Osteoporosis progresses uniformly throughout the lives of ERAP1-/- mice, but

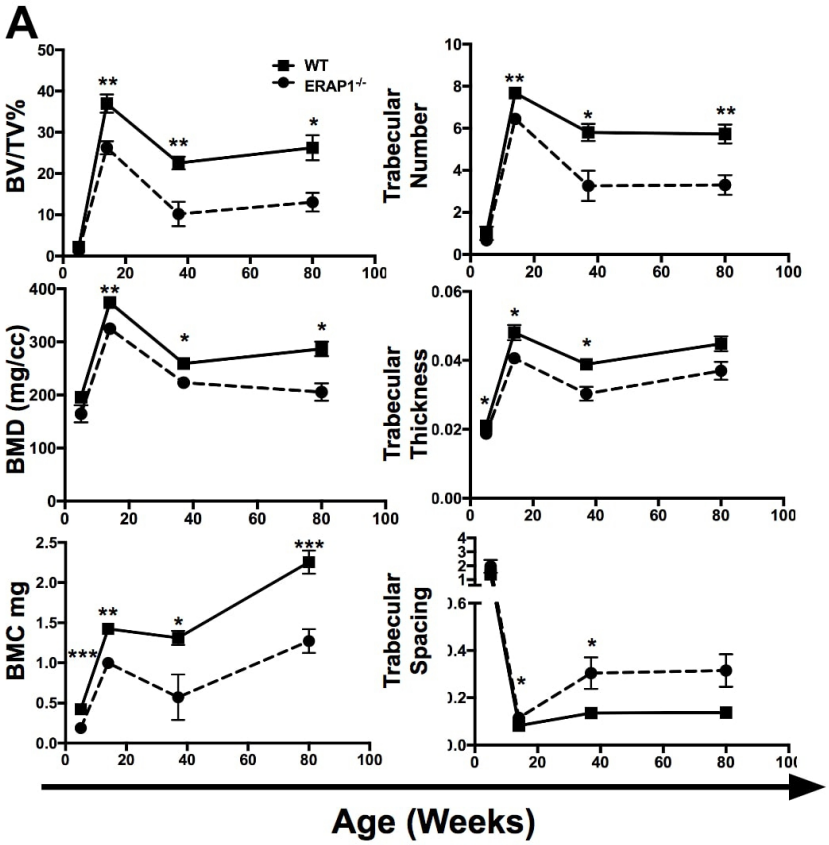

ankylosis is sporadic, similar to AS.

ERAP1-/- and WT mice were sacrificed at indicated ages and analyzed with μCT. **A)** Micromorphometry of trabecular bone was analyzed with Microview software and bone volume fraction (BV/TV%), bone mineral density (BMD), bone mineral content (BMC), trabecualr number, trabecular thickness, and trabecular spacing were calculated as a function of age. At 5 weeks of age WT and ERAP1-/- animals were similar, but as primary mineralization progressed, ERAP1-/- mice developed severe osteoporosis and poor trabecular architecture that was significantly different by 14 weeks and persisted out to 80 weeks. p value calculated by student's t-test. SEM shown.

Mice deficient in beta-2-microglobulin also develop osteoporosis and spinal ankylosis.

The primary known function of ERAP1 is MHC-I antigen presentation.[146,148,257,296,358] In the absence of ERAP1 there is a global change in which peptides are presented, and a net reduction in the steady state level of MHC-I on the surface of splenocytes and certain cancer cells.[148,257,359] Several other animal models with disruptions in the MHC-I pathway completely lack surface expression of MHC-I on all cells, including $\beta2m^{-/-}$ mice and transporter associated with antigen presentation $(TAP)^{-/-}$ mice.[206] Interestingly, previous reports suggest that $\beta2m^{-/-}$ mice and $TAP^{-/-}$ mice may spontaneously develop peripheral arthritis in their paws when housed in a non-SPF environment.[206] For this reason we wished to investigate if disruption of the MHC-I pathway by a different gene would also produce skeletal deformity of the spine and arthritis. We harvested bone marrow from $\beta2m^{-/-}$ mice, $ERAP1^{-/-}$ mice and WT mice and ran flow cytometry to confirm that loss of ERAP1 and β2m would have similar effects on the expression of MHC-I within the bone marrow (Figure 24A). Similar to previously published work done in cancer cells and splenocytes,[257,359] bone marrow cells from $\beta2m^{-/-}$ mice lacked all MHC-I expression, while bone marrow cells from $ERAP1^{-/-}$ mice had a significant decrease in MHC-I expression (Figure 24A). To determine if loss of MHC-I would also cause spinal deformity and osteoporosis, we harvested the axial skeletons and femurs of $\beta2m^{-/-}$ mice and performed uCT analysis. Similar to $ERAP1^{-/-}$ mice, $\beta2m^{-/-}$ mice spontaneously develop spinal ankylosis (Figure 24A). High variability in the prevalence of ankyloses was observed in $\beta2m^{-/-}$ mice. Only 20% of the 32-week old $\beta2m^{-/-}$ mice had signs of ankylosis, but 80% of the 50-week old animals had severe bilateral ankylosis (Figure 24E). Due to the high

variability it is unclear if this is due to a later development of the phenotype or random chance. However, the β2m$^{-/-}$ mice also suffered from osteoporosis and developed osteoporosis at a later age. The 32-week old β2m$^{-/-}$ mice had similar BV/TV% as WT mice, but by 50 weeks the β2m$^{-/-}$ mice had more severe osteoporosis than 80 week old ERAP1$^{-/-}$ and WT mice (Figure 24D). Specifically, β2m$^{-/-}$ mice had significantly less BMD, BMC, BV/TV%, and trabecular number (Chapter 5 Fig4D). While the conclusion is in contradiction to previous reports that identified no changes in bone homeostasis in β2m$^{-/-}$ mice,[360] this data and their data is consistent. Previous work in β2m$^{-/-}$ mice was limited as it only examined animals at 10 weeks of age.[360] Our data shows that β2m$^{-/-}$ mice appear to have similar BMD at that age, but develop severe osteoporosis by 50 weeks of age. Additionally, previous reports have found that transferring β2m$^{-/-}$ mice to non-specific pathogen-free (non-SPF) environments can trigger spontaneous arthritis in this strain,[208] it may be that environmental differences trigger or worsen the phenotype in these mice.

Figure 24: β2m-/- mice also develop spinal ankylosis and osteoporosis.

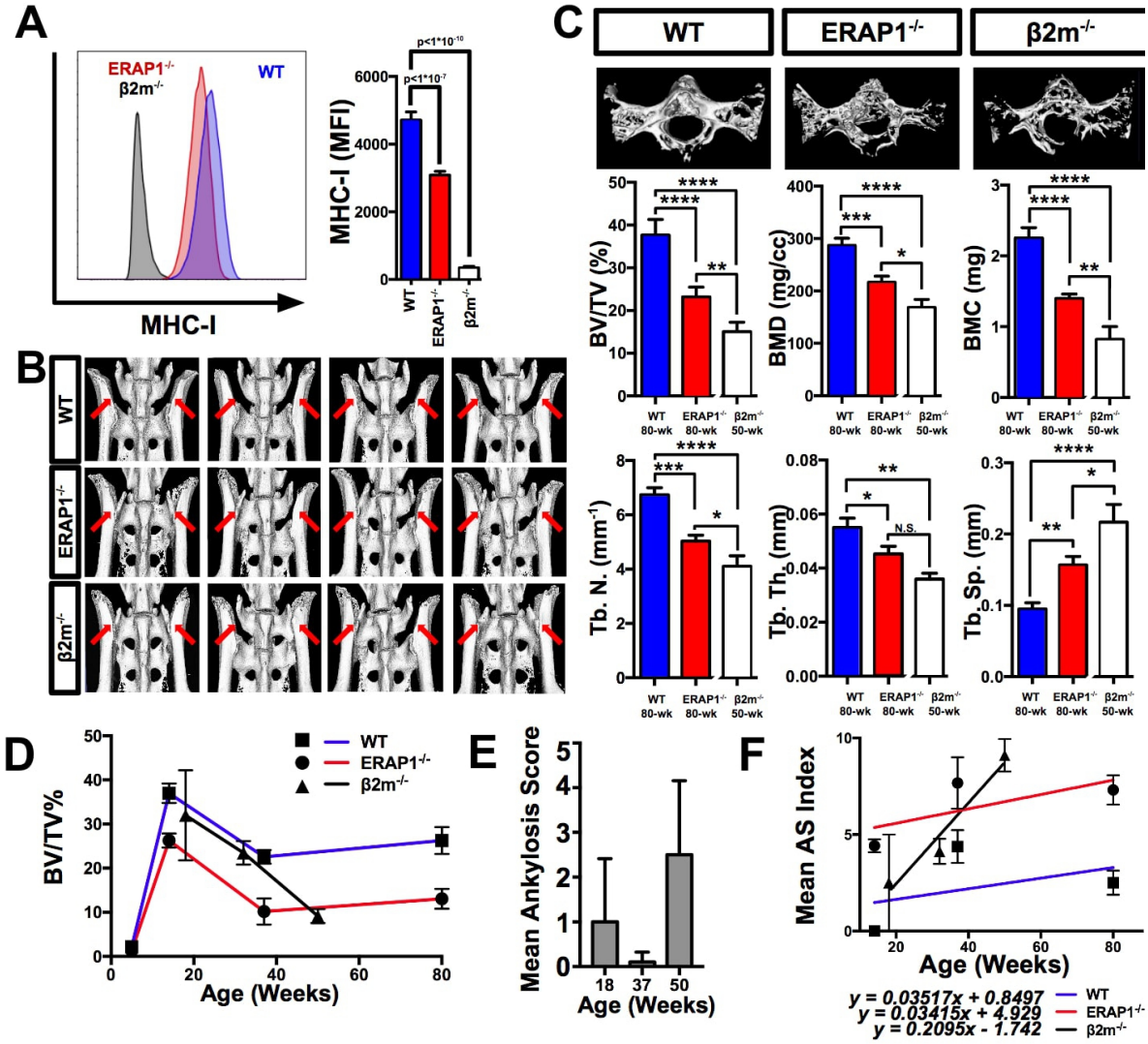

A) MHC-I (H2-Kb) was quantified on the surface of bone-marrow-derived cells via flow cytometry. Loss of ERAP1 reduces the steady state of MHC-I on the surface of cells, while loss of β2m almost completely oblates it. **B)** β2m-/-, ERAP1-/-, and WT mice were sacrificed at indicated ages and analyzed with μCT. Representative isosurfaces from μCT scans of β2m-/- ERAP1-/- and WT mice demonstrate that loss of MHC-I causes spinal ankylosis by 50 weeks of age. **C)** Micromorphometry of trabecular bone was analyzed in the sacrum with Microview

software and bone volume fraction (BV/TV%), bone mineral density (BMD), bone mineral content (BMC), trabecualr number, trabecular thickness, and trabecular spacing were calculated as a function of age. 50 week old β2m-/- had significantly more osteoporosis than 80 week old ERAP1-/- mice and WT mice. **D)** BV/TV% plotted as a function of time and demonstrates that unlike ERAP1-/- mice, β2m-/- maintain a similar bone volume until around 35 weeks of age, when they begin rapidly losing bone mass and become more osteoporotic than ERAP1-/- mice by 50 weeks of age. **E)** Similar to ERAP1-/- mice and AS patients, formation of spinal ankylosis is highly variable. **F)** The AS index for the mice as a function of age. AS index was calculated by stratifying BMD was stratified as follows: 0 for >350, 1 for between 350 and 300, 3 for between 300 and 250, 5 for between 250 and 200, and 7 for less than 200. This score was added to the average ankylosis score per side within a mouse to calculate the AS index. The disease progresses uniformly in ERAP1-/- mice as demonstrated by the same slope as WT mice, but the AS index for β2m-/- mice starts more similarly to WT and progresses with a significantly greater slope.

Deficiency of ERAP1 or β2m causes recruitment of plasma cells and macrophages to intervertebral joints.

Although the presence of inflammation within the intervertebral joints of AS is well established, it remains unclear if inflammation causes spinal ankylosis or is merely an associated symptom. The limited biopsies available from discovertebral lesions of AS patients have revealed the presence of plasma cells, macrophages, and less frequently T-cells.[361] To determine if immune infiltrate was present within the ankylosed joints of the ERAP1$^{-/-}$ mice, we harvested the L6/S1 joints and performed H&E staining and immunohistochemical analysis. As expected, the L6/S1 joint from an 80-week old WT mouse demonstrates a normal architecture (Figure 25A) of concentrically lamellated annulus fibrosus (Figure 25B) and nucleus pulposus with characteristic cells and matrix (Figure 25C). In contrast, the L6/S1 joint from ERAP1$^{-/-}$ mice demonstrates severe pathology (Figure 25D). The organized fibrous structure of annulus fibrosus is diminished and the structural organization of nucleus pulposus is changed, with diminished glycoprotein rich matrix and a unique cellular infiltrate (Figure 25F) instead of the fibroblast like cells observed in the joint of WT animals. Surrounding the unique cellular infiltrate, we noted ectopic bone formation within the joint (white arrows Figure 25D-E) with embedded resident osteocytes (black arrows Figure 25E). Ankylosed joints from β2m$^{-/-}$ mice also showed disruption of the disc by ectopic bone and cell infiltrate (Figure 25G-H). To determine if these infiltrative cells were immune cells, we performed immunohistochemistry for IgM and F4/80. This confirmed that many of the large mononuclear cells were IgM+ plasma cells (Figure 25K&M), and that the infiltrate was punctuated by F4/80+ macrophages (Figure 25L&N). CD3 staining failed to show evidence of T cells in these same areas (data not shown). These results

demonstrate that in the absence of *Erap1* and *β2m*, immune cells infiltrate and ectopic bone develops in intervertebral disk of the two bones where ankylosis is observed.

Figure 25: Deficiency or *Erap1* or *β2m* results in recruitment of immune cells to spinal joints.

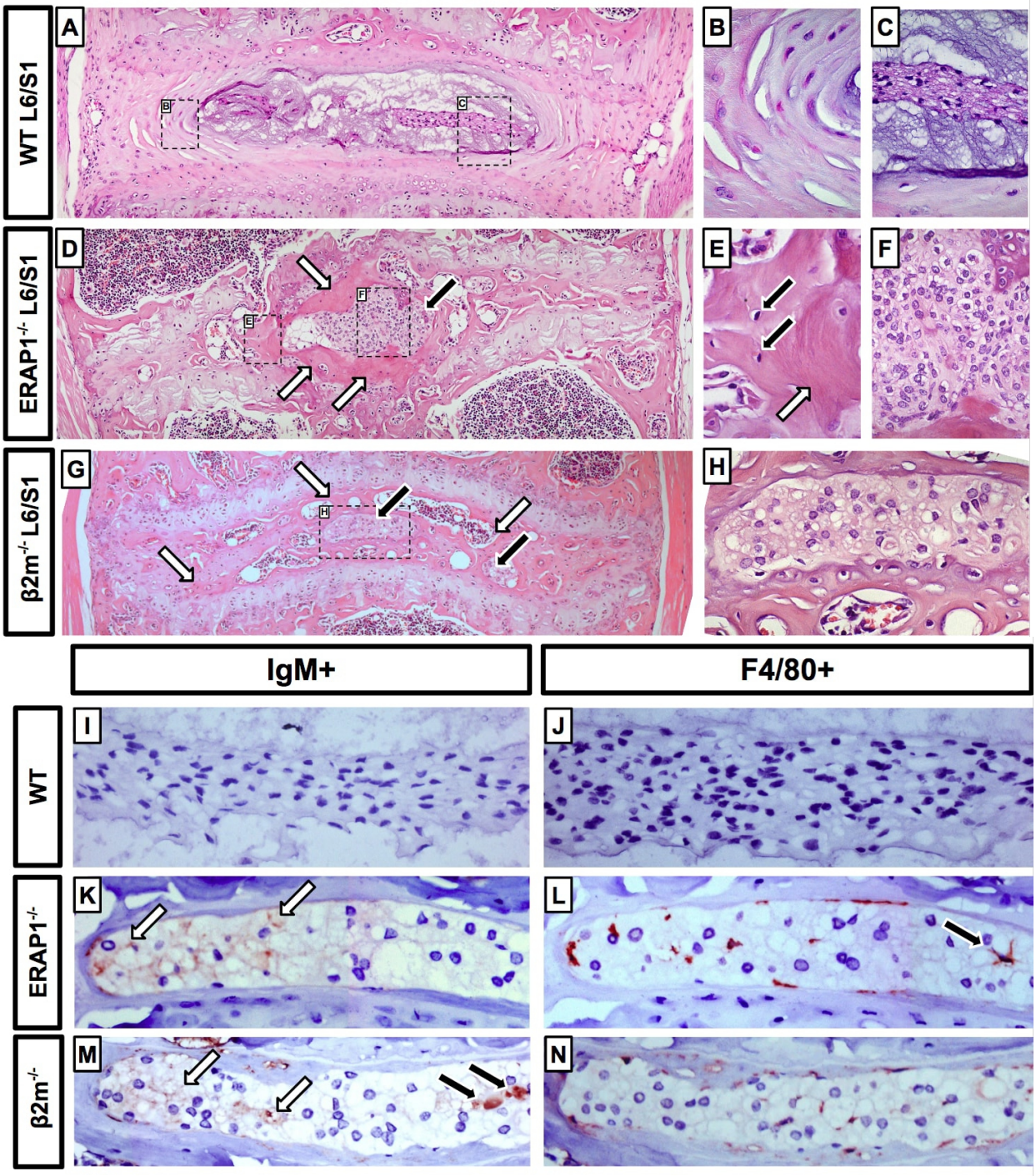

A) Representative H&E of a WT L6/SI joint demonstrating healthy annulus fibrosis **(B)**,

and nucleus pulposus **(C)**. **D)** Representative H&E of an ERAP1-/- L6/SI joint demonstrating disruption of the disc by a large infiltrative mass of cells (black arrow and F) and ectopic bone (white arrows and E) within the joint. **E)** 60x magnification of intervertebral bone formation with black arrows demonstrating osteocytes. **F)** 60x magnification of mononuclear infiltrating cells. **G&H)** Representative H&E of a β2m-/- L6/SI joint demonstrating immune infiltrate. Immunohistochemistry demonstrating IgM+ plasma cells within the L6/SI joints in ERAP1-/- **(K)** and β2m-/- **(M)** mice, but not WT mice **(I)** and F4/80+ macrophages within the L6/SI joints in ERAP1-/- **(J)** and β2m-/- **(L)** mice, but not WT mice **(N)**. Black arrow in **(L)** shows a macrophage in plane.

Deficiency *Erap1* or *β2m* results in dysregulation of osteoclasts and osteoblasts.

Osteoblasts and osteoclasts maintain healthy bones by balancing bone formation and resorption, respectively.[362] In our previous work we demonstrated that *Erap1*$^{-/-}$ mice secrete increased amounts of IL-6 and TNFα in response to innate stimulation.[171] These cytokines are known to impact osteoblast and osteoclast function,[362] so we investigated if loss of ERAP1 or β2m would alter osteoclast and osteoblast development or function. Bone marrow derived osteoclasts were cultured on fluorescently labeled dentin discs and confocal microscopy was utilized to measure the size of the resorption pits. Interestingly, osteoclasts derived from ERAP1$^{-/-}$ mice developed significantly ($p<0.05$) larger pits than WT osteoclasts, while osteoclasts derived from β2m$^{-/-}$ mice developed even larger pits than osteoclasts from WT mice ($p<0.01$) and ERAP1$^{-/-}$ mice ($p<0.01$) (Figure 26A&B). To determine the impact of ERAP1 and b2m deficiency on ostaoclastogenesis potential, bone marrow cells were differentiated into osteoclasts and TRAP stained. While we observed increased osteoclastogenesis of ERAP-/- marrow cells, β2m$^{-/-}$ outgrowths showed no difference (Figure 26C). Interestingly, we observed decreased osteoclast size of osteoclasts derived from ERAP-/- and β2m$^{-/-}$ bone marrow (Figure 26D-E).

To determine the steady-state level of osteoblast numbers in the spines of WT, ERAP1$^{-/-}$, and β2m$^{-/-}$ mice, we performed static histomorphometry analysis, as previously described.[363] ERAP1$^{-/-}$ mice had significantly reduced numbers of active osteoblasts per trabecular surface area in their sacra, as compared to WT mice (Figure 26A). Interestingly, β2m$^{-/-}$ mice had even fewer osteoblasts as compared to both WT and ERAP1$^{-/-}$ mice (Figure 26A). To assess osteoblast differentiation, bone marrow cells were harvested from age- and gender- matched WT,

ERAP1$^{-/-}$, and β2m$^{-/-}$ mice and differentiated into osteoblasts as described in methods. ERAP1$^{-/-}$ marrow cells had a heightened capacity to differentiate into osteoblasts compared to WT (Chapter 5 Fig. 6C), while they showed no difference in activity, as determined by production of mineralized extracellular matrix (Figure 26H). In contrast, β2m$^{-/-}$ cells differentiated into osteoblasts at a significantly ($p<0.0001$) reduced rate (Figure 26G) and failed to produce normal amounts of calcified extracellular matrix (Figure 26H). Dynamic histomorphometric analysis of the sacrum showed that neither Mineral Apposition Rate nor Bone Formation Rate were significantly different, indicating similar osteoblast activity in vivo, although, analysis was complicated by the increased bone formation rate of the sacrum (Data not shown). Consistent with these, findings, serum osteocalcin levels determined by ELISA were not different in ERAP-/- or β2m$^{-/-}$ mice compared to WT (Data not shown).

Figure 26: Deficiency or ERAP1 or β2m mediate different effects on osteoclasts and osteoblasts.

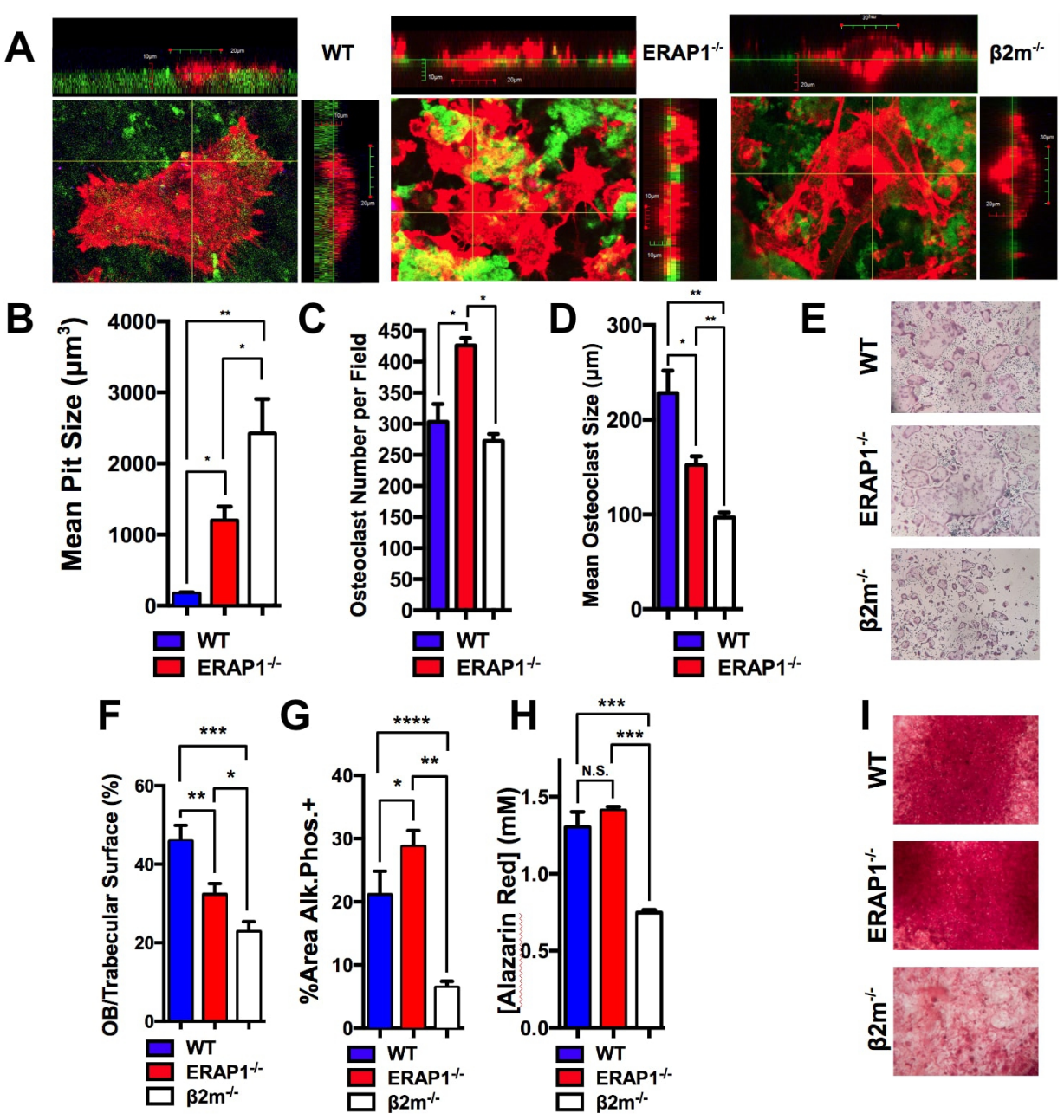

Osteoclasts were differentiated from bone marrow on stained dentin discs, allowed to mature and from pits in the dentin substrate, then stained and analyzed with confocal

microscopy. For each osteoclast, the area it had invaded past the dentin border was measured as a measure for osteoclast activity. ERAP1-/-osteoclasts had significantly larger pits compared to WT, and MHC-I deficient mice had significantly larger pits compared to the ERAP1-/- and WT mice seen in representative image **(A)** and quantified mean with SEM **(B)**. **C-D)** Osteoclastogenesis assay was performed on bone marrow from the indicated mice and both the number **(C)** and size **(D)** of osteoclasts were recorded and representative images shown **(E)**. **F)** Slides were taken and stained with TRAP and hematoxylin of the sacrum, then the ratio of surface area of trabecular bone covered by active osteoblasts (defined as mononuclear cuboidal cells adherent to the trabecular margin) to total trabecular surface was calculated and averaged for each genotype. Osteoblasts were derived from bone marrow of the indicated genotype (as described in methods) and the overall number was measured using the alkaline phosphatase assay **G)**. ERAP1-/- bone marrow cells had an increased ability to differentiate into osteoblasts. Osteoblasts were derived from bone marrow of the indicated genotype (as described in methods) and mineralization was measured using alizarin red. **H)** Osteoclasts derived from β2m-/- bone marrow had a significantly decreased amount of mineralization. **I)** Representative shown.

Discussion

The link between MHC-I and AS has been known for over 40 years,[23,24,348] yet the pathogenesis of AS is still not understood. There is now a large amount of genetic evidence that implicates the MHC-I pathway and ERAP1 in the pathogenesis of AS,[14,28,316] but despite these advances in understanding the genetic risks for AS, basic biological evidence has lagged behind. Prior to this study, to our knowledge, no direct link between antigen-presentation and bone homeostasis was known. Herein we demonstrate that genetic disruption of two genes responsible for normal MHC-I antigen presentation is sufficient to phenocopy the major skeletal findings of AS in mice.

Development of therapeutics for AS has also been slow, with many drugs failing clinical trials,[102,105,109] and other approved drugs providing symptomatic relief, but failing to halt the skeletal changes.[70,71] The difficulty of drug development is likely in part due to a lack of an animal model, as none of the preclinical efficacy studies justifying translation of these therapeutics into the clinical arena were conducted in animal models of AS.[92,98,102,105,109] This is likely because none of the currently described animal models consistently develop the key skeletal features of AS. In this chapter, we identify a simple genetic murine model that spontaneously and consistently develops the key skeletal features of AS. The ERAP1$^{-/-}$ model may be of great value to the field as a model to test the effect of potential AS therapeutics on the skeletal progression of the disease.

Within the ERAP1$^{-/-}$ model of AS two phenotypic features must be explained, bone loss and ectopic bone formation. The bone loss observed in ERAP1$^{-/-}$ mice, including osteoporosis and erosions can be explained by an increased osteoclast activity (Figure 26A&B) and decreased

osteoblast number (Figure 26F). From the experiments performed it is difficult to know whether the increased osteoclast activity is cell-intrinsic or is the effect of other bone-marrow resident cells (such as immune cells) communicating with osteoclasts. Our previous work studying inflammation in ERAP1$^{-/-}$ mice suggest that they produce increased amounts of several proinflammatory cytokines that increase osteoclast activity, including TNF-α and IL-6.[171] These same cytokines have been reported to be increased in AS,[59,350] suggesting that the increased osteoclast activity may be explained by increased inflammatory cytokines. The decreased number of osteoblasts in ERAP1$^{-/-}$ mice is almost certainly extrinsic, and not a property of the osteoblasts. This is because in identical environments, when we performed the osteoblastogenesis assay we observed an increased number of osteoblasts develop from ERAP1$^{-/-}$ bone marrow (Figure 26H), but we observed a decreased number of active osteoblasts in the bones of the mice (Figure 26F). This suggests that osteoblasts can develop normally, but are failing to do so in vivo because of changes in the microenvironment of the bone, such as cytokines or immune cell-cell interactions. It is therefore likely that the numerous changes in immune cell response and cytokine production that we and others have noted in the ERAP1$^{-/-}$ mice may be contributing to the osteoclast activity and osteoblast number.

The results from experiments on ERAP1$^{-/-}$ osteoblasts and osteoclasts both explain the global osteoporosis observed in the mice, but not the ectopic bone formation. Because new bone forms in very specific anatomical locations, we may expect that it is not due to systemic changes, but changes at these specific anatomical locations. To investigate if abnormal immune cells may be present at these sites we performed H&E and found immune cell infiltrate in the intervertebral space of ankylosed joints in both ERAP1$^{-/-}$ mice and β2m$^{-/-}$ mice. Immunohistochemistry

identified IgM+ plasma cells and F4/80+ macrophages. These pockets of immune infiltrate were surrounded by ectopic bone suggesting that they may be promoting this bone formation. Recruitment of these cells to this specific anatomic location may explain why ankylosis occurs only in the axial skeleton.

This work has important implications on the knowledge of how MHC-I and ERAP1 may be causing AS. Up until now, the majority of prominent hypotheses have suggested that the AS-associated MHC-I alleles have a gain-of-function mutation that causes AS. These theories include the hypothesis that HLA-B27 is activating the unfolded protein response,[220,233] or forming homo-dimers that activate specific immune receptors.[227] The observation that loosing ERAP1 or losing MHC-I triggers the AS phenotype in these mice, suggests that AS may be caused by a loss-of-function (rather than a gain-of-function) in the MHC-I antigen-presentation pathway. Consistent with this hypothesis, many AS-associated MHC-I molecules have difficulty presenting peptides, and our work has shown that the ERAP1 variant most strongly associated with AS over-trims peptides, reducing antigen presentation. Empty HLA-B*2705 molecules misfold in the endoplasmic reticulum and are frequently degraded without ever reaching the cell's surface.[220] Similarly, multiple forms of HLA-B*27 form peptide-free homodimers and can rise to the surface of the cell without presenting antigen.[226,230] Furthermore, previous reports observed the onset of arthritis in the feet of $\beta 2m^{-/-}$ mice when housed in certain non-SPF environments.[207] Interestingly, the same phenotype was observed in $TAP1^{-/-}$ mice, mice that also have a failure of antigen-presentation, although at a third location in the pathway.[206] These findings corroborate the idea that disruption of the MHC-I pathway may cause skeletal deformity. Interestingly, the development of arthritis in the $\beta 2m^{-/-}$ mice was not rescued by the

addition of HLA-B27,[206] demonstrating that, in mice, HLA-B27 has a loss of function that fails to rescue the onset of arthritis cause by insufficient MHC-I. These data suggest that bacteria may be contributing to the phenotype. In each of these models ($\beta 2m^{-/-}$, $TAP1^{-/-}$, and HLA-B27+ $\beta 2m^{-/-}$) arthritis was only observed when the mice were housed in a different non-SPF facility. The loss of function of the MHC-I system coupled with particular bacterial pathogens, may have triggered the arthritis, as the only difference was changed housing. Differences in bacterial exposure may also explain why we were unable to reproduce the finding of paw arthritis in these animals in our facility.

Herein we describe a novel impact of ERAP1 deficiency and β2m deficiency within the skeletal system, show that immune cells are spontaneously recruited to the precise anatomic locations of spinal ankylosis, and define and validate multiple assays that could be used in this model in future preclinical trials.

Chapter 6

Materials and Methods

Animal procedures

All animal procedures were approved by the Michigan State University Institutional Animal Care and Use Committee (http://iacuc.msu.edu.proxy2.cl.msu.edu/). Adult C57BL/6 WT mice were purchased from Taconic Farms (Hudson, NY, USA). Ad5 vectors were injected intramuscularly (I.M.) into 8-week-old mice. A total of 1×1010 viral particles per mouse were administered I.M. in a volume of 30 μl PBS solution (pH 7. 4) into the tibialis anterior of the right hindlimb. Numbers of animals used for each experiment are specified on the corresponding figure legends. Plasma and tissue samples were collected and processed at the indicated times.

ELISpot analysis

96-Well Multiscreen high protein binding Immobilon-P membrane plates (Millipore, Billerica, MA, USA) were pretreated with ethanol, coated with mouse anti-IFN-γ (or IL-4 or IL-2) capture antibody, incubated overnight and blocked with RPMI medium [with 10% fetal bovine serum (FBS), 1% PSF (penicillin, streptomycin, fungizone)] prior to the addition of 1.0×106 splenocytes per well (19). Ex vivo stimulation included the incubation of splenocytes in 100 μl of media alone (unstimulated), or media containing 2 μg per well of a single 15-mer peptide (indicated in the figure) for 18–24h in a 37°C, 5% CO2 incubator. Ready Set Go IFN-γ, IL-2 and IL-4 mouse ELISpot kits were purchased from eBioscience (San Diego, CA, USA). Staining of plates was completed per the manufacturer's protocol. Spots were counted and photographed by an automated ELISpot reader system (Cellular Technology, Cleveland, OH, USA).

Cell staining and flow cytometry

To evaluate intracellular cytokine responses, splenocytes from immunized mice were ex vivo stimulated with a pool of peptides that generated responses only in WT animals, WT immunodominant toxin-A-derived peptides (IDTAPs) (TGYTIINGKHFYFNT, FYFNTDGIMQIGVFK, ALTSY KIINGKHFYF, STGYTIISGKHFYFN, YTSINGKHFYFNTDG, SKMVTGVFKGPNGFE), or with a pool of peptides that generated responses only in ERAP1−/− animals, ERAP1−/− IDTAPs (AAIHLCTINNDKYYF, FEYFAPANTDANNIE, GFEYFA PANTDANNI, FAPANTDANNIEGQA, EYFAPANTDANNIEG, ANNIEGQAIRYQNRF), at a total mass of 2 μg per well. Subsequently, intracellular staining was performed as previously described (20). Briefly, cells were surface stained with allophycocyanin-Cy7-CD3, Alexa Fluor 700-CD8a and CD16/32 Fc-block antibodies, fixed with 2% formaldehyde (Polysciences, Warrington, PA, USA), permeabilized with 0.2% saponin (Sigma-Aldrich, St Louis, MO, USA) and stained for intracellular cytokines with PE-Cy7-TNF-α, allophycocyanin-granzyme B, PE-perforin, FITC-IFN-γ, Pacific Blue-CD62L, PerCP-Cy5.5-CD127 (4 μg ml−1) (all obtained from BD Biosciences, San Diego, CA, USA). Cells were incubated on ice with the appropriate antibodies for 30min, washed, and data were collected using an LSR II instrument (BD Biosciences, San Jose, CA, USA) and analyzed using FlowJo software (Tree Star Inc., Ashland, OR, USA).

In vivo CTL assay

An in vivo CTL assay was performed as previously described (19, 20). Briefly, ERAP1−/− or WT mice were immunized with Ad5-TA as described in the section describing Animal

procedures. Fourteen days following the injection, syngenic splenocytes were isolated and either pulsed with a pool of the WT IDTAPs (TGYTIINGKHFYFNT, FYFNTDGIMQIGVFK, ALTSYKIINGKHFYF, STGYTIISGKHFYFN, YTSINGKHFYF NTDG, SKMVTGVFKGPNGFE) and stained with 10 μM CFSE (CFSEhigh), or pulsed with a pool of ERAP1−/− IDTAPs (AAIHLC TINNDKYYF, FEYFAPANTDANNIE, GFEYFAPANTDANNI, FAPA NTDANNIEGQA, EYFAPANTDANNIEG, ANNIEGQAIRYQNRF) and stained with 1 μM CFSE (CFSElow). Naive and immunized mice were injected with equivalent amounts of both CFSElow- and CFSEhigh-stained cells (8×10^6 total cells per mouse) via the retroorbital sinus. After 20h, mice were terminally sacrificed and splenocytes were recovered and analyzed on an LSRII flow cytometer. FlowJo software was used to determine percentages of CFSE-stained cells as follows: % specific killing = 1 − [(% CFSEhigh/% CFSElow)immunized/(% CFSEhigh/% CFSElow)non-immunized].

Isolation of lymphocytes from spleen and liver tissues

Splenocytes from individual mice were harvested and processed as follows: spleen tissues were physically disrupted by passage through a 40-μm sieve, followed by RBC lysis by using 2ml of ACK lysis buffer (Invitrogen, Carlsbad, CA, USA) per homogenized spleen. Splenocytes were subsequently washed two times with RPMI medium (Invitrogen) supplemented with 10% FBS, 2mM l-glutamine, 1× PSF, re-suspended and counted. Liver tissue from individual mice was minced into small pieces, incubated in collagenase/DNase media containing RPMI supplemented with 10% FBS and 1× PSF, for 1h at 37°C, with vigorous vortexing every 15min. Following incubation, tissue was passed through a 40-μm sieve, followed by RBC lysis and

resuspension in complete RPMI media.

Cell-based antigen presentation assay (transfection and flow cytometry staining)

Construction of plasmids, encoding the respective ERAP1 alleles (summarized in Table I) was performed as previously described in pTracer-CMV-RFP, where the GFP/Zeo fusion protein was replaced with red fluorescent protein ORF.[249,296] Specific primers were designed to create point nucleotide mutations, resulting in corresponding ERAP1 amino acid substitutions, as shown in Table I. pTracer-CMV-RFP plasmids, encoding different ERAP1 alleles (Table I) were generated using a QuikChange II XL Site-Directed Mutagenesis Kit (Stratagene, La Jolla, CA). Integrity of ERAP1 genes, cloned into pTracer-CMV-RFP was confirmed by sequencing of the entire length of the ERAP1 ORF using primers listed in Supplemental Table I. An HA-tag (YPYDVPDYA) was introduced into the C-terminus of each ERAP1 allele constructed.

HeLa cells, stably expressing H-2Kb, human HLA-B*27 and Herpesvirus protein ICP47 (TAP1 blocker), (referred to as HeLa-Kb-B*27/47) were described previously.[146] To construct plasmids expressing HLA-B*27 restricted peptides (and their N-terminal precursors, Supplemental Table II), nucleotide sequences corresponding to specific peptides were subcloned into pTracer-CMV (Invitrogen, Carlsbad, CA). All peptides were designed to contain the ER-signal sequence MRYMILGLLALAAVCSA (from the Ad2E3gp19K protein) upstream of the peptide sequence.[249]

HeLa-Kb-B*27/47 cells (3×105 cells per well in 6-well plates) were transiently co-transfected with the indicated plasmids expressing specific HLA-B*27 specific peptides (1μg of pTracer-CMV-GFP-peptide) and ERAP1-expressing plasmids (1μg) for 48 hours using HeLa specific

TransIT HeLaMonster transfection kit (Mirus Bio LLC, Madison, WI). Transfection efficiency of 5–10% of GFP+/RFP+ was routinely achieved as verified by flow cytometry (Supplemental Figure 3). Surface expression of HLA-B*27 in transfected (GFP+/RFP+) cells was subsequently measured using flow cytometry, as previously described.[296] Briefly, at 48 hours post transfection, cells were incubated with ME1, an HLA-B*27-specific monoclonal antibody (from murine hybridoma supernatant) for 30 minutes on ice, rinsed and subsequently stained with the secondary antibody Cy5-AffiniPure Goat Anti-Mouse IgG (from Jackson Immunoresearch Laboratories; West Grove, PA)) for 30 min on ice (1:200 dilution). Samples were then analyzed on a BD LSR II, or Influx instruments and analyzed using FlowJo software (Tree Star, San Carlos, CA, USA).

Ad5-[E1-]-ICP (utilized in some antigen presentation experiments) was kindly provided by David. C. Johnson from Oregon Health and Science University (Portland, OR). For some experiments we have used ME1, HC10 and W6/32 monoclonal antibodies (all from murine hybridoma supernatant) to quantify levels of MHC class I antigen presentation as well as levels of HLA-B*27 free heavy chain (FHC) formation in HeLa-Kb-B*27/47 cells during transfection with different ERAP1 alleles and peptides. ME1 recognizes intact HLA-B*27 (and some other HLA-B alleles) complexes,[288,314] HC10 recognizes FHC of HLA-B*27 (and other HLA class I molecules),[288,314,315] W6/32 recognizes all intact HLA-B, -A, –C, -E, -G complexes.[315]

Recombinant enzyme expression and purification

ERAP1 alleles were purified from 293F cells after transfection with a plasmid (pTracer-CMV-RFP) carrying the appropriate allelic sequence (ERAP1_High and ERAP1_Low) as

described (20). Active enzyme was purified to homogeneity, by lysing the cells using a Potter-Elvehjem tissue homogenizer, and using affinity (anti-HA) and size-exclusion (S200) chromatography. Enzymes were stored in aliquots at −80° C in the presence of 10% glycerol and subjected to a single freeze-thaw cycle. This approach was found to retain full enzymatic activity during storage. All comparisons between alleles were made with enzyme preparations that were performed in parallel.

ERAP1 enzymatic assays

All enzymatic assays were performed in 50mM Hepes pH 7.0, 150mM NaCl as previously described.[296,364] Leucine 4-methyl-coumaryl-7-amide (L-AMC) assays were performed as previously described.[296,365] 100μM SIINFEKL peptide, shown previously to be resistant to ERAP1 hydrolysis and to stabilize the enzyme, was present in L-AMC assays.[255,296] Peptide VRYQSKNYY was purchased from JPT Peptide Technologies (Berlin, Germany) and purified by RP-HPLC to more than 95% purity. For peptide digestion assays, 50microM peptide was mixed with indicated concentrations of ERAP1 alleles and incubated at 25° C for 20 minutes. The reaction was stopped by the addition of trifluoroacetic acid to a final concentration of 0.1% (for HPLC analysis) or formic acid to a final concentration of 1% (for LC/MS analysis). Digestion products were analyzed by reversed-phase HPLC (C-18 chromolith™ column, Merck) using a linear acetonitrile gradient for elution. Chromatographic peaks were identified by running peptide controls and by mass spectrometry. Reaction rates were calculated by comparing the relative peak area of the product peak to the substrate peak measured by absorbance at 222nm and quantified by running peptide controls.

Western blotting

HeLa-Kb-B*27/47 cells were transfected with pTracer-CMV-RFP-ERAP1_High (or _Low). At 24 hours post transfection, protein was harvested in lysis buffer (20mM Tris-HCl, pH 7.4, 1mM EDTA, 150mM NaCl) containing 1% Triton X-100 with protease inhibitors. Lysed samples were then centrifuged at maximum speed (16,000×g) for 15 minutes at 4°C, after which the protein concentration of the supernatant was determined using the BCA method.[366] Equivalent concentrations of protein samples (5–15 μg) were electrophoretically separated in 7% polyacrylamide gels and transferred onto nitrocellulose membranes. Membranes were then probed with the mouse-anti-hTubulin monoclonal primary antibody (Sigma-Aldrich, St. Louis, MO) at 1:30000 dilution for 20 minutes and primary polyclonal rabbit-anti-hERAP1 (Proteintech, Chicago, IL) at 1:1000 dilution for 2–16 hours or rabbit anti-HA-tag (YPYDVPDYA) antibody (Rockland, Gilbertsville, PA) at 1:2000 dilution for 2–16 hours (to measure exogenous, plasmid derived levels of ERAP1). Following incubations, membranes were probed with fluorescent antibodies (IRDYE800 conjugated goat anti-mouse IgG (Rockland) and Alexa Fluor 680 conjugated goat anti-rabbit IgG (Invitrogen, Grand Island, NY)) for 45 minutes at 1:5000 dilution. Optimally exposed membranes were scanned, and indicated protein bands were quantified using Licor's Odyssey scanner (models 2.1 or 3.0).[367] For data analysis, the fluorescence of ERAP1 proteins was normalized to Tubulin levels.

Cytokine and chemokine analysis

A human-based 27-plex multiplex-based assay was used to determine the indicated cytokine/chemokine concentrations in the media collected from cultured HeLa-Kb-B*27/47 cells

transfected with ERAP1 alleles. Media was collected at 48 hours post transfection. Assay was performed according to the manufacturer's instructions (Bio-Rad, Hercules, CA) via Luminex 100 technology (Luminex, Austin, TX) as previously described.[368]

Statistical analysis

Statistically significant differences were determined using a one-way ANOVA with a Student–Newman–Keuls post hoc test or by using two-tailed homoscedastic Student's t-tests (P value of <0.05 was deemed statistically significant). Graphs in this thesis are presented as mean of the average ± SEM, unless otherwise specified. Statistical analyses were performed using GraphPad Prism (GraphPad Software).

µCT imaging

Vertebras and femurs were harvested, fixed and scanned using a GE Explore Locus microcomputed tomography (µCT) system using 20 µm voxel resolution obtained from 720 views. Beam angle of increment of 0.5, beam strength of 80 peak kV and 450 µA were used. Each run included age matched WT, ERAP-/- and b2m-/- bones, and a calibration phantom for standardization and consistency. An average thresholds of S1 calculated from multiple WT bone samples was determined as 1232 in 14-week-old age group and 1009 in 70-week-old group and were used to separate bone from bone marrow. Bone measurements were blinded until the final analysis. Trabecular bone analysis of the S1 vertebra was performed using advanced ROI generated using splines in the transverse plane outlining the entire length of the vertebral body excluding the outer cortical bone. Bone mineral density, content, bone volume fraction,

trabecular thickness, spacing and number values, as well as the representative isosurface images were generated using GE Healthcare MicroView software.

Osteoclast outgrowths

Bone marrow cells were differentiated into osteoclasts in cell culture as described previously (PMC4129456), with a few modifications. 250,000 cells per well were plated in 48-well plates. After overnight incubation in αMEM (Gibco) containing 10% FBS, and 50 µg/mL of penicillin and streptomycin the cells were treated with 5 ηg/ml RANKL (R&D Systems) and 30 ηg/ml M-CSF (Gibco) to induce osteoclastogenesis. After 5 days of culture, cells were stained with TRAP (Sigma) and imaged. Osteoclast size and number was determined using ImajeJ software.

Osteoclast pitting assay

Confocal osteoclast pitting assay was essentially performed as previously described. (PMID: 22130942) Briefly, dentine discs (Fisher, cat# NC0443942) were biotinylated with 0.5 mM Biotinylation Reagent (Fisher, cat# 50-492-586) for 1 hour at room temperature. Prior to seeding with osteoclasts, dentin disks were incubated in 96-well plates in αMEM (Gibco) containing 10% FBS, and 50 µg/mL of penicillin and streptomycin. Freshly isolated Bone marrow cells were seeded over dentin disks and incubated over night at 250,000 cells per well. The next day cell were supplemented with 5 ηg/ml RANKL (R&D Systems) and 30 ηg/ml M-CSF (Gibco). After 2 days of culture, media was replaced with acidic Resoption media. After 2 days of culture, cells were washed, fixed, and permeabilized with Triton-100. Cells were stained with FITC-streptavidin and Rhodamin Phallodin and analyzed as previously described. (PMID:

22130942).

Osteoblast outgrowths

Bone marrow cells were obtained from mouse femurs and tibias and plated overnight in 48 well plates at 500,00 cells per well in αMEM (Gibco) containing 10% FBS and 50 μg/mL of penicillin and streptomycin. The next day the cells were treated with 50 μg/mL of ascorbic acid (Sigma, 50-81-7) and 10 mM -glycerophosphate (Sigma, 154804-51-0) to promote osteoblastogenesis. Media was changed every 2-3 days. For osteblastogenesis analysis, after 5 days of culture cells were washed with PBS and fixed with 10% formalin for 60 seconds. Cells were incubated with BCIP/NBT substrate (Sigma, B5655) solution for 10 minutes and evaluated for alkaline phosphatase positive cells using imageJ software. For calcium deposition assay, after 28 days of incubation, cells were washed, fixed and stained with 2% Alazarin Red S (EMD Milipore, C.I. 58005) solution as described previously. For quantification of staining, alizarin release assay was performed as described before (PMID: 15136169) and absorbance at 405nm was measured.

Cross-fostering experiments

ERAP-/- and WT breeding cages were set up simultaneously to synchronize pregnancies. Upon showing physical signs of pregnancy, females were removed from males and housed separately. Immediately after birth, ERAP-/- pups were transferred to lactating WT mothers, and vice versa, WT pups were transferred to ERAP-/- mothers. Pups were weaned by 28 days of age. At 14 weeks of age mice were sacrificed and their sacra were harvested and fixed for μCT

analysis. Average threshold value of WT control mice of 1039 was used for trabecular bone analysis of S1 of cross-fostered and control animals using μCT.

Chapter 7

Significance and Future Directions

Significance

Over the past 40 years there has been an increasing amount of evidence from genetic studies that suggested that AS is due to changes in antigen presentation, yet the pathogenesis of the disease remains unknown. The first genetic link between AS and antigen presentation derived from familial studies that showed that carriers of *HLA-B*27* were hundreds of times more likely to develop the disease than non-carriers.[22–24] Since then, GWAS have confirmed the association of other *HLA-B* genes with AS[14] and identified a strong epistatic interaction between *HLA-B* and *ERAP1* that further increases the risk for developing AS.[13,14] All of this genetic evidence suggests that antigen presentation is critical to the pathogenesis of AS, however prior to our work there was no convincing biological evidence to support this, because prior to our work, no connection between antigen presentation and bone homeostasis was known. In this thesis, we demonstrate that ERAP1 can create and destroy epitopes, that human ERAP1 variants trim peptides at different rates, that human ERAP1 variants have the ability to shift immunodominance of antigen derived peptides, alter levels of MHC-I *in vivo*, and finally, that loss of ERAP1 or loss of MHC-I presentation in mice is sufficient to phenocopy the major skeletal findings of human AS. These findings constitute a breakthrough in the field of AS and open up many new areas of investigation. They also prove the findings made by genetic association studies by providing an animal model of AS that links ERAP1 to spinal ankylosis.

Role of ERAP1 in Antigen Presentation

In Chapters 2, 3, and 4 we advance the understanding of the impact that ERAP1 has upon antigen presentation. Prior to this work, it was understood that ERAP1 enhanced or reduced the presentation of certain antigens,[146,147,257] however the extent to which ERAP1 could destroy epitopes, and the effect that polymorphisms in ERAP1 have on antigen presentation were not known. In chapter 2 we demonstrated that absence of ERAP1 completely reshapes the immunodominant T-cell response to a model antigen. This was surprising, as it may have been previously assumed that the biological function of ERAP1 was facilitating this process,[147] however without ERAP1 an alternative immunodominant hierarchy appeared. This has two important implications: (1) the primary role of ERAP1 could not be in facilitating immunodominance, as immunodominance was intact in its absence, and (2) it appeared that ERAP1 was destroying the majority of epitopes that would otherwise become immunodominant. We confirmed that ERAP1 was destroying these important immunogenic epitopes by demonstrating that the addition of n-terminal residues prior to an immunogenic peptide provided linear protection from destruction by ERAP1 (Figure 2). Having demonstrated that ERAP1 both created and destroyed novel immunogenic epitopes, we next demonstrated that the same degree of differences in antigen presentation could be mediated by SNPs within ERAP1 (Chapter 3). We demonstrated that AS-associated ERAP1 SNPs increased the ability of ERAP1 to trim peptides, and reduced the overall abundance of MHC-I on the cell's surface, likely by over-trimming peptides and reducing the overall amounts of peptides that were appropriately sized for MHC-I display. Furthermore we demonstrated an additive effect of these ERAP1 SNPs on both enzymatic activity and antigen presentation, because the ERAP1 variant with all 5 AS-associated

ERAP1 SNPs had the highest enzymatic activity and the greatest decrease in antigen presentation in vitro and in vivo.

This work opens up new possibilities in the pathogenesis of AS and other ERAP1-associated diseases. While the predominant hypothesis prior to our work may have been the arthritogenic peptide hypothesis, our work supports two alternative hypotheses as well. In chapter 4 we demonstrate that ERAP1-High generates unique immunogenic peptides and provide evidence in support of the arthritogenic peptide hypothesis. We also demonstrate that ERAP1-High selectively destroys immunogenic peptides, suggesting that it could contribute to AS by destroying key tolerogenic peptides. Finally we demonstrate that ERAP1-High decreases the overall surface expression of MHC-I on multiple cell types, suggesting that decreased total MHC-I expression could play a role. Therefore, with the expanded understanding of ERAP1 provided in this work, three theories of the role of antigen presentation in AS are supported: (1) the arthritogenic peptide hypothesis, (2) the hypothesis that disease-associate HLA-B and ERAP1 combinations fail to present protective peptides, and (3) the hypothesis that disease-associate HLA-B and ERAP1 combinations decrease overall MHC-I expression causing AS.

While our work can not rule out any of these hypotheses, we provide evidence supporting the possibility that AS may be due to an overall reduction of surface MHC-I levels. In chapter 3 we demonstrate that disease-associated ERAP1 SNPs over-trim peptides, resulting in a decrease in the amount of HLA-B*27 presented on the surface of human cells. Furthermore these SNPs had an additive effect, with ERAP1-High (the variant with all 5 SNPs) having the highest enzymatic activity and the greatest reduction of MHC-I on the surface of cells. In chapter 4 we demonstrate that ERAP1-High has a similar effect in vivo, by showing that even at a relatively

low level of expression, ERAP1-High is capable of significantly reducing MHC-I levels on the surface of multiple cell types. Additional support for the MHC-I deficiency theory of AS comes from recent reports that note an overall decrease in peptide-presentation mediated by disease-associated HLA-B*27 isoforms.[222] While none of this evidence can prove causation, future work in the ERAP1$^{-/-}$ animal model of AS can help determine which of these hypotheses are correct.

This reduction in MHC-I could potentially mediate multiple effects on the immune system. As previously discussed each antigen presented in the thymus is critical for negative selection.[156] Decreased antigen presentation leads to an autoimmune disease, APS1 and therefore a decrease in MHC-I may create a 'leaky thymus' that allows autoreactive T-cells to escape negative selection.[156,158] The decreased level of antigen presentation could also impact the development or activation of NK cells. Developmentally, NK cells require MHC-I to become licensed and therefore a decrease in MHC-I may alter the licensing or maturation of NK cells.[151] This may be the case as we have shown that there is a higher percent of terminally differentiated NK cells from ERAP1-/- mice and that their licensing is altered. An overall decrease in MHC-I may also impact NK activation. Decreased MHC-I on target cells would increase NK activation, by decreasing the engagement of inhibitory receptors (KIRs in humans and Ly49 molecules in mice).[167,369] Additionally, MHC-I may act in cis, on the surface of NK cells to inhibit activation, so a decrease in MHC-I on the surface of the NK cells may also serve to increase their activity.[328]

Role of ERAP1 in Male Development

In this thesis we also uncover a role of ERAP1-High in male development, by showing that ERAP1-High is a dominant lethal autosomal allele. Historically very few dominant lethal autosomal alleles have been discovered, even fewer in mammals, and fewer still with a sex-specific effect.[339] The most direct hypothesis would be that male-derived antigens (antigens derived from proteins on the Y chromosome) were being differentially processed by ERAP1-High and affecting fetal development via antigen presentation events, such as the development of spiral arteries by NK cells.[320] However, the observation that ERAP1-High is lethal to males on a $\beta 2m^{-/-}$ background suggests that these effects are independent of antigen presentation. A possible explanation is that ERAP1 is interacting with a protein coded on the X chromosome, that is at a lower concentration in male fetuses. One such protein is RBMX. It is expressed at approximately 50% in male fetuses compared to female fetuses[370] and has been shown to bind to ERAP1 in a functional protein-protein complex.[340] The exact functions of RBMX are not known, however it has been shown to act by splicing mRNA, and therefore could have relatively broad effects on the expression of multiple genes.[371–373] Future studies into the role of the protein complex containing RBMX and ERAP1 may shed light on some of it's functions beyond antigen presentation.

Role of ERAP1 in Bone Homeostasis

Even more significant than our work in defining the role of ERAP1 and ERAP1 variants in antigen presentation and in male lethality, is our discovery of the important role ERAP1 plays in the skeletal system. Prior to the work presented in this thesis, no direct connection between

ERAP1 or antigen-presentation and bone homeostasis was known. In chapter 5 we demonstrated that deficiency of ERAP1 or β2m was sufficient to cause spontaneous spinal ankylosis, osteoporosis, and dysregulation of both osteoclasts and osteoblasts in vivo.

Although we did not demonstrate the mechanism, because both genes are critical to antigen-presentation, the simplest hypothesis would be that disruption of the antigen presentation pathway is responsible for the phenotype. More evidence in support of this theory can be provided by reapeating the study in TAP1$^{-/-}$ mice. TAP1$^{-/-}$ mice lack the ability to transport peptides into the ER and therefore have greatly reduced MHC-I antigen presentation on the surface of their cells. If TAP1$^{-/-}$ mice also develop a similar phenotype, it would strongly suggest that these phenotypes are caused by antigen presentation, because the alternative hypothesis would be that ERAP1, β2m, and TAP1 all have unknown functions outside antigen presentation in another pathway that regulates bone. However, if TAP1$^{-/-}$ mice do not develop the phenotype, then the non-canonical functions of ERAP1 and β2m can be investigated. These include the role of β2m in iron homeostasis via an MHC-I-like receptor[374,375] and the antigen-presentation independent role of ERAP1 in the innate immune system.[168–171,175] After the role of antigen presentation had been confirmed or ruled out, the exact cells that are responsible can be investigated using tissue-specific knockouts and chimeric mice.

Role of ERAP1 in Innate Immunity

We also show effects of ERAP1 on elements of the innate immune system such as NKG2D expression, NK activation, and the development of T-cell memory. These effects of ERAP1 are unlikely to be direct molecular interactions between ERAP1 and molecules in these

various pathways and are more likely secondary to changes in antigen presentation or yet-to-be discovered molecular mechanisms of ERAP1. In our previous work and unpublished work we demonstrated that ERAP1 variants differentially induced the inflammasome,[175] and that *ERAP1* deficient mice develop a more severe form of chemically induced colitis than WT counterparts (Aldhamen et al, manuscript submitted), similar to mice with deficiencies in genes critical to the inflammasome such as *ASC* (apoptosis-associated speck-like protein) and *NLRP6* (nucleotide-binding oligomerization domain protein-like receptor 6). The susceptibility to colitis in $ASC^{-/-}$ and $NLRP6^{-/-}$ was a result of changes in their gut microbiome, so it is possible that the increased susceptibility to colitis we observed in $ERAP1^{-/-}$ mice is also due to changes in the gut microbiome.[376] Antigen presentation may selectively curate the gut microbiome and dysregulation of antigen presentation (via loss of ERAP1, or addition of HLA-B*27) may cause dysbiosis that in turn affects the immune system. This could potentially explain many of the effects of ERAP1 on the immune system including the skeletal pathology. If we were able to demonstrate transmission of the AS phenotype from $ERAP1^{-/-}$ mice to WT mice, it would suggest that the osteoporosis and/or ankylosis was also mediated by interactions between gut flora and the immune system. A similar "gut-immune-spine axis" was recently shown in mice with spinal cord injuries, where dysbiosis of the gut resulted in enhanced recruitment immune cells to the spine at sights of trauma-induced inflammation.[244] If immune-mediated dysbiosis was present in $ERAP1^{-/-}$ mice, it could foster abnormal recruitment or migration of immune cells to sights of mechanical stress- in the spine. These results would then justify study of the skeletons of $ASC^{-/-}$ and $NLRP6^{-/-}$ mice, as well as therapeutic strategies targeting the microbiome, including fecal transplant (cross-fostering in mice), targeted antibiotics, and targeted dietary

alterations.

Future Directions

The work presented in this thesis constitutes a major breakthrough in the field of AS research and allows for novel avenues of scientific inquiry. Outlined below are a few key experiments that address immediate questions raised by this research and incrementally refine our understanding of the pathogenesis of AS.

Future Directions – Ankylosing Spondylitis in ERAP1^{High} Mice

One of the most straightforward investigations that can build upon this work is determining if ERAP1^{High} or ERAP1^{Low} also impact bone homeostasis. This investigation is justified by the observation that ERAP1^{High} and ERAP1^{Low} mediate a variety of effects on antigen presentation and the immune system similar to loss of ERAP1. For instance, both the loss of ERAP1 and the addition of ERAP1^{High} significantly reduced the amount of MHC-I presented on the surface of cells. If the skeletal phenotype observed in ERAP1$^{-/-}$ and β2m$^{-/-}$ mice was due to a reduction in the amount of MHC-I, then the ERAP1^{High} mice may develop a similar phenotype. For this reason the next step is determining if the changes in antigen-presentation mediated by ERAP1^{High} also impact bone homeostasis in a similar manner to ERAP1$^{-/-}$. The following six-arm trial could determine if ERAP1^{High} also causes ankylosing spondylitis and/or if ERAP1^{Low} is protective.

WT, ERAP1$^{-/-}$, ERAP1^{High}, ERAP1^{Low}, ERAP1^{High}/ERAP1$^{-/-}$, and ERAP1^{Low}/ERAP1$^{-/-}$ mice would be generated and raised under identical conditions and monitored for skeletal

pathology. We could use the assays and scoring systems developed and validated in our ERAP1$^{-/-}$ model to determine how human ERAP variants impact the skeletal system. Each group of mice could be scanned with μCT and monitored for spinal ankylosis, SI erosions, SI fusion, osteoporosis, and Andersson lesions over a 36 week period as described in Chapters 5 and 6. If no significant changes are observed by 36 weeks, mice coould be aged out to 2 years to ensure that the changes don't manifest at a later age. At the end of the study, the mice will be sacrificed and sections taken for H&E staining to count osteoblasts and adiposity and if any cellular infiltrate is observed, immunohistochemistry for IgM, CD3, and F4/80 will be performed to identify plasma cells, T-cells, and macrophages respectively. Osteoclastogenesis and osteoblastogenesis would also be performed from bone marrow to determine the differentiation potentials of the cells, and osteoclast activity assays will be performed as described in chapters 5 and 6.

These studies could help determine how human ERAP1 variants impact bone development. Our hypothesis would be that ERAP1^{High} may have a similar impact to loss of ERAP1 because ERAP1^{High} was able to reduce the amount of MHC-I on the surface of cells, similar to loss of ERAP1. If ERAP1^{High} mice develop a bony pathology it will indicate that a single extra copy of ERAP1^{High} is enough to override the effect of endogenous ERAP1, either by creating arthritogenic peptides, or by destroying protective tolerance-inducing peptides. However, if the ERAP1^{High} mice develop normally, it will be interesting to determine if the ERAP1^{High}/ERAP1$^{-/-}$ develop pathology. If the ERAP1^{High}/ERAP1$^{-/-}$ mice develop pathology, but the ERAP1^{Low}/ERAP1$^{-/-}$ mice do not, it would indicate that ERAP1^{High} is a loss-of-function mutation, as it would demonstrate that ERAP1^{High} is unable to rescue the ERAP1$^{-/-}$ phenotype,

while ERAP1^{Low} could. This outcome would suggest that murine ERAP1 and ERAP1^{Low} have a protective effect that ERAP1^{High} lacks. Alternatively, it may also be that these mice develop a different skeletal phenotype entirely, so we will carefully do full body scans with unbiased skeletal analyses performed by a blinded third party.

These relatively straightforward studies will determine the functional impacts of ERAP1^{High} and ERAP1^{Low} in vivo on the skeletal system.

Future Directions – Ankylosing Spondylitis in HLA-B*27 Mice

Another critical finding of this work is that β2m$^{-/-}$ develop spinal ankylosis and other characteristic features of AS, suggesting that disruption of the MHC-I pathway may be the cause of AS. If this is the case it would suggest that disease-linked HLA molecules such as HLA-B*27:05 cause AS through a loss-of-function, rather than-gain-of-function mutation, contrary to what has been assumed by the majority of the literature up to this point. To test this hypothesis we can generate two strains of mice transgenically expressing the disease-linked *HLA-B*27:05* or the protective *HLA-B*27:06* allele on the β2m$^{-/-}$ background.

If the skeletal disease in β2m$^{-/-}$ mice is due to lack MHC-I presentation on the surface of cells, then the addition of a transgenic HLA gene will restore MHC-I levels to the surface of cells and should rescue the skeletal phenotype. To test this we could cross β2m$^{-/-}$ mice with mice transgenically expressing the *HLA-B*27:06* transgene. *HLA-B*27:06* is not associated with AS, but differs from pathogenic HLA-B*27 molecules in only 1-2 amino acids.[120,377] We therefore expect that the addition of *HLA-B*27:06* to the β2m$^{-/-}$ background will result in mice with normal skeletal development. If this is the case, it will further demonstrate that β2m$^{-/-}$ mice

develop the skeletal phenotype due to altered antigen presentation.

Having established that *HLA-B*27:06* rescues the $\beta 2m^{-/-}$ phenotype, we could investigate the role of *HLA-B*27:05* in this pathway. As previously explained, the work presented in this thesis suggests that AS may be caused by decreased surface expression of MHC-I, which suggests that pathogenic HLA-B*27 variants may be loss-of-function mutations. If this is the case, we would expect that these HLA-B27 variants would fail to rescue the $\beta 2m^{-/-}$ phenotype. To determine this we can compare the skeletons of $\beta 2m^{-/-}$ mice, HLA-B*27:06/$\beta 2m^{-/-}$ mice, and HLA-B*27:05/$\beta 2m^{-/-}$ mice. If this hypothesis is correct, we would expect that HLA-B*27:05 will fail to rescue the $\beta 2m^{-/-}$ phenotype, and HLA-B*27:05/$\beta 2m^{-/-}$ mice will develop spinal ankylosis and osteoporosis.

There is previously published data suggesting that this may be the case. For instance two different strains of mice deficient in MHC-I surface expression ($\beta 2m^{-/-}$ mice and $TAP1^{-/-}$ mice) developed spontaneous arthritis in their paws when transferred to non-SPF environments.[206] The addition of the *HLA-B*27:05* transgene did not prevent arthritis in these mice.[207] At the time this result was interpreted as a negative finding, because the assumption was that HLA-B*27:05 must have a gain-of-function mutation, however in light of our findings, it may be that these data demonstrate a loss-of-function mutation in HLA-B*27:05 mice that causes arthritis. Unfortunately, those studies did not include a complete skeletal analysis and lacked an appropriate control. Therefore to determine the effect of HLA-B*27:05 on the skeleton, one could construct HLA-B*27:06/$\beta 2m^{-/-}$, and HLA-B*27:05/$\beta 2m^{-/-}$ mice and perform a complete skeletal analysis to test these hypotheses.

Future Directions – Therapeutic Tests

Development of therapeutics for AS has been slow, with many drugs failing clinical trials,[102,105,109] and other approved drugs providing symptomatic relief, but failing to halt progressive skeletal changes.[70,71] The difficulty of AS drug development is in part due to a lack of a robust animal model. Indeed, none of the FDA approved therapeutics for AS justified their original clinical trials with efficacy studies in animal models.[69,71,91,92,96,98,105,109,378] Prior to the work presented herein, there were likely no animal models that mimicked the disease closely enough to warrant such a study. Therefore our development of the ERAP1-/- mouse model of AS allows for efficacy studies of current and potential AS therapeutics in animals for the first time. Furthermore, our model allows for multiple readouts of drug efficacy, which is critical as many of the existing AS therapeutics treat pain and inflammation without preventing progressive spinal ankylosis. The key symptoms in AS are painful inflammation, new bone growth, and osteoporosis, so our goal is developing a readout for each of these pathologies in the ERAP1$^{-/-}$ mouse model.

For example, we have already established how we can measure spinal ankylosis and osteoporosis. In our AS prone animal models, putative therapeutics impact on osteoporosis could be measured via μCT as described in chapters 5 and 6. Six measures (BV/TV%, BMD, BMC, Tb. Th., Tb. N., and Tb. Sp.) taken in the sacrum, L6 vertebrae, and femur. Additionally the SI joint could be scored for erosions using the SI erosions scoring system described in chapter 5 and detailed in chapter 6. New bone formation could be measured with the AS fusion score at the L6/S1 joint using the system outlined in chapters 5 and 6. Due to the high variability of fusion in this model, the AS index will be used as well to score overall skeletal disease activity within AS

prone mice treated with a putative AS therapeutic.

Unlike measures of ankylosis and osteoporosis, we have yet to implement a measure for inflammation in ERAP1$^{-/-}$ mice, and we cannot use the same measurement used in AS clinical trials, the Assessment in SpondyloArthritis International Society improvement criteria (ASAS20).[90] The ASAS20 score consists almost entirely of patient subjective responses to questions regarding pain, stiffness, and their overall sense of disease activity.[90] In this system inflammation is measured as the patient's response to two questions: "how intense is your morning stiffness?" and "how long does your morning stiffness last?"[90] Not only is this impossible to implement in an animal model, but the responses in human patients may not necessarily be an accurate and reproducible measure of inflammation. Fortunately there are objective measures of inflammation in AS patients that can be used in animal models. The most powerful tool to accurately measure inflammation is likely magnetic resonance imaging (MRI) of the spine.[379,380] MR images have been used successfully in AS patients to monitor sites of inflammation within the spine,[65] and a similar protocol can be adapted for mice. Mice could be evaluated prior to therapy and each 6 weeks thereafter and scored with the AS spinal MRI activity (ASspiMRI-a) score, modified for mice.[381] For each vertebral unit, enhancement is scored on T1 sequence following gadolinium, edema is scored in short-tau inversion recovery sequence, and erosions are scored on enhancement of each vertebral unit with T1 sequence, as previously described.[68,379–381]

This measure of inflammation could be augmented with serum cytokine measures. Choosing which cytokines to assay is somewhat challenging because reports of the serum cytokine levels in AS patients have been highly variable.[382] Nonetheless, increased levels of of

TNF-α,[58–60] IL-6,[58–61] IL-17,[60,64] IL-23,[60,64] and IL-33[383,384] have been reported by multiple studies and correlated with disease activity or other measures of increased inflammation. For this reason blood could be harvested from mice every 6 weeks during treatment with a putative therapeutic, and assayed using a mutliplex bead-based assay system[171] for the cytokines listed above. Together MRI scoring and cytokine measures will quantify levels of inflammation within AS prone mice treated with putative AS therapeutics.

Together these three readouts cn be used to test the efficacy of AS therapeutics on treating inflammation, osteoporosis, and spinal ankylosis. In these trials 5-week old ERAP1-/- mice will have initial MRI and μCT scans taken (day 0) and then begin receiving the therapeutic or a placebo (defined below for each experiment). Each 6 weeks thereafter mice will have blood taken, receive MRI and μCT. The study will conclude at 36 weeks, as by 36 weeks a large effect size is observed in all parameters measured, and beyond this age only a marginal improvement in the effect size is observed (as shown in chapter 5). Naïve WT mice will be analyzed in tandem with the ERAP1-/- mice to provide a baseline measure for comparison.

These studies could begin by including known AS therapeutics, with a three-arm trial of placebo vs. NSAID vs. TNF-α blockade. NSIADs greatly reduce back pain in AS and decrease radiographic progression (ankylosis) in some, but not all, AS patients, so we expect that they will reduce both inflammation and skeletal pathology in the treated mice.[385] The initial trial with NSAIDs showed radiographic improvement with a dose of 100mg-200mg celecoxib twice daily,[91] which is approximately 1000-1,500ppm celecoxib mixed into mouse chow (a dose validated to be safe in previous experiments).[386] Compared to NSIADs, TNF-α blockade has shown a great effect on treating the pain and subjective measures of AS, but does not impact the

progression of skeletal disease.[70,387,388] For this reason we expect that TNF-α blockade may reduce inflammation in ERAP1$^{-/-}$ mice without improving the skeletal phenotype. We would use a dose of 5mg/kg of infliximab because this dose achieved success in treating inflammatory pain in the initial clinical trial with a TNF-α blocker.[98] Control mice would receive an injection of the previously described placebo used with infliximab, an antibody with the same Fc region, but a different Fv region that is non-functional.[389] At the end of 36 weeks the effect of these drugs on the progression of inflammation, osteoporosis, and ankylosis would then be measured and analyzed as described above. Based on results from clinical trials we expect that TNF-α blockade will improve signs of inflammation, but will not effect skeletal progression in the mice and that NSAID treatment will decrease both inflammation and skeletal disease.

These trials will serve to further validate this model by determining if the phenotype in ERAP1$^{-/-}$ mice responds similarly to currently approved AS therapeutics by reproducing findings observed in human trials. Furthermore if either therapeutic shows effects in a subset of animals, the improvement can be correlated with changes in serum cytokines and then further investigated, potentially shedding light on why NSAIDs and TNF-α are only effective in a subset of patients. Following these trials additional therapeutics can be tested.

Remaining Uncertainties and Limitations

Despite the increased understanding of the role of ERAP1 in antigen presentation and bone homeostasis provided by this work, limitations in the techniques and models used allow for specific uncertainties. Primary among these is the use of data obtained in animal models to extrapolate to human disease. Mice have many critical differences in their immune systems and skeletal systems that could potentially impact how our results translate to humans. For instance, the results we obtained in murine NK cells may fail to translate to human NK cells because the latter use different inhibitory receptors with different mechanisms of binding.[390] Human NK cells recognize MHC-I with KIR receptors that bind directly over the MHC-I-loaded peptide whereas the homologous murine Ly49 receptors don't make contact with bound peptide. This difference could potentially be critical, as ERAP1 could impact which peptides are loaded and alter the activation of human KIR+ NK cells, but not murine Ly49+ NK cells.

The murine skeletal system also has critical differences in both morphology and in the distribution of mechanical stress. Although it is not frequently discussed in AS literature, one common reason for inflammation within the axial skeleton is mechanical stress.[391,392] This may be playing a key role in triggering an inflammatory cascade in AS patients, and may explain some of the skeletal differences observed between the ERAP1$^{-/-}$ mice and AS patients. Specifically, sacroiliitis and sacroiliac fusion are hallmark radiographic features of AS, however we only observed sacroiliac erosions in ERAP1$^{-/-}$ mice, rather finding ankylosis as the murine Sacral-L6 joint. This difference may be due to anatomic differences as in humans, the SI joint is subjected to great mechanical strain because it transfers force from the upper body to the legs in a variety of activities.[393] Because mice are quadrupedal, a similar strain is not placed on their SI joints, and

this difference may explain why sacroiliac erosions fail to progress to full SI fusions in ERAP1$^{-/-}$ mice. In support of this, it has been shown in another pro-inflammatory murine model that mechanical stress triggered ankylosis.[394] Therefore, this limitation could be addressed by performing a similar study in ERAP1$^{-/-}$ mice, in which mechanical stress was applied to the sacroiliac joint and the joint was analyzed for ankylosis.

Additional limitations were encountered in Chapter 3, where the highly artificial model system that we used could have potentially produced a number of artifacts. In this system we were transfecting 2 plasmids (one containing ERAP1 and one containing the peptide) into TAP1-deficient cells. The very act of transfection can produce a strong immune response from cells and increase antigen presentation. We correctly controlled for this by demonstrating no significant difference between transfection of the ERAP1-High plasmid to the ERAP1-Low plasmid, making comparisons between groups valid, however all results that we obtained were post-transfection and therefore against the backdrop of an inflammatory response. Furthermore, this system only allowed us to assay a very small number of peptides, so from these studies alone, it would be impossible to know if our findings would be representative of larger peptide pools.

Most of the limitations introduced in chapter 3 were addressed by introducing ERAP1-High and ERAP1-Low into mice in chapter 4, however additional limitations were introduced. There are two large limitations of the ERAP1^{High} and ERAP1^{Low} mice. Firstly, these mice are expressing human ERAP1 from the promoter the Rosa26 locus. This resulted in a lower level of expression compared to endogenous murine ERAP1, and also removes the effect of the nascent ERAP1 promoters on the expression of ERAP1^{High} and ERAP1^{Low}. Whereas ERAP1 in its native locus is induced by IFN-γ,[249] p53,[395] and many other immune and non-immune transcription

factors, the transgenic ERAP1 genes we placed in the Rosa26 locus are not. Therefore the ERAP1^{High} and ERAP1^{Low} mice fail to model variation in ERAP1 expression mediated by cytokines, cell-specific transcription factors, and other signals that require ERAP1 to be in its native locus. Once again, this is properly controlled for, as the *ERAP1^{High}* and *ERAP1^{Low}* genes are identically constructed, making comparisons between these strains valid, however any differences between ERAP1^{High} and ERAP1^{Low} that require variations in transcription level will not be captured by our model. Solving this issue would require generating new transgenic mice with the human ERAP1 variants inserted into the native murine ERAP1 locus, however the observation that ERAP1^{High} is lethal in males even at ~1/10th expression, suggests that it may be lethal in all mice at full expression.

Another limitation in this work is inherent to studying a gene with multiple disease-associated SNPs. We chose to primarily study an ERAP1 variant containing all 5 disease-associate SNPs, and a control with no AS associated SNPs present, however these two alleles are not well represented in the population. A haplotype analysis was completed using HapMap and only 0.001% of humans that participated in published studies had the *ERAP1^{Low}* allele. Worse, no humans analyzed had the *ERAP1^{High}* allele. For this reason, studying *ERAP1^{High}* can not be directly justified using genetic studies, and is instead justified by our observation that in cells these 5 SNPs had an additive effect (chapter 3). While an alternative is studying the effect of individual SNPs, this is equally artificial, as many single-SNP ERAP1 variants also don't appear in the population due to strong linkage disequilibrium within ERAP1. The ideal solution would be to clone all commonly associated ERAP1 variants into mice and study the effect of each allele, rather than SNP. Interestingly, our observation that *ERAP1^{High}* is lethal in male mice may

explain why it is absent from the human population and why *ERAP1* has such strong linkage disequilibrium, as this strong selection bias would quickly remove it from the gene pool.

In fact, the lethal male phenotype is the largest remaining uncertainty presented in this work. Because it persists in the absence of MHC-I, it is likely due to one of ERAP1's functions outside of antigen presentation, such as the role of ERAP1 in blood pressure regulation. Recent work has shown that ERAP1 can affect the synthesis of nitric oxide,[174] and regulate blood pressure via the renin-angiotensin system.[396] These findings may explain why polymorphisms in ERAP1 are associated with blood pressure disorders of pregnancy, such as preeclampsia and HELP syndrome.[127] These mechanisms or other, yet unknown mechanisms may be causing the male-lethal phenotype in ERAP1-High mice, but those discoveries lie beyond the scope of this thesis.

Finally, while this thesis has been primarily focused on the canonical role of ERAP1 in antigen-presentation, recent research suggests that ERAP1 plays a host of other important functions in the immune system and beyond. It's been shown that ERAP1 is regulated by p53 and may play a role in cancer immunosurveillance,[395] that ERAP1 is critical in the renin-angiotensin system,[396] and that ERAP1 plays a role in innate immunity and inflammation.[171,175] At least some of these roles, or all of them contribute to the pathogenesis of AS.

Conclusion

In this thesis we set out to study ERAP1 based on its association to AS by GWAS. As a disease that is ~90% heritable,[111] AS was one of many complex genetic disorders that was to be solved by the GWAS revolution,[246] however after multiple large GWASs in AS, all known genes

only account for 24.4% of the heritable risk.[28] This demonstrates the importance of work like ours that builds upon probabilistic correlations from GWAS with biological evidence of causation.

Since we began our research ERAP1 has been associated with six other hereditary diseases and has found importance in an increasing number of fields beyond adaptive immunology. Our work has been critical in defining the role of ERAP1 in antigen presentation, and in identifying a new role for ERAP1 in bone homeostasis. Just as the experiments presented here build upon the results of genome-wide association studies, now these experiments can serve as foundations for future work dissecting the role of ERAP1 and antigen presentation in bone homeostasis. Furthermore, we predict that this new field of research will prove important for the understanding of the multiple diseases that are associated with epistasis between HLA and ERAP, including AS, Behçet's disease, and psoriasis.

REFERENCES

REFERENCES

1. Zochling, J. & Smith, E. U. R. Seronegative spondyloarthritis. *Best Pract. Res. Clin. Rheumatol.* **24,** 747–756 (2010).

2. Zochling, J., Brandt, J. & Braun, J. The current concept of spondyloarthritis with special emphasis on undifferentiated spondyloarthritis. *Rheumatology* **44,** 1483–1491 (2005).

3. Moll, J. M., Haslock, I., Macrae, I. F. & Wright, V. Associations between ankylosing spondylitis, psoriatic arthritis, Reiter's disease, the intestinal arthropathies, and Behcet's syndrome. *Medicine (Baltimore)* **53,** 343–364 (1974).

4. Braun, J. & Sieper, J. Ankylosing spondylitis. *The Lancet* **369,** 1379–1390 (2007).

5. Kerschbaumer, A., Fenzl, K. H., Erlacher, L. & Aletaha, D. An overview of psoriatic arthritis – epidemiology, clinical features, pathophysiology and novel treatment targets. *Wien. Klin. Wochenschr.* 1–5 (2016). doi:10.1007/s00508-016-1111-9

6. Lubrano, E. *et al.* The Definition and Measurement of Axial Psoriatic Arthritis. *J. Rheumatol. Suppl.* **93,** 40–42 (2015).

7. Ward, M. M. *et al.* American College of Rheumatology/Spondylitis Association of America/Spondyloarthritis Research and Treatment Network 2015 Recommendations for the Treatment of Ankylosing Spondylitis and Nonradiographic Axial Spondyloarthritis. *Arthritis Rheumatol. Hoboken NJ* **68,** 282–298 (2016).

8. Rosenbaum, J. T. Uveitis in spondyloarthritis including psoriatic arthritis, ankylosing spondylitis, and inflammatory bowel disease. *Clin. Rheumatol.* **34,** 999–1002 (2015).

9. Sampaio-Barros, P. D., Conde, R. A., Bonfiglioli, R., Bértolo, M. B. & Samara, A. M. Characterization and outcome of uveitis in 350 patients with spondyloarthropathies. *Rheumatol. Int.* **26,** 1143–1146 (2006).

10. Klingberg, E. *et al.* Osteoporosis in ankylosing spondylitis - prevalence, risk factors and methods of assessment. *Arthritis Res. Ther.* **14,** R108 (2012).

11. Cantini, F., Nannini, C., Cassarà, E., Kaloudi, O. & Niccoli, L. Uveitis in Spondyloarthritis: An Overview. *J. Rheumatol.* **93,** 27–29 (2015).

12. Palm, Ø., Moum, B., Jahnsen, J. & Gran, J. T. The prevalence and incidence of peripheral arthritis in patients with inflammatory bowel disease, a prospective population- based study (the IBSEN study). *Rheumatology* **40,** 1256–1261 (2001).

13. Evans, D. M. *et al.* Interaction between ERAP1 and HLA-B27 in ankylosing spondylitis implicates peptide handling in the mechanism for HLA-B27 in disease susceptibility. *Nat. Genet.* **43,** 761–767 (2011).

14. Cortes, A. *et al.* Major histocompatibility complex associations of ankylosing spondylitis are complex and involve further epistasis with ERAP1. *Nat. Commun.* **6,** 7146 (2015).

15. Conde-Jaldón, M. *et al.* Epistatic Interaction of ERAP1 and HLA-B in Behçet Disease: A Replication Study in the Spanish Population. *PLoS ONE* **9,** (2014).

16. Genetic Analysis of Psoriasis Consortium & the Wellcome Trust Case Control Consortium 2 *et al.* A genome-wide association study identifies new psoriasis susceptibility loci and an interaction between HLA-C and ERAP1. *Nat. Genet.* **42,** 985–990 (2010).

17. Pimentel-Santos, F. M. *et al.* Association of IL23R and ERAP1 genes with ankylosing spondylitis in a Portuguese population. *Clin. Exp. Rheumatol.* **27,** 800–806 (2009).

18. Cargill, M. *et al.* A large-scale genetic association study confirms IL12B and leads to the identification of IL23R as psoriasis-risk genes. *Am. J. Hum. Genet.* **80,** 273–290 (2007).

19. Duerr, R. H. *et al.* A Genome-Wide Association Study Identifies IL23R as an Inflammatory Bowel Disease Gene. *Science* **314,** 1461–1463 (2006).

20. Zhu, K.-J., Zhu, C.-Y., Shi, G. & Fan, Y.-M. Association of IL23R polymorphisms with psoriasis and psoriatic arthritis: a meta-analysis. *Inflamm. Res. Off. J. Eur. Histamine Res. Soc. Al* **61,** 1149–1154 (2012).

21. Davey-Ranasinghe, N. & Deodhar, A. Osteoporosis and vertebral fractures in ankylosing spondylitis. *Curr. Opin. Rheumatol.* **25,** 509–516 (2013).

22. Schlosstein, L., Terasaki, P. I., Bluestone, R. & Pearson, C. M. High association of an HL-A antigen, W27, with ankylosing spondylitis. *N. Engl. J. Med.* **288,** 704–706 (1973).

23. Brewerton, D. A. *et al.* Ankylosing spondylitis and HL-A 27. *Lancet Lond. Engl.* **1,** 904–907 (1973).

24. Caffrey, M. F. & James, D. C. Human lymphocyte antigen association in ankylosing spondylitis. *Nature* **242,** 121 (1973).

25. Burton, P. R. *et al.* Association scan of 14,500 nonsynonymous SNPs in four diseases identifies autoimmunity variants. *Nat. Genet.* **39,** 1329–1337 (2007).

26. Kastbom, A. *et al.* Genetic variants in CARD8 but not in NLRP3 are associated with

ankylosing spondylitis. *Scand. J. Rheumatol.* **42,** 465–468 (2013).

27. (tasc), T. A.-A.-A. S. C. Genome-wide association study of ankylosing spondylitis identifies non-MHC susceptibility loci. *Nat. Genet.* **42,** 123–127 (2010).

28. Cortes, A. *et al.* Identification of multiple risk variants for ankylosing spondylitis through high-density genotyping of immune-related loci. *Nat. Genet.* **45,** 730–738 (2013).

29. Brown, M. A. *et al.* The effect of HLA-DR genes on susceptibility to and severity of ankylosing spondylitis. *Arthritis Rheum.* **41,** 460–465 (1998).

30. Vargas-Alarcón, G. *et al.* Effect of HLA-B and HLA-DR genes on susceptibility to and severity of spondyloarthropathies in Mexican patients. *Ann. Rheum. Dis.* **61,** 714–717 (2002).

31. Said-Nahal, R. *et al.* The role of HLA genes in familial spondyloarthropathy: a comprehensive study of 70 multiplex families. *Ann. Rheum. Dis.* **61,** 201–206 (2002).

32. McGonagle, D. Enthesitis: an autoinflammatory lesion linking nail and joint involvement in psoriatic disease. *J. Eur. Acad. Dermatol. Venereol. JEADV* **23 Suppl 1,** 9–13 (2009).

33. Gladman, D. D., Anhorn, K. A., Schachter, R. K. & Mervart, H. HLA antigens in psoriatic arthritis. *J. Rheumatol.* **13,** 586–592 (1986).

34. Gudjónsson, J. E. *et al.* HLA-Cw6-positive and HLA-Cw6-negative patients with Psoriasis vulgaris have distinct clinical features. *J. Invest. Dermatol.* **118,** 362–365 (2002).

35. Rahman, P. *et al.* Association of Interleukin 23 Receptor Variants with Psoriatic Arthritis. *J. Rheumatol.* **36,** 137–140 (2009).

36. Nelson, G. W. *et al.* Cutting Edge: Heterozygote Advantage in Autoimmune Disease: Hierarchy of Protection/Susceptibility Conferred by HLA and Killer Ig-Like Receptor Combinations in Psoriatic Arthritis. *J. Immunol.* **173,** 4273–4276 (2004).

37. Colmegna, I., Cuchacovich, R. & Espinoza, L. R. HLA-B27-Associated Reactive Arthritis: Pathogenetic and Clinical Considerations. *Clin. Microbiol. Rev.* **17,** 348–369 (2004).

38. Bergboer, J. G. M. *et al.* Paediatric-onset psoriasis is associated with ERAP1 and IL23R loci, LCE3C_LCE3B deletion and HLA-C*06. *Br. J. Dermatol.* **167,** 922–925 (2012).

39. Zhang, X.-J. *et al.* Psoriasis genome-wide association study identifies susceptibility variants within LCE gene cluster at 1q21. *Nat. Genet.* **41,** 205–210 (2009).

40. Nair, R. P. *et al.* Genome-wide scan reveals association of psoriasis with IL-23 and NF-kappaB pathways. *Nat. Genet.* **41,** 199–204 (2009).

41. Sakane, T., Takeno, M., Suzuki, N. & Inaba, G. Behçet's Disease. *N. Engl. J. Med.* **341,** 1284–1291 (1999).

42. Bicer, A. Musculoskeletal Findings in Behcet's Disease. *Pathol. Res. Int.* **2012,** e653806 (2011).

43. Kirino, Y. *et al.* Genome-wide association analysis identifies new susceptibility loci for Behçet's disease and epistasis between HLA-B*51 and ERAP1. *Nat. Genet.* **45,** 202–207 (2013).

44. Orchard, T. R. *et al.* Clinical phenotype is related to HLA genotype in the peripheral arthropathies of inflammatory bowel disease. *Gastroenterology* **118,** 274–278 (2000).

45. Lyons, J. L. & Rosenbaum, J. T. Uveitis Associated With Inflammatory Bowel Disease Compared With Uveitis Associated With Spondyloarthropathy. *Arch. Ophthalmol.* **115,** 61–64 (1997).

46. Henckaerts, L. & Vermeire, S. NOD2/CARD15 disease associations other than Crohn's disease. *Inflamm. Bowel Dis.* **13,** 235–241 (2007).

47. Rudwaleit, M., Metter, A., Listing, J., Sieper, J. & Braun, J. Inflammatory back pain in ankylosing spondylitis: a reassessment of the clinical history for application as classification and diagnostic criteria. *Arthritis Rheum.* **54,** 569–578 (2006).

48. Taurog, J. D., Chhabra, A. & Colbert, R. A. Ankylosing Spondylitis and Axial Spondyloarthritis. *N. Engl. J. Med.* **374,** 2563–2574 (2016).

49. Van Praet, L. *et al.* Microscopic gut inflammation in axial spondyloarthritis: a multiparametric predictive model. *Ann. Rheum. Dis.* **72,** 414–417 (2013).

50. Leirisalo-Repo, M., Turunen, U., Stenman, S., Helenius, P. & Seppälä, K. High frequency of silent inflammatory bowel disease in spondylarthropathy. *Arthritis Rheum.* **37,** 23–31 (1994).

51. Ginsburg, W. W. & Cohen, M. D. Peripheral arthritis in ankylosing spondylitis. A review of 209 patients followed up for more than 20 years. *Mayo Clin. Proc.* **58,** 593–596 (1983).

52. Kim, T.-J. *et al.* The presence of peripheral arthritis delays spinal radiographic progression in ankylosing spondylitis: Observation Study of the Korean Spondyloarthropathy Registry. *Rheumatology* **53,** 1404–1408 (2014).

53. Fam, A. G., Rubenstein, J. D., Chin-Sang, H. & Leung, F. Y. Computed tomography in the diagnosis of early ankylosing spondylitis. *Arthritis Rheum.* **28,** 930–937 (1985).

54. Østergaard, M. & Lambert, R. G. W. Imaging in ankylosing spondylitis. *Ther. Adv. Musculoskelet. Dis.* **4,** 301–311 (2012).

55. Hermann, K.-G. A. *et al.* Spinal changes in patients with spondyloarthritis: comparison of MR imaging and radiographic appearances. *Radiogr. Rev. Publ. Radiol. Soc. N. Am. Inc* **25,** 559-569-570 (2005).

56. van den Berg, R. *et al.* ASAS modification of the Berlin algorithm for diagnosing axial spondyloarthritis: results from the SPondyloArthritis Caught Early (SPACE)-cohort and from the Assessment of SpondyloArthritis international Society (ASAS)-cohort. *Ann. Rheum. Dis.* **72,** 1646–1653 (2013).

57. Spoorenberg, A. *et al.* Relative value of erythrocyte sedimentation rate and C-reactive protein in assessment of disease activity in ankylosing spondylitis. *J. Rheumatol.* **26,** 980–984 (1999).

58. Gratacós, J. *et al.* Serum cytokines (IL-6, TNF-alpha, IL-1 beta and IFN-gamma) in ankylosing spondylitis: a close correlation between serum IL-6 and disease activity and severity. *Br. J. Rheumatol.* **33,** 927–931 (1994).

59. Bal, A. *et al.* Comparison of serum IL-1 beta, sIL-2R, IL-6, and TNF-alpha levels with disease activity parameters in ankylosing spondylitis. *Clin. Rheumatol.* **26,** 211–215 (2007).

60. Romero-Sanchez, C. *et al.* Association between Th-17 cytokine profile and clinical features in patients with spondyloarthritis. *Clin. Exp. Rheumatol.* **29,** 828–834 (2011).

61. Pedersen, S. J. *et al.* ASDAS, BASDAI and different treatment responses and their relation to biomarkers of inflammation, cartilage and bone turnover in patients with axial spondyloarthritis treated with TNFα inhibitors. *Ann. Rheum. Dis.* **70,** 1375–1381 (2011).

62. Sveaas, S. H. *et al.* Circulating levels of inflammatory cytokines and cytokine receptors in patients with ankylosing spondylitis: a cross-sectional comparative study. *Scand. J. Rheumatol.* **44,** 118–124 (2015).

63. Schulz, M., Dotzlaw, H. & Neeck, G. Ankylosing Spondylitis and Rheumatoid Arthritis: Serum Levels of TNF- and Its Soluble Receptors during the Course of Therapy with Etanercept and Infliximab. *BioMed Res. Int.* **2014,** e675108 (2014).

64. Chen, W.-S. *et al.* Association of serum interleukin-17 and interleukin-23 levels with disease activity in Chinese patients with ankylosing spondylitis. *J. Chin. Med. Assoc.* **75,** 303–308 (2012).

65. van der Heijde, D. *et al.* MRI inflammation at the vertebral unit only marginally predicts

new syndesmophyte formation: a multilevel analysis in patients with ankylosing spondylitis. *Ann. Rheum. Dis.* **71,** 369–373 (2012).

66. Bron, J. L., de Vries, M. K., Snieders, M. N., van der Horst-Bruinsma, I. E. & van Royen, B. J. Discovertebral (Andersson) lesions of the spine in ankylosing spondylitis revisited. *Clin. Rheumatol.* **28,** 883–892 (2009).

67. Appel, H. *et al.* Immunohistochemical analysis of osteoblasts in zygapophyseal joints of patients with ankylosing spondylitis reveal repair mechanisms similar to osteoarthritis. *J. Rheumatol.* **37,** 823–828 (2010).

68. Maksymowych, W. P. *et al.* Inflammatory lesions of the spine on magnetic resonance imaging predict the development of new syndesmophytes in ankylosing spondylitis: Evidence of a relationship between inflammation and new bone formation. *Arthritis Rheum.* **60,** 93–102 (2009).

69. Calin, A. *et al.* Outcomes of a multicentre randomised clinical trial of etanercept to treat ankylosing spondylitis. *Ann. Rheum. Dis.* **63,** 1594–1600 (2004).

70. Baraliakos, X. *et al.* Radiographic progression in patients with ankylosing spondylitis after 4 yrs of treatment with the anti-TNF-α antibody infliximab. *Rheumatology* **46,** 1450–1453 (2007).

71. Maas, F. *et al.* Spinal radiographic progression in patients with ankylosing spondylitis treated with TNF-α blocking therapy: a prospective longitudinal observational cohort study. *PloS One* **10,** e0122693 (2015).

72. Baraliakos, X., Listing, J., Rudwaleit, M., Sieper, J. & Braun, J. The relationship between inflammation and new bone formation in patients with ankylosing spondylitis. *Arthritis Res. Ther.* **10,** R104 (2008).

73. Bruijnen, S. T. *et al.* Bone formation rather than inflammation reflects Ankylosing Spondylitis activity on PET-CT: a pilot study. *Arthritis Res. Ther.* **14,** R71 (2012).

74. Toussirot, E., Michel, F. & Wendling, D. Bone density, ultrasound measurements and body composition in early ankylosing spondylitis. *Rheumatology* **40,** 882–888 (2001).

75. Nigil Haroon, N. *et al.* Alterations of bone mineral density, bone microarchitecture and strength in patients with ankylosing spondylitis: a cross-sectional study using high-resolution peripheral quantitative computerized tomography and finite element analysis. *Arthritis Res. Ther.* **17,** (2015).

76. Appel, H. *et al.* Immunohistochemical analysis of hip arthritis in ankylosing spondylitis: Evaluation of the bone–cartilage interface and subchondral bone marrow. *Arthritis Rheum.* **54,**

1805–1813 (2006).

77. Klingberg, E. *et al.* Bone microarchitecture in ankylosing spondylitis and the association with bone mineral density, fractures, and syndesmophytes. *Arthritis Res. Ther.* **15,** R179 (2013).

78. The prevalence of vertebral fractures in mild ankylosing spondylitis and their relationship to bone mineral density. Available at: http://rheumatology.oxfordjournals.org.proxy2.cl.msu.edu.proxy1.cl.msu.edu/content/39/1/85.full. (Accessed: 31st October 2016)

79. Ghasemi-rad, M. *et al.* Ankylosing spondylitis: A state of the art factual backbone. *World J. Radiol.* **7,** 236–252 (2015).

80. Stolwijk, C., van Tubergen, A., Castillo-Ortiz, J. D. & Boonen, A. Prevalence of extra-articular manifestations in patients with ankylosing spondylitis: a systematic review and meta-analysis. *Ann. Rheum. Dis.* **74,** 65–73 (2015).

81. Braun, J., Baraliakos, X., Listing, J. & Sieper, J. Decreased incidence of anterior uveitis in patients with ankylosing spondylitis treated with the anti–tumor necrosis factor agents infliximab and etanercept. *Arthritis Rheum.* **52,** 2447–2451 (2005).

82. Rudwaleit, M. *et al.* Adalimumab effectively reduces the rate of anterior uveitis flares in patients with active ankylosing spondylitis: results of a prospective open-label study. *Ann. Rheum. Dis.* **68,** 696–701 (2009).

83. Dougados, M. *et al.* The European Spondylarthropathy Study Group Preliminary Criteria for the Classification of Spondylarthropathy. *Arthritis Rheum.* **34,** 1218–1227 (1991).

84. Cohen, M. D. & Ginsburg, W. W. Late-onset peripheral joint disease in ankylosing spondylitis. *Ann. Rheum. Dis.* **41,** 574–578 (1982).

85. Rudwaleit, M. & Baeten, D. Ankylosing spondylitis and bowel disease. *Best Pract. Res. Clin. Rheumatol.* **20,** 451–471 (2006).

86. Kappelman, M. D. *et al.* The prevalence and geographic distribution of Crohn's disease and ulcerative colitis in the United States. *Clin. Gastroenterol. Hepatol. Off. Clin. Pract. J. Am. Gastroenterol. Assoc.* **5,** 1424–1429 (2007).

87. De Keyser, F. & Mielants, H. The gut in ankylosing spondylitis and other spondyloarthropathies: inflammation beneath the surface. *J. Rheumatol.* **30,** 2306–2307 (2003).

88. Rudwaleit, M. *et al.* The development of Assessment of SpondyloArthritis international

Society classification criteria for axial spondyloarthritis (part I): classification of paper patients by expert opinion including uncertainty appraisal. *Ann. Rheum. Dis.* **68,** 770–776 (2009).

89. Sieper, J. *et al.* The Assessment of SpondyloArthritis international Society (ASAS) handbook: a guide to assess spondyloarthritis. *Ann. Rheum. Dis.* **68,** ii1-ii44 (2009).

90. Landewé, R. & van Tubergen, A. Clinical Tools to Assess and Monitor Spondyloarthritis. *Curr. Rheumatol. Rep.* **17,** (2015).

91. Wanders, A. *et al.* Nonsteroidal antiinflammatory drugs reduce radiographic progression in patients with ankylosing spondylitis: A randomized clinical trial. *Arthritis Rheum.* **52,** 1756–1765 (2005).

92. Baeten, D. *et al.* Anti-interleukin-17A monoclonal antibody secukinumab in treatment of ankylosing spondylitis: a randomised, double-blind, placebo-controlled trial. *The Lancet* **382,** 1705–1713 (2013).

93. Baraliakos, X. *et al.* Long-term effects of secukinumab on MRI findings in relation to clinical efficacy in subjects with active ankylosing spondylitis: an observational study. *Ann. Rheum. Dis.* **75,** 408–412 (2016).

94. van der Heijde, D. *et al.* Efficacy and safety of infliximab in patients with ankylosing spondylitis: Results of a randomized, placebo-controlled trial (ASSERT). *Arthritis Rheum.* **52,** 582–591 (2005).

95. Haroon, N., Kim, T.-H. & Inman, R. D. NSAIDs and radiographic progression in ankylosing spondylitis Bagging big game with small arms? *Ann. Rheum. Dis.* **71,** 1593–1595 (2012).

96. van der Heijde, D. *et al.* Evaluation of the efficacy of etoricoxib in ankylosing spondylitis: Results of a fifty-two–week, randomized, controlled study. *Arthritis Rheum.* **52,** 1205–1215 (2005).

97. Gorman, J. D., Sack, K. E. & Davis, J. C. J. Treatment of Ankylosing Spondylitis by Inhibition of Tumor Necrosis Factor α. *N. Engl. J. Med.* **346,** 1349–1356 (2002).

98. Braun, J. *et al.* Treatment of active ankylosing spondylitis with infliximab: a randomised controlled multicentre trial. *The Lancet* **359,** 1187–1193 (2002).

99. van der Heijde, D. *et al.* Assessment of radiographic progression in the spines of patients with ankylosing spondylitis treated with adalimumab for up to 2 years. *Arthritis Res. Ther.* **11,** R127 (2009).

100. van der Heijde, D. *et al.* Radiographic progression of ankylosing spondylitis after up to two years of treatment with etanercept. *Arthritis Rheum.* **58,** 1324–1331 (2008).

101. Haberhauer, G., Strehblow, C. & Fasching, P. Observational study of switching anti-TNF agents in ankylosing spondylitis and psoriatic arthritis versus rheumatoid arthritis. *Wien. Med. Wochenschr.* **160,** 220–224 (2010).

102. Pathan, E. *et al.* Efficacy and safety of apremilast, an oral phosphodiesterase 4 inhibitor, in ankylosing spondylitis. *Ann. Rheum. Dis.* **72,** 1475–1480 (2013).

103. Sieper, J., Porter-Brown, B., Thompson, L., Harari, O. & Dougados, M. Assessment of short-term symptomatic efficacy of tocilizumab in ankylosing spondylitis: results of randomised, placebo-controlled trials. *Ann. Rheum. Dis.* **73,** 95–100 (2014).

104. Tan, A. L. Efficacy of anakinra in active ankylosing spondylitis: a clinical and magnetic resonance imaging study. *Ann. Rheum. Dis.* **63,** 1041–1045 (2004).

105. Haibel, H., Rudwaleit, M., Listing, J. & Sieper, J. Open label trial of anakinra in active ankylosing spondylitis over 24 weeks. *Ann. Rheum. Dis.* **64,** 296–298 (2005).

106. Spina, D. PDE4 inhibitors: current status. *Br. J. Pharmacol.* **155,** 308–315 (2008).

107. Edwards, C. J. *et al.* Apremilast, an oral phosphodiesterase 4 inhibitor, in patients with psoriatic arthritis and current skin involvement: a phase III, randomised, controlled trial (PALACE 3). *Ann. Rheum. Dis.* **75,** 1065–1073 (2016).

108. Celgene Reports Results from the Phase III POSTURE Study Evaluating Oral OTEZLA® in Ankylosing Spondylitis (NASDAQ:CELG). Available at: http://ir.celgene.com/releasedetail.cfm?releaseid=858785. (Accessed: 14th November 2016)

109. Sieper, J. *et al.* Sarilumab for the treatment of ankylosing spondylitis: results of a Phase II, randomised, double-blind, placebo-controlled study (ALIGN). *Ann. Rheum. Dis.* (2014). doi:10.1136/annrheumdis-2013-204963

110. Blécourt, J. J. de, Polman, A., Blécourt-Meindersma, T. de, Erlee, T. J. D. & Drion, E. F. Hereditary Factors in Rheumatoid Arthritis and Ankylosing Spondylitis. *Ann. Rheum. Dis.* **20,** 215 (1961).

111. Brown, M. A. *et al.* Susceptibility to ankylosing spondylitis in twins the role of genes, HLA, and the environment. *Arthritis Rheum.* **40,** 1823–1828 (1997).

112. Pedersen, O. B. *et al.* Ankylosing spondylitis in Danish and Norwegian twins: occurrence and the relative importance of genetic vs. environmental effectors in disease causation. *Scand. J. Rheumatol.* **37,** 120–126 (2008).

113. Brown, M. A., Laval, S. H., Brophy, S. & Calin, A. Recurrence risk modelling of the genetic susceptibility to ankylosing spondylitis. *Ann. Rheum. Dis.* **59,** 883–886 (2000).

114. van der Linden, S., Valkenburg, H. & Cats, A. The risk of developing ankylosing spondylitis in HLA-B27 positive individuals: a family and population study. *Br. J. Rheumatol.* **22,** 18–19 (1983).

115. Calin, A., Marder, A., Becks, E. & Burns, T. Genetic differences between B27 positive patients with ankylosing spondylitis and B27 positive healthy controls. *Arthritis Rheum.* **26,** 1460–1464 (1983).

116. Liu, Y. *et al.* Predominant association of HLA-B*2704 with ankylosing spondylitis in Chinese Han patients. *Tissue Antigens* **75,** 61–64 (2010).

117. Paladini, F. *et al.* Distribution of HLA-B27 subtypes in Sardinia and continental Italy and their association with spondylarthropathies. *Arthritis Rheum.* **52,** 3319–3321 (2005).

118. D'Amato, M. *et al.* Frequency of the new HLA-B*2709 allele in ankylosing spondylitis patients and healthy individuals. *Dis. Markers* **12,** 215–217 (1995).

119. Mathieu, A. & Sorrentino, R. HLA–B*2709 and spondylarthropathies: Comment on the concise communication by Olivieri et al. *Arthritis Rheum.* **48,** 866–867 (2003).

120. Van Gaalen, F. A. Does HLA-B*2706 protect against ankylosing spondylitis? A meta-analysis. *Int. J. Rheum. Dis.* **15,** 8–12 (2012).

121. Uddin, M. *et al.* Integrated Genomics Identifies Convergence of Ankylosing Spondylitis with Global Immune Mediated Disease Pathways. *Sci. Rep.* **5,** (2015).

122. Díaz-Peña, R. *et al.* Genetic study confirms association of HLA-DPA1(π)01:03 subtype with ankylosing spondylitis in HLA-B27-positive populations. *Hum. Immunol.* **74,** 764–767 (2013).

123. Brown, M. A., Kenna, T. & Wordsworth, B. P. Genetics of ankylosing spondylitis—insights into pathogenesis. *Nat. Rev. Rheumatol.* **12,** 81–91 (2016).

124. Zvyagin, I. V. *et al.* Association of ERAP1 Allelic Variants with Risk of Ankylosing Spondylitis. *Acta Naturae* **2,** 72–77 (2010).

125. Stratikos, E., Stamogiannos, A., Zervoudi, E. & Fruci, D. A Role for Naturally Occurring Alleles of Endoplasmic Reticulum Aminopeptidases in Tumor Immunity and Cancer Pre-Disposition. *Front. Oncol.* **4,** (2014).

126. Guerini, F. R. *et al.* A functional variant in ERAP1 predisposes to multiple sclerosis. *PloS One* **7,** e29931 (2012).

127. Haram, K., Mortensen, J. H. & Nagy, B. Genetic aspects of preeclampsia and the HELLP syndrome. *J. Pregnancy* **2014,** 910751 (2014).

128. Filer, C. *et al.* Investigation of association of the IL12B and IL23R genes with psoriatic arthritis. *Arthritis Rheum.* **58,** 3705–3709 (2008).

129. Xu, W.-D., Xie, Q.-B., Zhao, Y. & Liu, Y. Association of Interleukin-23 receptor gene polymorphisms with susceptibility to Crohn's disease: A meta-analysis. *Sci. Rep.* **5,** (2015).

130. Yu, P. *et al.* Association of Single Nucleotide Polymorphisms of IL23R and IL17 with Ulcerative Colitis Risk in a Chinese Han Population. *PLOS ONE* **7,** e44380 (2012).

131. Robinson, P. C. *et al.* ERAP2 is associated with ankylosing spondylitis in HLA-B27-positive and HLA-B27-negative patients. *Ann. Rheum. Dis.* **74,** 1627–1629 (2015).

132. Ivanova, M. *et al.* AB0050 Association of il12b gene polymorphisms with ankylosing spondylitis. *Ann. Rheum. Dis.* **72,** A800–A801 (2013).

133. Kloetzel, P.-M. Antigen processing by the proteasome. *Nat. Rev. Mol. Cell Biol.* **2,** 179–188 (2001).

134. Kisselev, A. F., Akopian, T. N., Woo, K. M. & Goldberg, A. L. The Sizes of Peptides Generated from Protein by Mammalian 26 and 20 S Proteasomes IMPLICATIONS FOR UNDERSTANDING THE DEGRADATIVE MECHANISM AND ANTIGEN PRESENTATION. *J. Biol. Chem.* **274,** 3363–3371 (1999).

135. Boguski, M. S. & McIntosh, M. W. Biomedical informatics for proteomics. *Nature* **422,** 233–237 (2003).

136. Ferrington, D. A. & Gregerson, D. S. Immunoproteasomes: structure, function, and antigen presentation. *Prog. Mol. Biol. Transl. Sci.* **109,** 75–112 (2012).

137. Momburg, F. *et al.* Selectivity of MHC-encoded peptide transporters from human, mouse and rat. *Nature* **367,** 648–651 (1994).

138. Chang, S.-C., Momburg, F., Bhutani, N. & Goldberg, A. L. The ER aminopeptidase, ERAP1, trims precursors to lengths of MHC class I peptides by a 'molecular ruler' mechanism. *Proc. Natl. Acad. Sci. U. S. A.* **102,** 17107–17112 (2005).

139. Piertney, S. B. & Oliver, M. K. The evolutionary ecology of the major histocompatibility complex. *Heredity* **96,** 7–21 (2006).

140. Buhler, S. & Sanchez-Mazas, A. HLA DNA Sequence Variation among Human Populations: Molecular Signatures of Demographic and Selective Events. *PLOS ONE* **6,** e14643 (2011).

141. Aguilar, A. *et al.* High MHC diversity maintained by balancing selection in an otherwise genetically monomorphic mammal. *Proc. Natl. Acad. Sci. U. S. A.* **101,** 3490–3494 (2004).

142. Barber, L. D. *et al.* Polymorphism in the alpha 1 helix of the HLA-B heavy chain can have an overriding influence on peptide-binding specificity. *J. Immunol.* **158,** 1660–1669 (1997).

143. Sommer, S. The importance of immune gene variability (MHC) in evolutionary ecology and conservation. *Front. Zool.* **2,** 16 (2005).

144. Oosterhout, C. van. A new theory of MHC evolution: beyond selection on the immune genes. *Proc. R. Soc. Lond. B Biol. Sci.* **276,** 657–665 (2009).

145. Gandhi, A., Lakshminarasimhan, D., Sun, Y. & Guo, H.-C. Structural insights into the molecular ruler mechanism of the endoplasmic reticulum aminopeptidase ERAP1. *Sci. Rep.* **1,** (2011).

146. York, I. A. *et al.* The ER aminopeptidase ERAP1 enhances or limits antigen presentation by trimming epitopes to 8–9 residues. *Nat. Immunol.* **3,** 1177–1184 (2002).

147. York, I. A., Brehm, M. A., Zendzian, S., Towne, C. F. & Rock, K. L. Endoplasmic reticulum aminopeptidase 1 (ERAP1) trims MHC class I-presented peptides in vivo and plays an important role in immunodominance. *Proc. Natl. Acad. Sci.* **103,** 9202–9207 (2006).

148. Rastall, D. P. W., Aldhamen, Y. A., Seregin, S. S., Godbehere, S. & Amalfitano, A. ERAP1 functions override the intrinsic selection of specific antigens as immunodominant peptides, thereby altering the potency of antigen-specific cytolytic and effector memory T-cell responses. *Int. Immunol.* **26,** 685–695 (2014).

149. Seregin, S. S. *et al.* Endoplasmic reticulum aminopeptidase-1 alleles associated with increased risk of ankylosing spondylitis reduce HLA-B27 mediated presentation of multiple antigens. *Autoimmunity* **46,** 497–508 (2013).

150. Tscharke, D. C., Croft, N. P., Doherty, P. C. & La Gruta, N. L. Sizing up the key determinants of the CD8+ T cell response. *Nat. Rev. Immunol.* **15,** 705–716 (2015).

151. Kim, S. *et al.* Licensing of natural killer cells by host major histocompatibility complex class I molecules. *Nature* **436,** 709–713 (2005).

152. Bevan, M. J. Helping the CD8+ T-cell response. *Nat. Rev. Immunol.* **4,** 595–602 (2004).

153. Kisielow, P., Teh, H. S., Blüthmann, H. & von Boehmer, H. Positive selection of antigen-specific T cells in thymus by restricting MHC molecules. *Nature* **335,** 730–733 (1988).

154. Ernst, B., Lee, D.-S., Chang, J. M., Sprent, J. & Surh, C. D. The Peptide Ligands Mediating Positive Selection in the Thymus Control T Cell Survival and Homeostatic Proliferation in the Periphery. *Immunity* **11,** 173–181 (1999).

155. Timothy K. Starr, Stephen C. Jameson & Hogquist, and K. A. Positive and Negative Selection of T Cells. *Annu. Rev. Immunol.* **21,** 139–176 (2003).

156. Liston, A., Lesage, S., Wilson, J., Peltonen, L. & Goodnow, C. C. Aire regulates negative selection of organ-specific T cells. *Nat. Immunol.* **4,** 350–354 (2003).

157. Pitkänen, J. & Peterson, P. Autoimmune regulator: from loss of function to autoimmunity. *Genes Immun.* **4,** 12–21 (2003).

158. Liston, A. *et al.* Gene Dosage–limiting Role of *Aire* in Thymic Expression, Clonal Deletion, and Organ-specific Autoimmunity. *J. Exp. Med.* **200,** 1015–1026 (2004).

159. Vilches, C. & Parham, P. KIR: Diverse, Rapidly Evolving Receptors of Innate and Adaptive Immunity. *Annu. Rev. Immunol.* **20,** 217–251 (2002).

160. Malnati, M. S. *et al.* Peptide specificity in the recognition of MHC class I by natural killer cell clones. *Science* **267,** 1016–1018 (1995).

161. Peruzzi, M., Parker, K. C., Long, E. O. & Malnati, M. S. Peptide sequence requirements for the recognition of HLA-B*2705 by specific natural killer cells. *J. Immunol.* **157,** 3350–3356 (1996).

162. Rajagopalan, S. & Long, E. O. The Direct Binding of a p58 Killer Cell Inhibitory Receptor to Human Histocompatibility Leukocyte Antigen (HLA)-Cw4 Exhibits Peptide Selectivity. *J. Exp. Med.* **185,** 1523–1528 (1997).

163. Boyington, J. C., Motyka, S. A., Schuck, P., Brooks, A. G. & Sun, P. D. Crystal structure of an NK cell immunoglobulin-like receptor in complex with its class I MHC ligand. *Nature* **405,** 537–543 (2000).

164. Fan, Q. R., Long, E. O. & Wiley, D. C. Crystal structure of the human natural killer cell inhibitory receptor KIR2DL1–HLA-Cw4 complex. *Nat. Immunol.* **2,** 452–460 (2001).

165. Orihuela, M., Margulies, D. H. & Yokoyama, W. M. The natural killer cell receptor Ly-49A recognizes a peptide-induced conformational determinant on its major histocompatibility complex class I ligand. *Proc. Natl. Acad. Sci. U. S. A.* **93,** 11792–11797 (1996).

166. Marquez, E. A. & Kane, K. P. Identities of P2 and P3 Residues of H-2Kb-Bound Peptides Determine Mouse Ly49C Recognition. *PLoS ONE* **10,** (2015).

167. Franksson, L. *et al.* Peptide dependency and selectivity of the NK cell inhibitory receptor Ly-49C. *Eur. J. Immunol.* **29,** 2748–2758 (1999).

168. Cui, X., Rouhani, F. N., Hawari, F. & Levine, S. J. An aminopeptidase, ARTS-1, is required for interleukin-6 receptor shedding. *J. Biol. Chem.* **278,** 28677–28685 (2003).

169. Cui, X. *et al.* Identification of ARTS-1 as a novel TNFR1-binding protein that promotes TNFR1 ectodomain shedding. *J. Clin. Invest.* **110,** 515–526 (2002).

170. Cui, X., Rouhani, F. N., Hawari, F. & Levine, S. J. Shedding of the type II IL-1 decoy receptor requires a multifunctional aminopeptidase, aminopeptidase regulator of TNF receptor type 1 shedding. *J. Immunol. Baltim. Md 1950* **171,** 6814–6819 (2003).

171. Aldhamen, Y. A. *et al.* Endoplasmic reticulum aminopeptidase-1 functions regulate key aspects of the innate immune response. *PloS One* **8,** e69539 (2013).

172. Goto, Y., Ogawa, K., Nakamura, T. J., Hattori, A. & Tsujimoto, M. TLR-mediated secretion of endoplasmic reticulum aminopeptidase 1 from macrophages. *J. Immunol. Baltim. Md 1950* **192,** 4443–4452 (2014).

173. Goto, Y., Ogawa, K., Hattori, A. & Tsujimoto, M. Secretion of endoplasmic reticulum aminopeptidase 1 is involved in the activation of macrophages induced by lipopolysaccharide and interferon-gamma. *J. Biol. Chem.* **286,** 21906–21914 (2011).

174. Goto, Y., Ogawa, K., Nakamura, T. J., Hattori, A. & Tsujimoto, M. Substrate-dependent nitric oxide synthesis by secreted endoplasmic reticulum aminopeptidase 1 in macrophages. *J. Biochem. (Tokyo)* **157,** 439–449 (2015).

175. Aldhamen, Y. A. *et al.* Autoimmune disease-associated variants of extracellular endoplasmic reticulum aminopeptidase 1 induce altered innate immune responses by human immune cells. *J. Innate Immun.* **7,** 275–289 (2015).

176. Vignali, D. A. A. & Kuchroo, V. K. IL-12 family cytokines: immunological playmakers. *Nat. Immunol.* **13,** 722–728 (2012).

177. Prevention of experimental autoimmune encephalomyelitis by antibodies against interleukin 12. *J. Exp. Med.* **181,** 381–386 (1995).

178. Cua, D. J. *et al.* Interleukin-23 rather than interleukin-12 is the critical cytokine for autoimmune inflammation of the brain. *Nature* **421,** 744–748 (2003).

179. Stritesky, G. L., Yeh, N. & Kaplan, M. H. IL-23 promotes maintenance but not commitment to the Th17 lineage. *J. Immunol. Baltim. Md 1950* **181,** 5948–5955 (2008).

180. Zielinski, C. E. *et al.* Pathogen-induced human TH17 cells produce IFN-γ or IL-10 and are regulated by IL-1β. *Nature* **484,** 514–518 (2012).

181. Kinugasa, T., Sakaguchi, T., Gu, X. & Reinecker, H. C. Claudins regulate the intestinal barrier in response to immune mediators. *Gastroenterology* **118,** 1001–1011 (2000).

182. Iwakura, Y., Ishigame, H., Saijo, S. & Nakae, S. Functional Specialization of Interleukin-17 Family Members. *Immunity* **34,** 149–162 (2011).

183. Lee, E. *et al.* Increased expression of interleukin 23 p19 and p40 in lesional skin of patients with psoriasis vulgaris. *J. Exp. Med.* **199,** 125–130 (2004).

184. Wilson, N. J. *et al.* Development, cytokine profile and function of human interleukin 17-producing helper T cells. *Nat. Immunol.* **8,** 950–957 (2007).

185. Piskin, G., Sylva-Steenland, R. M. R., Bos, J. D. & Teunissen, M. B. M. In vitro and in situ expression of IL-23 by keratinocytes in healthy skin and psoriasis lesions: enhanced expression in psoriatic skin. *J. Immunol. Baltim. Md 1950* **176,** 1908–1915 (2006).

186. Lin, A. M. *et al.* Mast Cells and Neutrophils Release IL-17 through Extracellular Trap Formation in Psoriasis. *J. Immunol.* **187,** 490–500 (2011).

187. Lowes, M. A. *et al.* Psoriasis vulgaris lesions contain discrete populations of Th1 and Th17 T cells. *J. Invest. Dermatol.* **128,** 1207–1211 (2008).

188. Chi, W. *et al.* Upregulated IL-23 and IL-17 in Behçet patients with active uveitis. *Invest. Ophthalmol. Vis. Sci.* **49,** 3058–3064 (2008).

189. Chi, W. *et al.* Production of interleukin-17 in Behcet's disease is inhibited by cyclosporin A. *Mol. Vis.* **16,** 880–886 (2010).

190. Mei, Y. *et al.* Increased serum IL-17 and IL-23 in the patient with ankylosing spondylitis. *Clin. Rheumatol.* **30,** 269–273 (2011).

191. Sherlock, J. P. *et al.* IL-23 induces spondyloarthropathy by acting on ROR-γt+ CD3+CD4-CD8- entheseal resident T cells. *Nat. Med.* **18,** 1069–1076 (2012).

192. Hammer, R. E., Maika, S. D., Richardson, J. A., Tang, J. P. & Taurog, J. D. Spontaneous inflammatory disease in transgenic rats expressing HLA-B27 and human beta 2m: an animal model of HLA-B27-associated human disorders. *Cell* **63,** 1099–1112 (1990).

193. Sherlock, J. P., Buckley, C. D. & Cua, D. J. The critical role of interleukin-23 in spondyloarthropathy. *Mol. Immunol.* **57,** 38–43 (2014).

194. Dougados, M. & Baeten, D. Spondyloarthritis. *The Lancet* **377,** 2127–2137 (2011).

195. Taurog, J. D. *et al.* Spondylarthritis in HLA-B27/human beta2-microglobulin-transgenic rats is not prevented by lack of CD8. *Arthritis Rheum.* **60,** 1977–1984 (2009).

196. May, E. *et al.* CD8 alpha beta T cells are not essential to the pathogenesis of arthritis or colitis in HLA-B27 transgenic rats. *J. Immunol. Baltim. Md 1950* **170,** 1099–1105 (2003).

197. van Duivenvoorde, L. M. *et al.* Relationship between inflammation, bone destruction, and osteoproliferation in spondyloarthritis in HLA-B27/Huβ2m transgenic rats. *Arthritis Rheum.* **64,** 3210–3219 (2012).

198. Perfetto, F. *et al.* Systemic amyloidosis: a challenge for the rheumatologist. *Nat. Rev. Rheumatol.* **6,** 417–429 (2010).

199. Miyata, T. *et al.* Identification of pentosidine as a native structure for advanced glycation end products in beta-2-microglobulin-containing amyloid fibrils in patients with dialysis-related amyloidosis. *Proc. Natl. Acad. Sci.* **93,** 2353–2358 (1996).

200. Armen, R. S. & Daggett, V. Characterization of Two Distinct β2-Microglobulin Unfolding Intermediates that May Lead to Amyloid Fibrils of Different Morphology. *Biochemistry (Mosc.)* **44,** 16098–16107 (2005).

201. Dulgheru, E. C., Balos, L. L. & Baer, A. N. Gastrointestinal complications of β2-microglobulin amyloidosis: A case report and review of the literature. *Arthritis Care Res.* **53,** 142–145 (2005).

202. Kuntz, D. *et al.* Destructive spondylarthropathy in hemodialyzed patients. A new syndrome. *Arthritis Rheum.* **27,** 369–375 (1984).

203. Vignes, J.-R., Eimer, S., Dupuy, R., Donois, E. & Liguoro, D. β2-Microglobulin amyloidosis caused spinal cord compression in a long-term haemodialysis patient. *Spinal Cord* **45,** 322–326 (2006).

204. Tran, T. M. *et al.* Additional human beta2-microglobulin curbs HLA-B27 misfolding and promotes arthritis and spondylitis without colitis in male HLA-B27-transgenic rats. *Arthritis Rheum.* **54,** 1317–1327 (2006).

205. Fukunishi, S., Yoh, K., Kamae, S. & Yoshiya, S. Beta 2-microglobulin amyloid deposit in HLA-B27 transgenic rats. *Mod. Rheumatol. Jpn. Rheum. Assoc.* **17,** 380–384 (2007).

206. Kingsbury, D. J. *et al.* Development of spontaneous arthritis in β2-microglobulin–deficient mice without expression of HLA–B27: Association with deficiency of endogenous major histocompatibility complex class I expression. *Arthritis Rheum.* **43,** 2290–2296 (2000).

207. Khare, S. D., Luthra, H. S. & David, C. S. Spontaneous inflammatory arthritis in HLA-B27 transgenic mice lacking beta 2-microglobulin: a model of human spondyloarthropathies. *J. Exp. Med.* **182,** 1153–1158 (1995).

208. Kingsbury, D. J. *et al.* Development of spontaneous arthritis in beta2-microglobulin-deficient mice without expression of HLA-B27: association with deficiency of endogenous major histocompatibility complex class I expression. *Arthritis Rheum.* **43,** 2290–2296 (2000).

209. Shultz, L. D. *et al.* Generation of functional human T-cell subsets with HLA-restricted immune responses in HLA class I expressing NOD/SCID/IL2r gamma(null) humanized mice. *Proc. Natl. Acad. Sci. U. S. A.* **107,** 13022–13027 (2010).

210. Jaiswal, S. *et al.* Enhanced humoral and HLA-A2-restricted dengue virus-specific T-cell responses in humanized BLT NSG mice. *Immunology* **136,** 334–343 (2012).

211. Brand, D. D., Latham, K. A. & Rosloniec, E. F. Collagen-induced arthritis. *Nat. Protoc.* **2,** 1269–1275 (2007).

212. Rosloniec, E. F. *et al.* An HLA-DR1 transgene confers susceptibility to collagen-induced arthritis elicited with human type II collagen. *J. Exp. Med.* **185,** 1113–1122 (1997).

213. Rosloniec, E. F. *et al.* Induction of autoimmune arthritis in HLA-DR4 (DRB1*0401) transgenic mice by immunization with human and bovine type II collagen. *J. Immunol. Baltim. Md 1950* **160,** 2573–2578 (1998).

214. Glant, T. T., Mikecz, K., Arzoumanian, A. & Poole, A. R. Proteoglycan-induced arthritis in balb/c mice. *Arthritis Rheum.* **30,** 201–212 (1987).

215. Bardos, T. A longitudinal study on an autoimmune murine model of ankylosing spondylitis. *Ann. Rheum. Dis.* **64,** 981–987 (2005).

216. Mikecz, K., Glant, T. T., Buzás, E. & Poole, A. R. Proteoglycan-induced polyarthritis and spondylitis adoptively transferred to naive (nonimmunized) BALB/c mice. *Arthritis Rheum.* **33,** 866–876 (1990).

217. Tseng, H.-W. *et al.* Inflammation-driven bone formation in a mouse model of ankylosing spondylitis: sequential not parallel processes. *Arthritis Res. Ther.* **18,** 35 (2016).

218. Gould, H. J. Complete Freund's adjuvant-induced hyperalgesia: a human perception: *Pain*

85, 301–303 (2000).

219. Benjamin, R. & Parham, P. Guilt by association: HLA-B27 and ankylosing spondylitis. *Immunol. Today* **11,** 137–142 (1990).

220. Colbert, R. A., Tran, T. M. & Layh-Schmitt, G. HLA-B27 misfolding and ankylosing spondylitis. *Mol. Immunol.* **57,** 44–51 (2014).

221. Kollnberger, S. *et al.* HLA-B27 Heavy Chain Homodimers Are Expressed in HLA-B27 Transgenic Rodent Models of Spondyloarthritis and Are Ligands for Paired Ig-Like Receptors. *J. Immunol.* **173,** 1699–1710 (2004).

222. Schittenhelm, R. B., Sian, T. C. C. L. K., Wilmann, P. G., Dudek, N. L. & Purcell, A. W. Revisiting the arthritogenic peptide theory: quantitative not qualitative changes in the peptide repertoire of HLA-B27 allotypes. *Arthritis Rheumatol. Hoboken NJ* **67,** 702–713 (2015).

223. A Review of the Pathogenesis of Ankylosing Spondylitis. *Medscape* Available at: http://www.medscape.com/viewarticle/570733. (Accessed: 30th November 2016)

224. May, E. *et al.* Conserved TCR beta chain usage in reactive arthritis; evidence for selection by a putative HLA-B27-associated autoantigen. *Tissue Antigens* **60,** 299–308 (2002).

225. Atagunduz, P. *et al.* HLA-B27-restricted CD8+ T cell response to cartilage-derived self peptides in ankylosing spondylitis. *Arthritis Rheum.* **52,** 892–901 (2005).

226. Kollnberger, S. *et al.* Cell-surface expression and immune receptor recognition of HLA-B27 homodimers. *Arthritis Rheum.* **46,** 2972–2982 (2002).

227. Kollnberger, S. *et al.* Interaction of HLA-B27 homodimers with KIR3DL1 and KIR3DL2, unlike HLA-B27 heterotrimers, is independent of the sequence of bound peptide. *Eur. J. Immunol.* **37,** 1313–1322 (2007).

228. Zambrano-Zaragoza, J. *et al.* Ankylosing Spondylitis: From Cells to Genes, Ankylosing Spondylitis: From Cells to Genes. *Int. J. Inflamm. Int. J. Inflamm.* **2013, 2013,** e501653 (2013).

229. Campbell, E. C., Fettke, F., Bhat, S., Morley, K. D. & Powis, S. J. Expression of MHC class I dimers and ERAP1 in an ankylosing spondylitis patient cohort. *Immunology* **133,** 379–385 (2011).

230. Cauli, A. *et al.* Increased level of HLA- B27 expression in ankylosing spondylitis patients compared with healthy HLA- B27- positive subjects: a possible further susceptibility factor for the development of disease. *Rheumatology* **41,** 1375–1379 (2002).

231. Antoniou, A. N., Ford, S., Taurog, J. D., Butcher, G. W. & Powis, S. J. Formation of HLA-B27 Homodimers and Their Relationship to Assembly Kinetics. *J. Biol. Chem.* **279,** 8895–8902 (2004).

232. Ciccia, F. *et al.* Evidence that autophagy, but not the unfolded protein response, regulates the expression of IL-23 in the gut of patients with ankylosing spondylitis and subclinical gut inflammation. *Ann. Rheum. Dis.* **73,** 1566–1574 (2014).

233. Neerinckx, B., Carter, S. & Lories, R. J. No evidence for a critical role of the unfolded protein response in synovium and blood of patients with ankylosing spondylitis. *Ann. Rheum. Dis.* **73,** 629–630 (2014).

234. Zeng, L., Lindstrom, M. J. & Smith, J. A. Ankylosing spondylitis macrophage production of higher levels of interleukin-23 in response to lipopolysaccharide without induction of a significant unfolded protein response. *Arthritis Rheum.* **63,** 3807–3817 (2011).

235. Rashid, T., Wilson, C. & Ebringer, A. The Link between Ankylosing Spondylitis, Crohn's Disease, *Klebsiella* , and Starch Consumption. *Clin. Dev. Immunol.* **2013,** 1–9 (2013).

236. Zeidler, H. & Rihl, M. Time to prove the infective etiology of ankylosing spondylitis and related spondylarthritides: Comment on the article by Carter et al. *Arthritis Rheum.* **60,** 3519–3520 (2009).

237. Zindl, C. L. *et al.* IL-22–producing neutrophils contribute to antimicrobial defense and restitution of colonic epithelial integrity during colitis. *Proc. Natl. Acad. Sci. U. S. A.* **110,** 12768–12773 (2013).

238. Gaffen, S. L., Jain, R., Garg, A. V. & Cua, D. J. IL-23-IL-17 immune axis: Discovery, Mechanistic Understanding, and Clinical Testing. *Nat. Rev. Immunol.* **14,** 585–600 (2014).

239. Thjodleifsson, B., Geirsson, A. J., Björnsson, S. & Bjarnason, I. A common genetic background for inflammatory bowel disease and ankylosing spondylitis: a genealogic study in Iceland. *Arthritis Rheum.* **56,** 2633–2639 (2007).

240. De Vos, M. *et al.* Ileocolonoscopy in seronegative spondylarthropathy. *Gastroenterology* **96,** 339–344 (1989).

241. De Vos, M., Mielants, H., Cuvelier, C., Elewaut, A. & Veys, E. Long-term evolution of gut inflammation in patients with spondyloarthropathy. *Gastroenterology* **110,** 1696–1703 (1996).

242. Lin, P. *et al.* HLA-B27 and Human β2-Microglobulin Affect the Gut Microbiota of Transgenic Rats. *PLOS ONE* **9,** e105684 (2014).

243. Costello, M.-E. *et al.* Intestinal dysbiosis in ankylosing spondylitis. *Arthritis Rheumatol.*

Hoboken NJ (2014). doi:10.1002/art.38967

244. Kigerl, K. A. *et al.* Gut dysbiosis impairs recovery after spinal cord injury. *J. Exp. Med.* jem.20151345 (2016). doi:10.1084/jem.20151345

245. Scher, J. U. *et al.* Expansion of intestinal Prevotella copri correlates with enhanced susceptibility to arthritis. *eLife* **2,** e01202 (2013).

246. Visscher, P. M., Brown, M. A., McCarthy, M. I. & Yang, J. Five Years of GWAS Discovery. *Am. J. Hum. Genet.* **90,** 7–24 (2012).

247. Lin, Z. *et al.* A genome-wide association study in Han Chinese identifies new susceptibility loci for ankylosing spondylitis. *Nat. Genet.* **44,** 73–77 (2012).

248. Zuk, O., Hechter, E., Sunyaev, S. R. & Lander, E. S. The mystery of missing heritability: Genetic interactions create phantom heritability. *Proc. Natl. Acad. Sci. U. S. A.* **109,** 1193–1198 (2012).

249. Saric, T. *et al.* An IFN-γ–induced aminopeptidase in the ER, ERAP1, trims precursors to MHC class I–presented peptides. *Nat. Immunol.* **3,** 1169–1176 (2002).

250. Serwold, T., Gonzalez, F., Kim, J., Jacob, R. & Shastri, N. ERAAP customizes peptides for MHC class I molecules in the endoplasmic reticulum. *Nature* **419,** 480–483 (2002).

251. Kochan, G. *et al.* Crystal structures of the endoplasmic reticulum aminopeptidase-1 (ERAP1) reveal the molecular basis for N-terminal peptide trimming. *Proc. Natl. Acad. Sci.* **108,** 7745–7750 (2011).

252. Rock, K. L., Farfán-Arribas, D. J. & Shen, L. Proteases in MHC Class I Presentation and Cross-Presentation. *J. Immunol.* **184,** 9–15 (2010).

253. van Endert, P. Post-proteasomal and proteasome-independent generation of MHC class I ligands. *Cell. Mol. Life Sci.* **68,** 1553–1567 (2011).

254. Stratikos, E. & Stern, L. J. Antigenic peptide trimming by ER aminopeptidases—Insights from structural studies. *Mol. Immunol.* **55,** 212–219 (2013).

255. Nguyen, T. T. *et al.* Structural basis for antigenic peptide precursor processing by the endoplasmic reticulum aminopeptidase ERAP1. *Nat. Struct. Mol. Biol.* **18,** 604–613 (2011).

256. Blanchard, N. *et al.* Endoplasmic Reticulum Aminopeptidase Associated with Antigen Processing Defines the Composition and Structure of MHC Class I Peptide Repertoire in Normal and Virus-Infected Cells. *J. Immunol.* **184,** 3033–3042 (2010).

257. Hammer, G. E., Gonzalez, F., James, E., Nolla, H. & Shastri, N. In the absence of aminopeptidase ERAAP, MHC class I molecules present many unstable and highly immunogenic peptides. *Nat. Immunol.* **8,** 101–108 (2007).

258. Yan, J. *et al.* In vivo role of ER-associated peptidase activity in tailoring peptides for presentation by MHC class Ia and class Ib molecules. *J. Exp. Med.* **203,** 647–659 (2006).

259. Yewdell, J. W. Confronting Complexity: Real-World Immunodominance in Antiviral CD8+ T Cell Responses. *Immunity* **25,** 533–543 (2006).

260. Kanaseki, T., Blanchard, N., Hammer, G. E., Gonzalez, F. & Shastri, N. ERAAP Synergizes with MHC Class I Molecules to Make the Final Cut in the Antigenic Peptide Precursors in the Endoplasmic Reticulum. *Immunity* **25,** 795–806 (2006).

261. Seregin, S. S., Aldhamen, Y. A., Rastall, D. P. W., Godbehere, S. & Amalfitano, A. Adenovirus-based vaccination against Clostridium difficile toxin A allows for rapid humoral immunity and complete protection from toxin A lethal challenge in mice. *Vaccine* **30,** 1492–1501 (2012).

262. Blanchard, N. *et al.* Immunodominant, protective response to the parasite Toxoplasma gondii requires antigen processing in the endoplasmic reticulum. *Nat. Immunol.* **9,** 937–944 (2008).

263. Thomas, P. G. *et al.* Hidden Epitopes Emerge in Secondary Influenza Virus-Specific CD8+ T Cell Reponses. *J. Immunol.* **178,** 3091–3098 (2007).

264. Jenkins, M. R., Webby, R., Doherty, P. C. & Turner, S. J. Addition of a Prominent Epitope Affects Influenza A Virus-Specific CD8+ T Cell Immunodominance Hierarchies When Antigen Is Limiting. *J. Immunol.* **177,** 2917–2925 (2006).

265. Hearn, A., York, I. A. & Rock, K. L. The Specificity of Trimming of MHC Class I-Presented Peptides in the Endoplasmic Reticulum. *J. Immunol.* **183,** 5526–5536 (2009).

266. Reeves, E., Edwards, C. J., Elliott, T. & James, E. Naturally Occurring ERAP1 Haplotypes Encode Functionally Distinct Alleles with Fine Substrate Specificity. *J. Immunol.* **191,** 35–43 (2013).

267. Aldhamen, Y. A. *et al.* Expression of the SLAM Family of Receptors Adapter EAT-2 as a Novel Strategy for Enhancing Beneficial Immune Responses to Vaccine Antigens. *J. Immunol.* **186,** 722–732 (2011).

268. Kaech, S. M. & Cui, W. Transcriptional control of effector and memory CD8+ T cell differentiation. *Nat. Rev. Immunol.* **12,** 749–761 (2012).

269. Hansen, S. G. *et al.* Effector memory T cell responses are associated with protection of rhesus monkeys from mucosal simian immunodeficiency virus challenge. *Nat. Med.* **15,** 293–299 (2009).

270. Hansen, S. G. *et al.* Profound early control of highly pathogenic SIV by an effector memory T-cell vaccine. *Nature* **473,** 523–527 (2011).

271. Sallusto, F., Lenig, D., Förster, R., Lipp, M. & Lanzavecchia, A. Two subsets of memory T lymphocytes with distinct homing potentials and effector functions. *Nature* **401,** 708–712 (1999).

272. Aldhamen, Y. A. *et al.* Vaccines Expressing the Innate Immune Modulator EAT-2 Elicit Potent Effector Memory T Lymphocyte Responses despite Pre-Existing Vaccine Immunity. *J. Immunol.* **189,** 1349–1359 (2012).

273. Tsai, F.-J. *et al.* Identification of Novel Susceptibility Loci for Kawasaki Disease in a Han Chinese Population by a Genome-Wide Association Study. *PLoS ONE* **6,** e16853 (2011).

274. Fierabracci, A., Milillo, A., Locatelli, F. & Fruci, D. The putative role of endoplasmic reticulum aminopeptidases in autoimmunity: Insights from genomic-wide association studies. *Autoimmun. Rev.* **12,** 281–288 (2012).

275. Lunemann, J. D. *et al.* Increased Frequency of EBV-Specific Effector Memory CD8+ T Cells Correlates with Higher Viral Load in Rheumatoid Arthritis. *J. Immunol.* **181,** 991–1000 (2008).

276. Cho, B.-A. *et al.* Characterization of Effector Memory CD8+ T Cells in the Synovial Fluid of Rheumatoid Arthritis. *J. Clin. Immunol.* **32,** 709–720 (2012).

277. Epstein, F. H., Albert, L. J. & Inman, R. D. Molecular Mimicry and Autoimmunity. *N. Engl. J. Med.* **341,** 2068–2074 (1999).

278. Wucherpfennig, K. W. & Strominger, J. L. Molecular mimicry in T cell-mediated autoimmunity: viral peptides activate human T cell clones specific for myelin basic protein. *Cell* **80,** 695–705 (1995).

279. Guilherme, L., Kalil, J. & Cunningham, M. Molecular mimicry in the autoimmune pathogenesis of rheumatic heart disease. *Autoimmunity* **39,** 31–39 (2006).

280. Beeton, C. Targeting Effector Memory T Cells with a Selective Peptide Inhibitor of Kv1.3 Channels for Therapy of Autoimmune Diseases. *Mol. Pharmacol.* **67,** 1369–1381 (2005).

281. Diz, R. *et al.* Autoreactive effector/memory CD4+ and CD8+ T cells infiltrating grafted and endogenous islets in diabetic NOD mice exhibit similar T cell receptor usage. *PloS One* **7,**

e52054 (2012).

282. Belz, G. T., Zhang, L., Lay, M. D. H., Kupresanin, F. & Davenport, M. P. Killer T cells regulate antigen presentation for early expansion of memory, but not naive, CD8+ T cell. *Proc. Natl. Acad. Sci.* **104,** 6341–6346 (2007).

283. Helft, J. *et al.* Antigen-specific T-T interactions regulate CD4 T-cell expansion. *Blood* **112,** 1249–1258 (2008).

284. Wong, P. & Pamer, E. G. Feedback regulation of pathogen-specific T cell priming. *Immunity* **18,** 499–511 (2003).

285. Brown, M. A. Breakthroughs in genetic studies of ankylosing spondylitis. *Rheumatology* **47,** 132–137 (2008).

286. Tsui, F. W. L. *et al.* Association of an ERAP1 ERAP2 haplotype with familial ankylosing spondylitis. *Ann. Rheum. Dis.* **69,** 733–736 (2010).

287. Consortium, T. W. T. C. C. Genome-wide association study of 14,000 cases of seven common diseases and 3,000 shared controls. *Nature* **447,** 661 (2007).

288. Haroon, N., Tsui, F. W., Uchanska-Ziegler, B., Ziegler, A. & Inman, R. D. Endoplasmic reticulum aminopeptidase 1 (ERAP1) exhibits functionally significant interaction with HLA-B27 and relates to subtype specificity in ankylosing spondylitis. *Ann. Rheum. Dis.* **71,** 589–595 (2012).

289. Rock, K. L. *et al.* Inhibitors of the proteasome block the degradation of most cell proteins and the generation of peptides presented on MHC class I molecules. *Cell* **78,** 761–771 (1994).

290. Craiu, A., Akopian, T., Goldberg, A. & Rock, K. L. Two distinct proteolytic processes in the generation of a major histocompatibility complex class I-presented peptide. *Proc. Natl. Acad. Sci.* **94,** 10850–10855 (1997).

291. Cerundolo, V. *et al.* The proteasome-specific inhibitor lactacystin blocks presentation of cytotoxic T lymphocyte epitopes in human and murine cells. *Eur. J. Immunol.* **27,** 336–341 (1997).

292. Schwarz, K. *et al.* The selective proteasome inhibitors lactacystin and epoxomicin can be used to either up- or down-regulate antigen presentation at nontoxic doses. *J. Immunol. Baltim. Md 1950* **164,** 6147–6157 (2000).

293. Stoltze, L. *et al.* Generation of the vesicular stomatitis virus nucleoprotein cytotoxic T lymphocyte epitope requires proteasome-dependent and -independent proteolytic activities. *Eur. J. Immunol.* **28,** 4029–4036 (1998).

294. Breban, M. *et al.* T cells, but not thymic exposure to HLA-B27, are required for the inflammatory disease of HLA-B27 transgenic rats. *J. Immunol.* **156,** 794–803 (1996).

295. Bowness, P. *et al.* Th17 Cells Expressing KIR3DL2+ and Responsive to HLA-B27 Homodimers Are Increased in Ankylosing Spondylitis. *J. Immunol.* **186,** 2672–2680 (2011).

296. Evnouchidou, I. *et al.* Cutting Edge: Coding Single Nucleotide Polymorphisms of Endoplasmic Reticulum Aminopeptidase 1 Can Affect Antigenic Peptide Generation In Vitro by Influencing Basic Enzymatic Properties of the Enzyme. *J. Immunol.* **186,** 1909–1913 (2011).

297. Chen, R., Yao, L., Meng, T. & Xu, W. The association between seven ERAP1 polymorphisms and ankylosing spondylitis susceptibility: a meta-analysis involving 8,530 cases and 12,449 controls. *Rheumatol. Int.* **32,** 909–914 (2012).

298. York, I. A., Grant, E. P., Dahl, A. M. & Rock, K. L. A Mutant Cell with a Novel Defect in MHC Class I Quality Control. *J. Immunol.* **174,** 6839–6846 (2005).

299. Hill, A. *et al.* Herpes simplex virus turns off the TAP to evade host immunity. *Nature* **375,** 411–415 (1995).

300. Evnouchidou, I. *et al.* The Internal Sequence of the Peptide-Substrate Determines Its N-Terminus Trimming by ERAP1. *PLOS ONE* **3,** e3658 (2008).

301. Scofield, R. H. *et al.* HLA-B27 binding of peptide from its own sequence and similar peptides from bacteria: implications for spondyloarthropathies. *The Lancet* **345,** 1542–1544 (1995).

302. Rock, K. L., York, I. A. & Goldberg, A. L. Post-proteasomal antigen processing for major histocompatibility complex class I presentation. *Nat. Immunol.* **5,** 670–677 (2004).

303. Saveanu, L. *et al.* Concerted peptide trimming by human ERAP1 and ERAP2 aminopeptidase complexes in the endoplasmic reticulum. *Nat. Immunol.* **6,** 689–697 (2005).

304. Jensen, P. E. Recent advances in antigen processing and presentation. *Nat. Immunol.* **8,** 1041–1048 (2007).

305. Rufer, E., Leonhardt, R. M. & Knittler, M. R. Molecular Architecture of the TAP-Associated MHC Class I Peptide-Loading Complex. *J. Immunol.* **179,** 5717–5727 (2007).

306. Harvey, D. *et al.* Investigating the genetic association between ERAP1 and ankylosing spondylitis. *Hum. Mol. Genet.* **18,** 4204–4212 (2009).

307. Lopez de Castro, J. A. *et al.* HLA-B27: a registry of constitutive peptide ligands. *Tissue Antigens* **63,** 424–445 (2004).

308. Fiorillo, M. T., Maragno, M., Butler, R., Dupuis, M. L. & Sorrentino, R. CD8+ T-cell autoreactivity to an HLA-B27–restricted self-epitope correlates with ankylosing spondylitis. *J. Clin. Invest.* **106,** 47 (2000).

309. Cheuk, E. & Chamberlain, J. W. Strong memory CD8+ T cell responses against immunodominant and three new subdominant HLA-B27-restricted influenza A CTL epitopes following secondary infection of HLA-B27 transgenic mice. *Cell. Immunol.* **234,** 110–123 (2005).

310. Ugrinovic, S., Mertz, A., Wu, P., Braun, J. & Sieper, J. A single nonamer from the Yersinia 60-kDa heat shock protein is the target of HLA-B27-restricted CTL response in Yersinia-induced reactive arthritis. *J. Immunol.* **159,** 5715–5723 (1997).

311. Brooks, J. M., Murray, R. J., Thomas, W. A., Kurilla, M. G. & Rickinson, A. B. Different HLA-B27 subtypes present the same immunodominant Epstein-Barr virus peptide. *J. Exp. Med.* **178,** 879–887 (1993).

312. Appel, H. *et al.* Use of HLA-B27 tetramers to identify low-frequency antigen-specific T cells in Chlamydia-triggered reactive arthritis. *Arthritis Res. Ther.* **6,** R521 (2004).

313. Kuon, W. *et al.* Identification of HLA-B27-Restricted Peptides from the Chlamydia trachomatis Proteome with Possible Relevance to HLA-B27-Associated Diseases. *J. Immunol.* **167,** 4738–4746 (2001).

314. Boyle, L. H., Goodall, J. C., Opat, S. S. & Gaston, J. S. H. The Recognition of HLA-B27 by Human CD4+ T Lymphocytes. *J. Immunol.* **167,** 2619–2624 (2001).

315. Perosa, F. *et al.* β2-Microglobulin-Free HLA Class I Heavy Chain Epitope Mimicry by Monoclonal Antibody HC-10-Specific Peptide. *J. Immunol.* **171,** 1918–1926 (2003).

316. Evans, D. M. *et al.* Interaction between ERAP1 and HLA-B27 in ankylosing spondylitis implicates peptide handling in the mechanism for HLA-B27 in disease susceptibility. *Nat. Genet.* **43,** 761–767 (2011).

317. García-Medel, N. *et al.* Functional Interaction of the Ankylosing Spondylitis-associated Endoplasmic Reticulum Aminopeptidase 1 Polymorphism and HLA-B27 in Vivo. *Mol. Cell. Proteomics MCP* **11,** 1416 (2012).

318. Schatz, M. M. *et al.* Characterizing the N-Terminal Processing Motif of MHC Class I Ligands. *J. Immunol.* **180,** 3210–3217 (2008).

319. Neefjes, J., Jongsma, M. L. M., Paul, P. & Bakke, O. Towards a systems understanding of MHC class I and MHC class II antigen presentation. *Nat. Rev. Immunol.* **11,** 823–836 (2011).

320. Kieckbusch, J., Gaynor, L. M., Moffett, A. & Colucci, F. MHC-dependent inhibition of uterine NK cells impedes fetal growth and decidual vascular remodelling. *Nat. Commun.* **5,** 3359 (2014).

321. Mao, X., Fujiwara, Y., Chapdelaine, A., Yang, H. & Orkin, S. H. Activation of EGFP expression by Cre-mediated excision in a new ROSA26 reporter mouse strain. *Blood* **97,** 324–326 (2001).

322. Srinivas, S. *et al.* Cre reporter strains produced by targeted insertion of EYFP and ECFP into the ROSA26 locus. *BMC Dev. Biol.* **1,** 4 (2001).

323. Kaer, L. V., Ashton-Rickardt, P. G., Ploegh, H. L. & Tonegawa, S. TAP1 mutant mice are deficient in antigen presentation, surface class I molecules, and CD4−8+ T cells. *Cell* **71,** 1205–1214 (1992).

324. Zhou, F. Molecular Mechanisms of IFN-γ to Up-Regulate MHC Class I Antigen Processing and Presentation. *Int. Rev. Immunol.* **28,** 239–260 (2009).

325. Liu, M. K. P. *et al.* Vertical T cell immunodominance and epitope entropy determine HIV-1 escape. *J. Clin. Invest.* (2012). doi:10.1172/JCI65330

326. Stratikos, E. Modulating antigen processing for cancer immunotherapy. *Oncoimmunology* **3,** (2014).

327. Höllsberg, P., Hansen, H. J. & Haahr, S. Altered CD8+ T cell responses to selected Epstein–Barr virus immunodominant epitopes in patients with multiple sclerosis. *Clin. Exp. Immunol.* **132,** 137–143 (2003).

328. Held, W. & Mariuzza, R. A. Cis interactions of immunoreceptors with MHC and non-MHC ligands. *Nat. Rev. Immunol.* **8,** 269–278 (2008).

329. Nausch, N. & Cerwenka, A. NKG2D ligands in tumor immunity. *Oncogene* **27,** 5944–5958 (2008).

330. Chang, S. T., Linderman, J. J. & Kirschner, D. E. Effect of Multiple Genetic Polymorphisms on Antigen Presentation and Susceptibility to Mycobacterium tuberculosis Infection. *Infect. Immun.* **76,** 3221–3232 (2008).

331. Azuz-Lieberman, N. *et al.* The involvement of NK cells in ankylosing spondylitis. *Int. Immunol.* **17,** 837–845 (2005).

332. Mousavi, T. *et al.* Phenotypic Study of Natural Killer Cell Subsets in Ankylosing Spondylitis Patients. *Iran. J. Allergy Asthma Immunol.* **8,** 193–198 (2009).

333. Ogasawara, K. *et al.* NKG2D blockade prevents autoimmune diabetes in NOD mice. *Immunity* **20,** 757–767 (2004).

334. Groh, V., Bruhl, A., El-Gabalawy, H., Nelson, J. L. & Spies, T. Stimulation of T cell autoreactivity by anomalous expression of NKG2D and its MIC ligands in rheumatoid arthritis. *Proc. Natl. Acad. Sci. U. S. A.* **100,** 9452–9457 (2003).

335. Zhou, X. *et al.* MICA, a gene contributing strong susceptibility to ankylosing spondylitis. *Ann. Rheum. Dis.* **73,** 1552–1557 (2014).

336. Amroun, H. *et al.* Early-onset ankylosing spondylitis is associated with a functional MICA polymorphism. *Hum. Immunol.* **66,** 1057–1061 (2005).

337. Wiemann, K. *et al.* Systemic NKG2D down-regulation impairs NK and CD8 T cell responses in vivo. *J. Immunol. Baltim. Md 1950* **175,** 720–729 (2005).

338. Oppenheim, D. E. *et al.* Sustained localized expression of ligand for the activating NKG2D receptor impairs natural cytotoxicity in vivo and reduces tumor immunosurveillance. *Nat. Immunol.* **6,** 928–937 (2005).

339. Dandapat, A. *et al.* Dominant Lethal Pathologies in Male Mice Engineered to Contain an X-Linked DUX4 Transgene. *Cell Rep.* **8,** 1484–1496 (2014).

340. Adamik, B. *et al.* An association between RBMX, a heterogeneous nuclear ribonucleoprotein, and ARTS-1 regulates extracellular TNFR1 release. *Biochem. Biophys. Res. Commun.* **371,** 505–509 (2008).

341. Yadav, M. *et al.* Predicting immunogenic tumour mutations by combining mass spectrometry and exome sequencing. *Nature* **515,** 572–576 (2014).

342. Gubin, M. M., Artyomov, M. N., Mardis, E. R. & Schreiber, R. D. Tumor neoantigens: building a framework for personalized cancer immunotherapy. *J. Clin. Invest.* **125,** 3413+ (2015).

343. Yang, X. & Yu, X. An introduction to epitope prediction methods and software. *Rev. Med. Virol.* **19,** 77–96 (2009).

344. Zhang, L., Udaka, K., Mamitsuka, H. & Zhu, S. Toward more accurate pan-specific MHC-peptide binding prediction: a review of current methods and tools. *Brief. Bioinform.* bbr060 (2011). doi:10.1093/bib/bbr060

345. Kotturi, M. F. *et al.* Of mice and humans: how good are HLA transgenic mice as a model of human immune responses? *Immunome Res.* **5,** 3 (2009).

346. Jacobson, J. A., Girish, G., Jiang, Y. & Resnick, D. Radiographic Evaluation of Arthritis: Inflammatory Conditions. *Radiology* **248,** 378–389 (2008).

347. Mitra, D. The prevalence of vertebral fractures in mild ankylosing spondylitis and their relationship to bone mineral density. *Rheumatology* **39,** 85–89 (2000).

348. Schlosstein, L., Terasaki, P. I., Bluestone, R. & Pearson, C. M. High association of an HL-A antigen, W27, with ankylosing spondylitis. *N. Engl. J. Med.* **288,** 704–706 (1973).

349. McGonagle, D., Aydin, S. Z., Gül, A., Mahr, A. & Direskeneli, H. 'MHC-I-opathy'—unified concept for spondyloarthritis and Behcet disease. *Nat. Rev. Rheumatol.* **11,** 731–740 (2015).

350. Gratacós, J. *et al.* SERUM CYTOKINES (IL-6, TNF-α, IL-1β AND IFN-γ) IN ANKYLOSING SPONDYLITIS: A CLOSE CORRELATION BETWEEN SERUM IL-6 AND DISEASE ACTIVITY AND SEVERITY. *Rheumatology* **33,** 927–931 (1994).

351. Ritchlin, C. T., Haas-Smith, S. A., Li, P., Hicks, D. G. & Schwarz, E. M. Mechanisms of TNF-alpha- and RANKL-mediated osteoclastogenesis and bone resorption in psoriatic arthritis. *J. Clin. Invest.* **111,** 821–831 (2003).

352. Kwan Tat, S., Padrines, M., Théoleyre, S., Heymann, D. & Fortun, Y. IL-6, RANKL, TNF-alpha/IL-1: interrelations in bone resorption pathophysiology. *Cytokine Growth Factor Rev.* **15,** 49–60 (2004).

353. Glant, T. T. *et al.* Proteoglycan-induced arthritis and recombinant human proteoglycan aggrecan G1 domain-induced arthritis in BALB/c mice resembling two subtypes of rheumatoid arthritis. *Arthritis Rheum.* **63,** 1312–1321 (2011).

354. Brand, D. D., Latham, K. A. & Rosloniec, E. F. Collagen-induced arthritis. *Nat. Protoc.* **2,** 1269–1275 (2007).

355. Khare, S. D. *et al.* Spontaneous inflammatory disease in HLA-B27 transgenic mice does not require transporter of antigenic peptides. *Clin. Immunol. Orlando Fla* **98,** 364–369 (2001).

356. Donnelly, S. *et al.* Bone mineral density and vertebral compression fracture rates in ankylosing spondylitis. *Ann. Rheum. Dis.* **53,** 117–121 (1994).

357. Glatt, V., Canalis, E., Stadmeyer, L. & Bouxsein, M. L. Age-Related Changes in Trabecular Architecture Differ in Female and Male C57BL/6J Mice. *J. Bone Miner. Res.* **22,** 1197–1207 (2007).

358. Nguyen, T. T. *et al.* Structural basis for antigenic peptide precursor processing by the endoplasmic reticulum aminopeptidase ERAP1. *Nat. Struct. Mol. Biol.* **18,** 604–613 (2011).

359. Cifaldi, L. *et al.* ERAP1 regulates natural killer cell function by controlling the engagement of inhibitory receptors. *Cancer Res.* **75,** 824–834 (2015).

360. Marusić, A., Katavić, V., Stimac, D., Kusec, V. & Jonjić, S. Bone turnover in homozygous beta 2-microglobulin knock-out mice does not differ from that of their heterozygous littermates. *Eur. J. Clin. Chem. Clin. Biochem. J. Forum Eur. Clin. Chem. Soc.* **33,** 915–918 (1995).

361. Dhakad, U. & Das, S. K. Andersson lesion in ankylosing spondylitis. *BMJ Case Rep.* **2013,** (2013).

362. Amarasekara, D. S., Yu, J. & Rho, J. Bone Loss Triggered by the Cytokine Network in Inflammatory Autoimmune Diseases. *J. Immunol. Res.* **2015,** 832127 (2015).

363. Britton, R. A. *et al.* Probiotic *L. reuteri* Treatment Prevents Bone Loss in a Menopausal Ovariectomized Mouse Model: PROBIOTICS SUPPRESS ESTROGEN DEFICIENCY-INDUCED BONE LOSS. *J. Cell. Physiol.* **229,** 1822–1830 (2014).

364. Georgiadou, D. *et al.* Placental Leucine Aminopeptidase Efficiently Generates Mature Antigenic Peptides In Vitro but in Patterns Distinct from Endoplasmic Reticulum Aminopeptidase 1. *J. Immunol.* **185,** 1584–1592 (2010).

365. Zervoudi, E. *et al.* Probing the S1 specificity pocket of the aminopeptidases that generate antigenic peptides. *Biochem. J.* **435,** 411–420 (2011).

366. Seregin, S. S. *et al.* TRIF Is a Critical Negative Regulator of TLR Agonist Mediated Activation of Dendritic Cells In Vivo. *PLoS ONE* **6,** e22064 (2011).

367. Arrestin-2 and G Protein-coupled Receptor Kinase 5 Interact with NFκB1 p105 and Negatively Regulate Lipopolysaccharide-stimulated ERK1/2 Activation in Macrophages. Available at: http://www.jbc.org.proxy2.cl.msu.edu/content/281/45/34159.long. (Accessed: 31st October 2016)

368. Seregin, S. S. *et al.* Transient Pretreatment With Glucocorticoid Ablates Innate Toxicity of Systemically Delivered Adenoviral Vectors Without Reducing Efficacy. *Mol. Ther.* **17,** 685–696 (2009).

369. Long, E. O. Negative signalling by inhibitory receptors: the NK cell paradigm. *Immunol. Rev.* **224,** 70–84 (2008).

370. Lowe, R., Gemma, C., Rakyan, V. K. & Holland, M. L. Sexually dimorphic gene expression emerges with embryonic genome activation and is dynamic throughout development. *BMC Genomics* **16,** 295 (2015).

371. Adamson, B., Smogorzewska, A., Sigoillot, F. D., King, R. W. & Elledge, S. J. A genome-wide homologous recombination screen identifies the RNA-binding protein RBMX as a component of the DNA-damage response. *Nat. Cell Biol.* **14,** 318–328 (2012).

372. Elliott, D. J. The role of potential splicing factors including RBMY, RBMX, hnRNPG-T and STAR proteins in spermatogenesis*. *Int. J. Androl.* **27,** 328–334 (2004).

373. Elliott, D. J. *et al.* An evolutionarily conserved germ cell-specific hnRNP is encoded by a retrotransposed gene. *Hum. Mol. Genet.* **9,** 2117–2124 (2000).

374. Muckenthaler, M. U. *et al.* Molecular analysis of iron overload in beta2-microglobulin-deficient mice. *Blood Cells. Mol. Dis.* **33,** 125–131 (2004).

375. Schaible, U. E., Collins, H. L., Priem, F. & Kaufmann, S. H. E. Correction of the iron overload defect in beta-2-microglobulin knockout mice by lactoferrin abolishes their increased susceptibility to tuberculosis. *J. Exp. Med.* **196,** 1507–1513 (2002).

376. Elinav, E. *et al.* NLRP6 inflammasome regulates colonic microbial ecology and risk for colitis. *Cell* **145,** 745–757 (2011).

377. Ren, E. C. *et al.* Possible protective role of HLA-B*2706 for ankylosing spondylitis. *Tissue Antigens* **49,** 67–69 (1997).

378. Keystone, E. C. *et al.* Radiographic, clinical, and functional outcomes of treatment with adalimumab (a human anti-tumor necrosis factor monoclonal antibody) in patients with active rheumatoid arthritis receiving concomitant methotrexate therapy: A randomized, placebo-controlled, 52-week trial. *Arthritis Rheum.* **50,** 1400–1411 (2004).

379. Baraliakos, X. *et al.* Inflammation in ankylosing spondylitis: a systematic description of the extent and frequency of acute spinal changes using magnetic resonance imaging. *Ann. Rheum. Dis.* **64,** 730–734 (2005).

380. Braun, J. & Sieper, J. Early diagnosis of spondyloarthritis. *Nat. Clin. Pract. Rheumatol.* **2,** 536–545 (2006).

381. Braun, J. *et al.* Magnetic resonance imaging examinations of the spine in patients with ankylosing spondylitis, before and after successful therapy with infliximab: evaluation of a new scoring system. *Arthritis Rheum.* **48,** 1126–1136 (2003).

382. Reveille, J. D. Biomarkers for diagnosis, monitoring of progression, and treatment

responses in ankylosing spondylitis and axial spondyloarthritis. *Clin. Rheumatol.* **34,** 1009–1018 (2015).

383. Li, X. *et al.* Elevated Serum Level of IL-33 and sST2 in Patients With Ankylosing Spondylitis. *J. Investig. Med.* **61,** 848–851 (2013).

384. Han, G.-W. *et al.* Serum levels of IL-33 is increased in patients with ankylosing spondylitis. *Clin. Rheumatol.* **30,** 1583–1588 (2011).

385. Wang, R., Dasgupta, A. & Ward, M. M. Comparative efficacy of non-steroidal anti-inflammatory drugs in ankylosing spondylitis: a Bayesian network meta-analysis of clinical trials. *Ann. Rheum. Dis.* **75,** 1152–1160 (2016).

386. Drachman, D. B. *et al.* Cyclooxygenase 2 inhibition protects motor neurons and prolongs survival in a transgenic mouse model of ALS. *Ann. Neurol.* **52,** 771–778 (2002).

387. Heijde, D. van der *et al.* Radiographic findings following two years of infliximab therapy in patients with ankylosing spondylitis. *Arthritis Rheum.* **58,** 3063–3070 (2008).

388. Maas, F. *et al.* SAT0343 Spinal Radiographic Progression during 6 Years of Tnf-Alpha Blocking Therapy in Patients with Ankylosing Spondylitis: Results from the GLAS Cohort. *Ann. Rheum. Dis.* **73,** 716–717 (2014).

389. Sandborn, W. J. *et al.* Colectomy Rate Comparison After Treatment of Ulcerative Colitis With Placebo or Infliximab. *Gastroenterology* **137,** 1250–1260 (2009).

390. Cassidy, S. A., Cheent, K. S. & Khakoo, S. I. Effects of Peptide on NK Cell-Mediated MHC I Recognition. *Front. Immunol.* **5,** (2014).

391. Furukawa, K.-I. Current Topics in Pharmacological Research on Bone Metabolism: Molecular Basis of Ectopic Bone Formation Induced by Mechanical Stress. *J. Pharmacol. Sci.* **100,** 201–204 (2006).

392. N, B., Ww, B., Ch, G., J, C. & Lw, S. Validation study of WOMAC: a health status instrument for measuring clinically important patient relevant outcomes to antirheumatic drug therapy in patients with osteoarthritis of the hip or knee. *J. Rheumatol.* **15,** 1833–1840 (1988).

393. De, H., Dd, H. & Sj, T. The sacroiliac joint: a review of anatomy and biomechanics with clinical implications. *J. Manipulative Physiol. Ther.* **20,** 607–617 (1996).

394. Jacques, P. *et al.* Proof of concept: enthesitis and new bone formation in spondyloarthritis are driven by mechanical strain and stromal cells. *Ann. Rheum. Dis.* annrheumdis-2013-203643 (2013). doi:10.1136/annrheumdis-2013-203643

395. Wang, B., Niu, D., Lai, L. & Ren, E. C. p53 increases MHC class I expression by upregulating the endoplasmic reticulum aminopeptidase ERAP1. *Nat. Commun.* **4,** 2359 (2013).

396. Hisatsune, C. *et al.* ERp44 Exerts Redox-Dependent Control of Blood Pressure at the ER. *Mol. Cell* 58, 1015–1027 (2015).